Russian Original Vol. 34, No. 2, February, 1973

August, 1973

SATEAZ 34(2) 101-192 (1973)

SOVIET ATOMIC ENERGY

АТОМНАЯ ЭНЕРГИЯ
(ATOMNAYA ÉNERGIYA)

TRANSLATED FROM RUSSIAN

CONSULTANTS BUREAU, NEW YORK

SOVIET ATOMIC ENERGY

Soviet Atomic Energy is a cover-to-cover translation of *Atomnaya Énergiya*, a publication of the Academy of Sciences of the USSR.

An arrangement with Mezhdunarodnaya Kniga, the Soviet book export agency, makes available both advance copies of the Russian journal and original glossy photographs and artwork. This serves to decrease the necessary time lag between publication of the original and publication of the translation and helps to improve the quality of the latter. The translation began with the first issue of the Russian journal.

Consultants Bureau journals appear about six months after the publication of the original Russian issue. For bibliographic accuracy, the English issue published by Consultants Bureau carries the same number and date as the original Russian from which it was translated. For example, a Russian issue published in December will appear in a Consultants Bureau English translation about the following June, but the translation issue will carry the December date. When ordering any volume or particular issue of a Consultants Bureau journal, please specify the date and, where applicable, the volume and issue numbers of the original Russian. The material you will receive will be a translation of that Russian volume or issue.

Subscription
$80 per volume (6 issues)
2 volumes per year
(Add $5 for orders outside the United States and Canada.)

Single Issue: $30
Single Article: $15

CONSULTANTS BUREAU, NEW YORK AND LONDON

227 West 17th Street
New York, New York 10011

Davis House
8 Scrubs Lane
Harlesden, NW10 6SE
England

Published monthly. Second-class postage paid at Jamaica, New York 11431.

SOVIET ATOMIC ENERGY

A translation of *Atomnaya Énergiya*
August, 1973

Volume 34, Number 2 February, 1973

CONTENTS

CONTENTS

(continued)

The Russian press date (podpisano k pechati) of this issue was 1/31/1973. Publication therefore did not occur prior to this date, but must be assumed to have taken place reasonably soon thereafter.

DISCRETE MONITORING OF THE POWER DISTRIBUTION IN THE ACTIVE ZONES OF NUCLEAR REACTORS

I. Ya. Emel'yanov, V. N. Vetyukov,
L. V. Konstantinov, V. G. Nazaryan,
I. K. Pavlov, and V. V. Postnikov

UDC 621.039.564.2

The achievement of precise and reliable monitoring of the power distribution in a reactor is a necessary condition for the economically effective and safe use of a powerful nuclear installation. At the present time it is a generally accepted practice to use sensors discretely sited within the active zone [1]. An analysis of signals arising from the sensors within the reactor by means of an information store and computer facilitates operative monitoring of the precritical thermal-loading reserve of every fuel element, and hence helps in optimizing the fields of energy evolution, with a view to increasing the power and heat-technological reliability of the reactor and also the mean integrated power development of the fuel charge.

Despite the fact that an optimization of the methods of mathematically analyzing discrete measurements of power distribution inside the reactor would provide a great increase in monitoring accuracy, and hence in the accessible power potential of the fuel (or the heat-technological reliability of the reactor), insufficient attention has as yet been paid to this problem in the literature.

In the present investigation we studied two methods of discretely monitoring the energy distribution: empirical and experimental – computing. The first method constitutes an engineer's solution of the problem, and is based on the use of simple empirical relationships obtained in experiments relating to the starting and initial period of use of the fundamental reactor of the type in question; the second method is based on the simultaneous use of the results of a physical calculation and discrete measurements of the power distribution. The use of both methods is illustrated by reference to the Beloyarsk Nuclear Power Station.

The empirical method of monitoring the power distribution W(r) is based on the concepts of a macroscopic field $W_M(r)$ and a field microstructure $\varphi(r)$ [1-3]. The problem of discrete monitoring in this case reduces to a determination of the values of the macrofield at the sensor sites:

TABLE 1. Comparison between Various Interpolation Methods

Interpolation procedure	Empirical method			Experimental–computer method		
	A	B	$\sigma^2_{W_I}$ (%)²	A	B	$\sigma^2_{V_I}$ (%)²
Plane interpolation	0,380	0,333	45,35	0,309	0,333	20,03
Method of least squares	0,398	0,258	47,36	0,345	0,258	22,11
Interpolation by Lagrange polynomials						
$m=1$, $N_s=4$	0,353	0,250	42,04	0,280	0,250	18,04
$m=3$, $N_s=16$	0,318	0,409	38,29	0,258	0,409	17,02
$m=5$, $N_s=36$	0,320	0,498	38,72	0,283	0,498	18,78
$m=7$, $N_s=64$	0,490	0,115	57,83	0,381	0,115	24,04
Statistical interpolation						
$n=N_s=4$	0,334	0,356	40,04	0,276	0,352	18,02
$n=N_s=16$	0,315	0,402	37,92	0,251	0,397	16,56
$n=N_s=36$	0,315	0,404	37,92	0,252	0,360	16,54

Translated from Atomnaya Énergiya, Vol. 34, No. 2, pp. 75-80, February, 1973. Original article submitted April 20, 1972; revision submitted August 28, 1972.

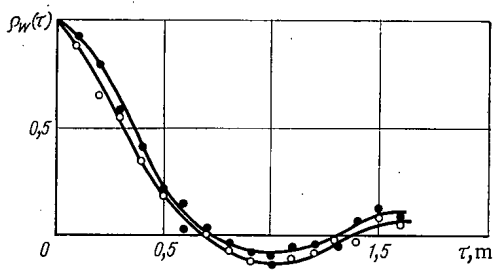

Fig. 1

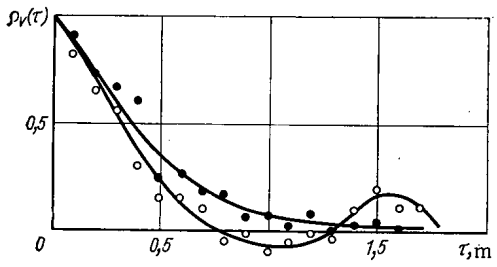

Fig. 2

Fig. 1. Relative correlation functions of the distribution $W^0_M(\mathbf{r})$ obtained by measurements in the reactor of the second unit of the Beloyarsk Nuclear Power Station, using small-scale fission chambers at "zero" power for the whole active zone (○) and for the central part of the latter (⊙).

Fig. 2. Relative correlation functions of the distribution $V^0(\mathbf{r})$ for the reactor in the second unit of the Beloyarsk Nuclear Power Station obtained by fission chambers at "zero" power (⊙) and derived from the residual activity of the fuel channels for the central part of the shut-down reactor (○).

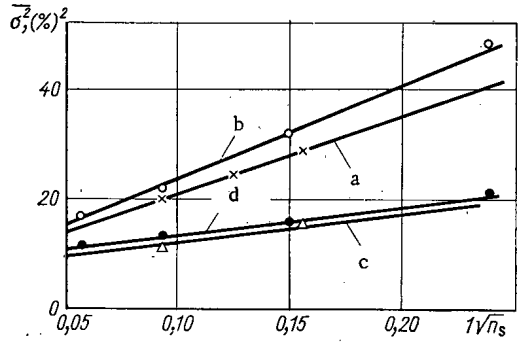

Fig. 3. Dependence of $\bar{\sigma}^2_{WI}$ and $\bar{\sigma}^2_{VI}$ on $1/\sqrt{n_s}$ for the reactor of the second unit in Beloyarsk Nuclear Power Station, obtained by the empirical (a, b) and experimental – computing (c, d) methods using Eq. (4) (a, c) and by direct calculation [4] (b, d) from the results of experiments at "zero" power.

$$W_M(\mathbf{r}) = \frac{W(\mathbf{r})}{\varphi(\mathbf{r})}, \qquad (1)$$

the interpolation of these values over the whole reactor, and the subsequent introduction of corrections allowing for the microstructure of the power distribution for every fuel element [3]. We note that the direct interpolation of the distribution $W(\mathbf{r})$ rather than $W_M(\mathbf{r})$ leads to a considerably greater error in monitoring the power distribution.

The $W_M(\mathbf{r})$ distribution may, in general, be formally considered as a nonuniform, random distribution with a varying mathematical expectancy, dispersion, etc., since in addition to the general variation in $W_M(\mathbf{r})$ due to the dimensions of the reactor and the averaged distribution of the fuel load and control units, there are also purely random deviations associated with technological scatter in the disposition of the fuel elements and absorption units, and also local quasirandom deviations associated with various localized inhomogeneities, which cannot be completely taken into account in the manner represented by Eq. (1). In view of all this, we employed the elementary concepts of the theory of random functions [4], in addition to other methods [2, 3], when choosing a method of interpolating the macrofield and analyzing the results obtained.

In order to avoid the difficulties arising from a direct interpolation of nonuniform random distributions, we used the operation of macrofield centering [5]

$$\overset{0}{W}_M(\mathbf{r}_s) = W_M(\mathbf{r}_s) - \tilde{W}_M(\mathbf{r}_s), \qquad (2)$$

where $\overset{0}{W}_M(\mathbf{r}_s)$ is the centered random distribution, $\tilde{W}_M(\mathbf{r}_s)$ is the mathematical expectancy of the macrofield, constituting the result of approximating the discretely measured distribution $W_M(\mathbf{r}_s)$.

By way of expressions approximating the values of $W_M(\mathbf{r}_s)$ in the sensor sites for the two-dimensional case, we considered a series of Bessel functions and trigonometrical functions, a polynomial of the second degree, and a unidimensional radial distribution, obtained by mathematical smoothing of the measured quantities. In the absence of sensors on the periphery of the reactor, $\tilde{W}_M(\mathbf{r})$ may be derived by "sewing together" the distribution in the central region and the distribution on the periphery of the active zone determined experimentally or by physical calculations.

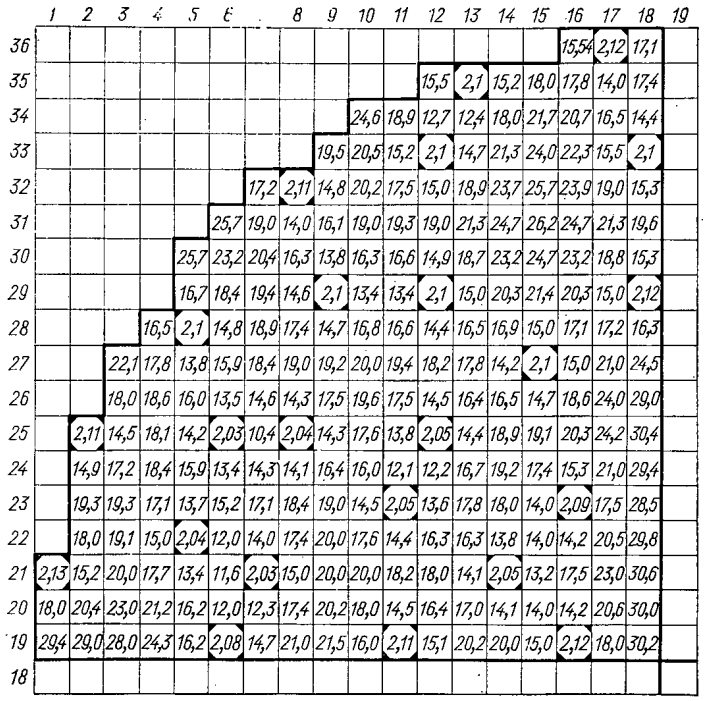

Fig. 4. Distribution of $\sigma^2(\%)^2$ with respect to the fuel channels of one quadrant of the active zone in the second unit of the Beloyarsk Nuclear Power Station (shaded corners indicate channels containing sensors).

The latter two means of approximation were the most convenient for the practical analysis of discrete measurements in a computer. It should be noted that the correctness of our choice of approximating expression may be confirmed by finding whether the discrete monitoring errors derived from correlation analysis agree (see Eq. (4)), and also by comparing the calculated and measured power distributions [3].

In accordance with (2), the unknown distribution of the macrofield over the reactor was determined as the sum of $\tilde{W}_M(\mathbf{r})$ and the interpolated distribution of $\overset{0}{W}_M(\mathbf{r})$.

Taking a square lattice of sensors as an example, we studied four methods of interpolating $\overset{0}{W}_M(\mathbf{r})$: 1) plane interpolation in which the value of $\overset{0}{W}_M$ is determined for each fuel channel as the z coordinate of the plane drawn through the values of $\overset{0}{W}_M(\mathbf{r})$ for the three nearest sensors; 2) successive approximation (by the method of least squares) of the values of $\overset{0}{W}_M(\mathbf{r})$ derived from sensors separated distances of no more thatn ~1/6 of the reactor diameter by a polynomial of the second degree; 3) successive interpolation along the x and y axes by Lagrange polynomials of degree m, equal to 1, 3, 5, 7; 4) statistical interpolation [4] based on the theory of random functions.

In a number of cases the interpolation indicated in 1)-3) may be carried out directly for the values of $W_M(\mathbf{r})$ without serious loss of accuracy, without first carrying out the centering operation.

The essence of the latter interpolation (proposed earlier [6] for unidimensional stationary random processes) lies in finding the unknown coefficients a_i of the interpolation series

$$\overset{0}{W}_M(\mathbf{r}) = \sum_{i=1}^{n} a_i \overset{0}{W}_{Mi}(\mathbf{r}_i) \qquad (3)$$

from the minimum interpolation error of the spatial distribution of $\overset{0}{W}_M(\mathbf{r})$. In Eq. (3), n is the order of interpolation, equal to the chosen number of neighboring sensors measuring the quantities $W_i(\mathbf{r})$ used in calculating $\overset{0}{W}_M(\mathbf{r})$.

The dispersion of the interpolation error for an arbitrary fuel channel may be expressed as the dispersion of a linear combination of random functions [6]:

$$\sigma^2_{W\cdot I} = A\sigma^2_W + B\sigma_S$$
$$A = 1 + \sum_{i=1}^{n}\sum_{j=1}^{n} a_i a_j \rho_{ij} - 2\sum_{i=1}^{n} a_i \rho_i; \qquad (4)$$
$$B = \sum_{i=1}^{n} a_i^2,$$

where σ^2_W is the dispersion of the random field $\overset{0}{W}_M$; σ^2_S is the dispersion of the sensor error $\rho_{ij} = K_W(|\mathbf{r}_i - \mathbf{r}_j|)/\sigma^2_W$ is the normalized value of the correlation function $K_W(|\mathbf{r}_i - \mathbf{r}_j|)$ of the random field $\overset{0}{W}_M(\mathbf{r})$

$$\rho_i = \frac{K_W(|\mathbf{r} - \mathbf{r}_i|)}{\sigma^2_W}.$$

Equating to zero the derivatives of σ^2_{WI} with respect to each of the coefficients a_i, we obtain a system of equations for finding the values of these:

$$\left.\begin{aligned}
(1 + \sigma_S^2/\sigma_W^2)\, a_1 + \rho_{12} a_2 + \ldots + \rho_{1n} a_n &= \rho_1;\\
\rho_{21} a_1 + (1 + \sigma_S^2/\sigma_W^2)\, a_2 + \ldots + \rho_{2n} a_n &= \rho_2;\\
\ldots\ldots\ldots\ldots\ldots\ldots\ldots\ldots\ldots\ldots\ldots\ldots\\
\rho_{n1} a_1 + \rho_{n2} a_2 + \ldots + (1 + \sigma_S^2/\sigma_W^2)\, a_n &= \rho_n.
\end{aligned}\right\} \qquad (5)$$

In Eq. (4) the errors of the sensors are regarded as mutally uncorrelated quantities, and the dispersion of the random field $\sigma^2_W = K_W(0)$ is taken as constant over the active zone. If the latter condition is not satisfied, it is essential to center $\overset{0}{W}_M(\mathbf{r})$ with respect to the dispersion [5].

The correlation functions $K_W(\tau)$ of the distribution of $\overset{0}{W}_M(\mathbf{r})$, like the coefficients characterizing the microstructure of the power distribution, may be obtained by experiments or physical calculations.

Figure 1 illustrates the relative correlation functions $\rho_W(\tau)$ for the centered power macrofield of the fuel channels in the reactor of the second unit of Beloyarsk Nuclear Power Station. The $\rho_W(\tau)$ curves determined for different parts of the reactor lie close to one another in the initial section (τ < 1.0-1.2 m), which is of practical interest in the processing of the discrete measurements. Calculations showed that in this case the coefficients a_i approached zero for $|\mathbf{r} - \mathbf{r}_i| > 1.2$-1.4 m. Thus the most appropriate order of statistical interpolation n is determined by the number of sensors lying within this distance of the fuel channels.

An advantage of statistical interpolation lies in the fact that exactly the same computing method may be used for both interpolation and extrapolation, as well as for refining the measurements at the sensor sites by reference to the readings of neighboring sensors.

The foregoing procedures for interpolating the centered macrofield on the empirical principle are compared in Table 1 for a fuel channel lying in the center of a rectangular lattice of N_S sensors, by comparing the values of σ^2_W calculated from Eq. (4) and $\rho_W(\mathbf{r})$ illustrated in Fig. 1.

The experimental – computing method of monitoring the power distribution is based (as in [7]) on determining a quantity $V(\mathbf{r})$ for each sensor, this being the ratio of the measured signal to the signal derived from a physical calculation of the neutron flux or power distribution. The relative distribution of $W(\mathbf{r})$ was determined as the product of the power distribution obtained from the physical calculation and the distribution of $V(\mathbf{r})$ [1, 4]. The absolute value of the power distribution was determined, as in the empirical method, by normalizing the relative distribution to the thermal power of the reactor.

In order to optimize the experimental – computing method, we studied various ways of interpolating the distribution $V(\mathbf{r})$. An analysis of many calculated and experimental power distribution showed that $\overset{0}{V}(\mathbf{r}) = V(\mathbf{r}) - \overline{V}(\mathbf{r})$ might be considered as a homogeneous random distribution. The relative correlation functions

$\rho_V(\tau) = K_V(\tau)/K_V(0)$ of the distribution $\overset{0}{V}(\mathbf{r})$ shown in Fig. 2, corresponding to two different states of the reactor in the second unit of the Beloyarsk Nuclear Power Station, are similar to one another in the range $\tau < 0.5$ m.

It should be noted that the distances τ at which the correlation functions of the radial – azimuthal distributions of $\overset{0}{W}_M(\mathbf{r})$ and $\overset{0}{V}(\mathbf{r})$ fall by a factor of two are practically identical, and amount to 0.08–0.1 of the radius of the active zone for the Beloyarsk reactors. This is evidently associated with the fact that the relative ranges of propagation of the distortions introduced into the power distribution by random local perturbations in the active zones of these reactors are identical.

The results of our investigation into the four methods of interpolating the $V(\mathbf{r})$ distribution under the conditions indicated when considering the empirical method are shown in Table 1. The values of σ^2_V were calculated from (4) using the correlation function of Fig. 2. The tabulated values of the mean square errors σ_{WI} and σ_{VI} for the various methods of interpolation and the values of A and B for statistical interpolation correspond to $\sigma_s = 1.5\%$; $\sigma_W = 10.8\%$ and $\sigma_V = 7.9\%$.

It follows from an analysis of the tabulated data that the best accuracy is given by statistical interpolation in both the empirical and the experimental – computing methods. The latter method gives a smaller error in discrete monitoring as compared with the empirical, but it requires regular physical calculations of the power distribution on a fairly powerful (usually external) electronic computer. The frequency of these calculations may be reduced with the aid of the station's own computer by introducing corrections based on Eqs. (1) and (2) to allow for slight changes in the positions of the control devices and the charging of the reactor.

A reliable estimation of the error committed in the discrete monitoring of the power distribution during the service life of the reactor is of particular importance for choosing safe and efficient operating conditions for the fuel channels.

In order to verify the validity of the method of estimating the monitoring accuracy, we compared the values of $\overline{\sigma^2}$ averaged over the reactor obtained in accordance with (4) and by comparing [3] the interpolated and measured values (Fig. 3). The dependence of $\overline{\sigma^2}$ on $1\sqrt{n_s}$, which is proportional to the spacing in the lattice of n_s sensors uniformly distributed in the reactor of the second unit of the Beloyarsk Nuclear Power Station, is closely described by the linear relationship generally characteristic of such cases. The results of Fig. 3 demonstrate the satisfactory accuracy of the method of computing σ based on Eq. (4).

It should be noted that the results of Figs. 3 and 4 and Table 1 correspond to measurements of the power of individual fuel elements in the fuel channels made during the physical initiation period, using a charge of considerable inhomogeneity. During actual serivce, the errors in the two methods were in general 1.5–2.0 times lower for the fuel channels.

As an example of the calculation of σ for individual fuel channels, Figure 4 illustrates the distribution of σ^2_{WI} over part of the active zone of the reactor in the second unit of the Beloyarsk Nuclear Power Station, corresponding to statistical interpolation in the empirical method.

A comparison of the experimental and calculated values shows that the error in the discrete monitoring obeys a normal distribution law.

The reliability which is essential for the discrete monitoring of the power distribution can only be achieved if measures are taken to eliminate coarse errors (faults or oversights) in the measurements and general (systematic) failures associated with maladjustments of the sensors, breakdown of the computer, operator errors, etc. The power distribution should therefore be monitored by at least two different methods. Mistakes in measurements committed in, for example, the Beloyarsk Nuclear Power Station, may then be revealed by applying statistical "unacceptability" criteria to the relative differences in the distributions obtained by the different methods and analyzing these on a computer. In the same way, it is desirable to compare $\overset{0}{V}(\mathbf{r})$ or $\overset{0}{W}(\mathbf{r})$ over a specific range, and at the symmetrical points of the active zone, and also to compare analogous quantities measured at a specific point over a certain time interval.

The methods of discrete monitoring of multidimensional distributions considered in this paper are intended for use in conjuction with the algorithms fed into the information and computing equipment of the Nuclear Power Station in order to monitor the power distribution. However, after making certain slight

changes, these methods may also be used for other problems of discrete measurements (for example, in determining the temperature fields in the reactor, radiation fields and spectra in the biological shielding, and so on).

In conclusion, the authors wish to thank I. S. Akimov for the results of the physical calculations relating to the Beloyarsk Nuclear Power Station and also M. P. Bodrilin, Yu. I. Volod'ko, and V. O. Steklov for help in the measurements.

LITERATURE CITED

1. I. Ya. Emel'yanov et al., At. Energ., 30, 275 (1971).
2. B. G. Dubovskii et al., International Conference on Physical Problems in the Design of Thermal Reactors, London, June (1967).
3. I. Ya. Emel'yanov et al., At Energ., 30, 422 (1971).
4. I. Ya. Emel'yanov, L. V. Konstantinov, and V. V. Postnikov, Transactions of a Conference of International Atomic-Energy Agency Experts, IAEA-119 (1969).
5. E. S. Wentzel, Theory of Probabilities [Russian translation], Nauka, Moscow (1964).
6. Yu. L. Rozov et al., Avtometriya, No. 5, 7 (1968).
7. W. Legget, Trans. ANS, 9, 484 (1966).

DEPOSITS ON VK-50 FUEL ELEMENTS

A. I. Zabelin, B. V. Pshenichnikov,
and T. S. Svyatysheva

UDC 621.039.524.4-97:621.03.955.336

The VK-50 water-cooled water-moderated pressure-vessel boiling-water reactor incorporates a cylindrical pressure vessel with a removable cover. The pressure vessel and the cover are hardfaced with 1Kh18N9T austenitic steel. The in-core operating pressure is 70-100 kg/cm^2.

The core fuel volume, also known as the small core, consists of 91 fuel assemblies. The natural coolant circulation speed while the fuel assembly is present in the core was 0.5 m/sec. The mean irradiation level of the core was 36 kW/liter.

The character of the deposits depends on the heat-transfer and hydrodynamical operating conditions of the fuel assemblies, and on the composition of impurities in the coolant. The latter are in turn a function of the water – chemical conditions and of the stability of the structural materials against corrosion and erosion. The contact area presented by the structural materials to the coolant is cited below (in percentage of total areas):

Brass (L-68)	52.1
Carbon steel (St. 3, St. 20, St. 22^k)	39.1
Stainless steels (1Kh18N9T, 1Kh13, 3Kh13)	5.6
Zirconium alloys	3.2

The corrosion rate and the yield of corrosion products affecting the coolant both depend on the quality of the coolant (see Table 1). Corrosion products, upon leaving the surface of the corroding materials and entering the coolant stream, become activated in the reactor core and migrate through the loop.

This article cites some of the results obtained in studies of deposits formed on the surface of a fuel element that had seen 155 effective full days of service in core from the start of the reactor campaign. The exposure time involved was longer than ten months.

Sampling and Sample Analysis Procedure

Visual inspection of the surface of the fuel element revealed that the fuel element becomes coated with a reddish-brown film composed of corrosion products. At a distance of 1 m from the top of the fuel element, we find a white incrustation breaking through at sites where the top film cover is impaired.

TABLE 1. Basic Criteria for Water – Chemical Conditions

Physicochemical variables	Coolant		
	feed-water	reactor loop water	reactor loop steam
pH value	8,3	9,5	—
Dissolved oxygen, mg/kg	0,05	0,20	30,00
Total amount of corrosion products, mg/kg	0,50	1,00	0,05

Five samples scraped off the surface of the fuel element were found to be flaky formations which were sparingly soluble in acids even after heating. The chemical composition of the deposits was determined on the basis of standard physicochemical procedures of analysis.

These samples were also subjected to γ-ray spectrometric analysis. The detector employed was a FEU-56

Translated from Atomnaya Énergiya, Vol. 34, No. 2, pp. 81-84, February, 1973. Original article submitted May 4, 1972.

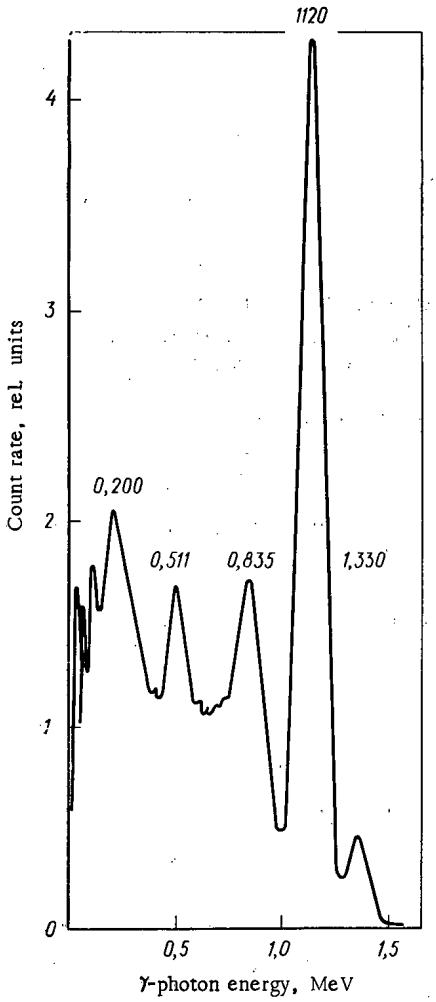

Fig. 1

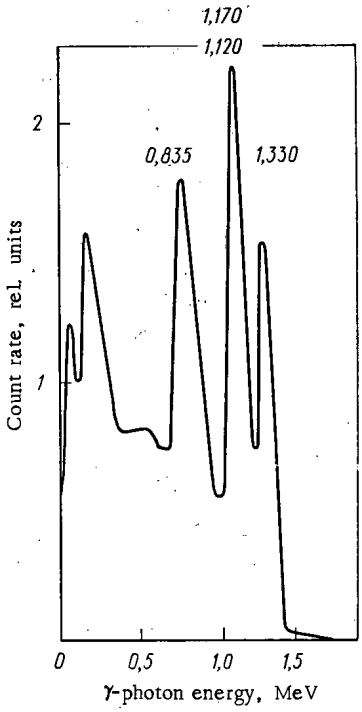

Fig. 2

Fig. 1. Typical γ-ray spectrum of deposits on VK-50 fuel elements.

Fig. 2. γ-Ray spectrum of deposits on VK-50 fuel elements (zinc-depleted sample).

photomultiplier with a NaI(Tl) 70 × 70 mm crystal. Pulses from the detector were amplified by a quantity-manufactured UIS-2 broadbanded amplifier and were placed across the input of an AI-256 multichannel pulse height analyzer. The γ-ray spectra obtained on the multichannel analyzer were recorded by a BZ-15 digital printout and by an EPP-09 automatic electronic potentiometric recorder.

The spectrometer resolution was 10% at the Cs^{137} γ-line (0.661 MeV). The FEU-56 photomultiplier was supplied from a type VS-22 quantity-manufactured stabilized voltage power supplies package. Fluctuations of the output voltage from ratings were not greater than 0.01% in response to 10% changes in line voltage or power supplies voltage.

Four peaks are clearly in evidence in γ-ray spectrum shown in Fig. 1, in the energy range beyond 0.2 MeV: 0.511, 0.835, 1.120, and 1.330 MeV. Those peaks can be interpreted as photopeaks due to γ-photons emitted by Mn^{54} (0.834 MeV), Zn^{65} (1.120 MeV), and Co^{60} (1.330 MeV), with the 0.511 MeV peak considered an outlier. This last peak is identified as the photopeak of annihilation radiation of positrons formed in the decay of the nuclide Zn^{65}. Consequently, gamma-ray spectrometry of the specimens made it possible to determine the presence of the radioactive isotopes Mn^{54}, Zn^{65}, and Co^{60} in the deposits on the fuel elements.

The isotopes Na^{22}, Fe^{59}, Co^{58}, and Zr^{95} + Nb^{95} were also detectable in the deposits. But photopeaks due to the γ-photons emitted by Na^{22} (1.277 MeV), Fe^{59} (1.289 and 1.098 MeV), and Co^{60} (1.170 MeV) lie in the region of the photopeak due to γ-photons emitted by Zn^{65} (1.120 MeV) and Co^{60} (1.330 MeV). The

TABLE 2. Averaged Content of Elements in Deposits of Corrosion Products on Fuel Element

Chemical composition of deposits		Sources of origin	
element	content, wt.%	reactor loop facilities and equipment	structural materials
Iron	39,0	Turbine condensers, condenser piping, deaerators, feedwater lines, steam piping, turbine	Carbon steel (St. 3, St. 20, St. 22k)
Manganese Nickel Chromium	5,0 0,5 0,2	In-pile surfaces, HPS* steam lines, feedwater header, louvered control devices in HPS and LPS† systems, evaporation plant. steam turbine buckets, scramming and control system screws	Stainless steel (1Kh18N9T, and (0Kh18N10T) and chromium steel (1Kh13 and 3Kh13)
Copper Zinc	35,0 20,0	Piping system of turbine condensers and LPH‡	Brass (L-68)
Cobalt	$\ll$ 0,1	Thrust bearings of feedwater pumps, hardfacing of third and fourth stages of turbine low-pressure cylinder	Stellite (45-50% Co) and T15K6 alloy (6% Co)

*High-pressure steam separators.

†Low-pressure steam separators.

‡Low-pressure heaters.

TABLE 3. Relationship of Radioisotopes in Deposits on Fuel Elements (%)

Radioisotope	Relative activity*
Mn^{54}	2,5±0,4
Zn^{65}	92,0±3,7
Co^{60}	5,1±0,4

*Averaged from five samples

maximum in the spectrum of Compton electrons due to Zn^{65} γ-photons, and the photopeaks due to the γ-photons emitted by Co^{58} (0.805 and 0.814 MeV) and by $Zr^{95} + Nb^{95}$ (0.756, 0.723, and 0.768 MeV) are found in the region of the Mn^{54} (0.835 MeV) photopeak. Control experiments were staged in order to ascertain whether nuclides, of which the photopeaks might be masked by strong lines, were also present.

A weighed aliquot of the sample scraped off the outer surface of fuel elements was fused with a fivefold excess of potassium hydrogen sulfate ($KHSO_4$) in a muffle furnace at temperatures 900-950°C. The resulting amalgam or alloy was dissolved in 20% hydrochloric acid upon heating, and was diluted with desalinated water. The solution resulting was then passed down a chromatographic column, and mixtures of isotopes or individual isotopes were isolated with the aid of radiochemical techniques.

Filter paper moistened in appropriately prepared solutions was sealed in a polyethylene packet, and the γ-ray spectrum of the sample was then taken.

The spectrum of a zinc-depleted sample is shown in Fig. 2. It is clear from a comparison of the γ-ray spectrum so obtained and the primary spectrum (see Fig. 1) that the intensity of the Zn^{65} photopeak decreased appreciably, while the Co^{60} photopeak (1.330 MeV) gained in intensity. Because of the decline in the annihilation radiation peak, a peak began to show up in the vicinity of 0.6 MeV, as the maximum in the spectrum of Compton electrons due to the 0.835 MeV γ-photons. It is clear in Fig. 2 that no new γ-lines were detected in the spectrum.

Sodium is then isolated by chemical means from the zinc-depleted sample obtained in the preceding control experiment. The γ-ray spectrum of the sample depleted of zinc and sodium does not differ from that of the sample depleted of zinc alone. In order to check for the presence of Na^{22} and Fe^{59} in the sample, we ran repeat tests to determine the content of those isotopes, using independent methods. Cobalt was isolated from the working sample. Manganese was isolated along with the cobalt. The resulting γ-ray spectrum of the sample now coincided with that of pure Zn^{65}. Filtrates from the same samples were tested as an additional check. No new γ-emission lines were detected in the spectrum.

The relationship between radioisotopes present in the deposits bulit up on the fuel elements was specific for each power station tested, and depends on the structural materials used [1].

Discussion of Results of Measurements

Elements traceable to corrosion and erosion in the stream (iron, manganese, chromium, nickel, copper, zinc) or to naturally occurring impurities in the water (calcium, magnesium, silicon) were found in aliquot volumes of solutions of five samples scraped off the surfaces of the fuel elements.

It is clear from Table 2 that the deposits consist primarily of compounds of iron (39%), copper (35%), and zinc (20%). Manganese is represented much less conspicuously in the deposits, and there is very little nickel or chromium present. Considerable quantities of zirconium and niobium (elements found in corrosion products of the fuel-element cladding) were not detected.

Table 3 displays the relationship between the activities of corrosion products incorporating the isotopes Zn^{65}, Mn^{54}, and Co^{60}, all calculated for the time of reactor shutdown. As pointed out earlier, the fuel element under investigation was kept for over ten months in the cooling pond. During that time, the activity of all of the other isotopes decreased to such an extent that the photopeaks associated with the γ-photons they emitted were masked by far more intense γ-lines (mainly those due to Zn^{65}). One curious fact is the level of over 90% activity of the samples attributable to γ-emission by Zn^{65}, a nuclide formed in the reaction $Zn^{64}(n, \gamma)Zn^{65}$ (abundance 48.89%). We can infer from those data that brass should be avoided as a structural material in a power station loop, in the case of a single-loop system of the type selected for the VK-50 reactor power station, in order to improve the radiation situation.

The isotope Mn^{54} is formed principally in a (n, p) reaction, from the isotope Fe^{54} (abundance 5.81%) [2], and to a much lesser extent in a (n, 2n) reaction from the isotope Mn^{55} (abundance 100%). The activity of Mn^{54} is therefore proportional to the concentration of iron corrosion products. The isotope Co^{60} is formed primarily through the reactions $Co^{50}(n, \gamma)Co^{60}$ (abundance 100%) and $Ni^{60}(n, p)Co^{60}$ (abundance 26.16%). Since no cobalt was detected through chemical analysis of the samples, it may be surmised that the isotope Co^{60} owes its origin here principally to the second reaction, from the nickel.

CONCLUSIONS

1. Nuclear electric power generating stations based around a VK-50 reactor differ from other power stations based around boiling-water reactors in the typically high content of copper and zinc compounds in the deposits, on account of the brass used in the turbine condenser and in the low-pressure heater on stream in the primary loop.

2. The principal component of the deposits on the fuel element, responsible for ~90% of the long-lived isotope, is the isotope Zn^{65}.

3. Despite the very limited dimensions of the stainless steel surfaces, some Co^{60} was nevertheless detected in the deposits.

LITERATURE CITED

1. V. P. Pogodin (editor), Corrosion of Structural Materials in Water-Cooled Reactors [in Russian], Atomizdat, Moscow (1965).
2. I. P. Selinov, The Nuclides (Reference Tables) [in Russian], Nauka, Moscow (1970).

SOME PHYSICAL AND MECHANICAL PROPERTIES OF URANIUM – ZIRCONIUM ALLOYS AT LOW TEMPERATURES

G. B. Fedorov, M. T. Zuev,
E. A. Smirnov, and A. E. Kissil'

UDC 537.311.31:669.822:539.67

Earlier investigations into the thermodynamic [1] and diffusion [1, 2] properties as well as the specific heat [3] of uranium – zirconium alloys at high temperatures have shown that the extrema appearing on the concentration dependences of these properties lie in a range of compositions which, at lower temperatures, correspond to the δ_1 phase [4]. In this range of compositions (22-35 at. % uranium*) the integrated thermodynamic functions (molar free energy and molar enthalpy) exhibit their maximum negative deviations from ideal behavior [1], while the specific heat exhibits its maximum deviations from the Neuman and Kopp rule [3]; the mutual diffusion coefficients pass through a minimum and the activation energy reaches a maximum [1, 2]. Further analysis of the results of [3] in relation to the specific heat of uranium – zirconium alloys showed that, even at room temperature, there was a slight deviation from the additivity law, with a maximum in the region of the δ_1 phase.

In this paper we shall present the results of a fresh study of certain physical properties of uranium – zirconium alloys at room and negative temperatures. We examined the following properties: specific electrical resistance (resistivity), integrated low-temperature thermo-emf, internal friction, Young's modulus, and hardness.

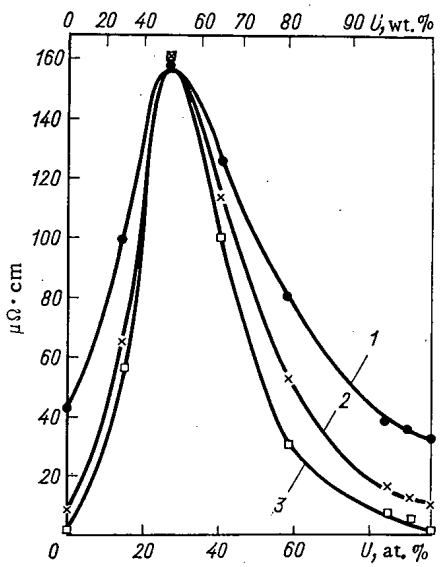

Fig. 1. Concentration dependence of the resistivity of uranium – zirconium alloys at temperatures of: 1) 295°K; 2) 77.4°K; 3) 4.2°K.

Alloys and Method of Investigation. We studied samples of pure zirconium and uranium as well as alloys of these containing (according to measurements of the charge) 14.1; 27.7; 41.6; 60.5; 87.9 and 94 at. % of uranium. The method of preparation and the dimensions of the samples were analogous to those described in [3]. The samples were studied in the annealed state (being first held in a dynamic oil vacuum of 3.10^{-4} mm Hg at 1000°C and then cooled slowly).

The electrical resistance was measured at room temperature, T_r = (295 ± 3)°K, in liquid nitrogen at T_n = (77.4 ± 0.7)°K, and in liquid helium at T_h = (4.22 ± 0.02)°K by a four-contact potentiometric method, with two directions of the low-density current (0.1 A/cm^2). In calculating the resistivity at low temperatures, the geometry of the samples was taken to be exactly the same in each case.

The low-temperature thermo-emf was determined [9] relative to copper, using a constant temperatue gradient $\Delta T = T_r - T_n$ = (216 ± 5), and also by using the recording of a preamplified signal.

*According to other investigations, the range of compositions corresponding to this phase (denoted in different ways by different authors) extends from ~26.6 to ~33.4 [5], from 24.5-25 to ~31.5 [6], or from ~24.5 to 29.5-30 at. % uranium [7, 8].

Translated from Atomnaya Énergiya, Vol. 34, No. 2, pp. 85-88, February, 1973. Original article submitted December 30, 1971.

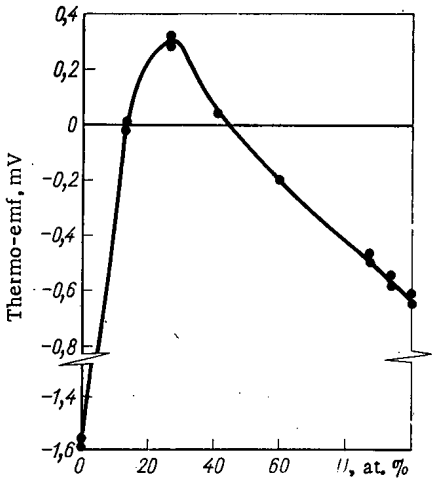

Fig. 2

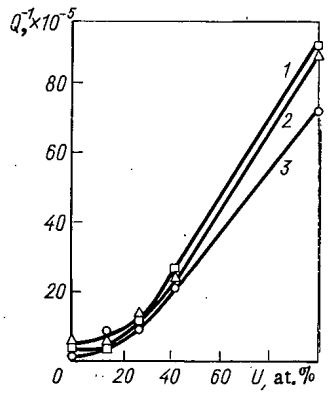

Fig. 3

Fig. 2. Dependence of the integrated thermo-emf of uranium – zirconium alloys (ΔT = 216°K) on the uranium concentration.

Fig. 3. Dependence of the background of the internal friction on the composition of uranium – zirconium alloys at temperatures: 1) 273°K; 2) 173°K; 3) 77.4°K.

The elastic modulus and internal friction at temperatures between T_n and T_r were determined by a method based on resonance bending vibrations at a frequency of ~1 KHz [10]. The hardness was measured in a Rockwell apparatus with a load of 100 kg. At least ten measurements were made with each sample.

Electrical Resistance. The concentration dependence of the resistivity (Fig. 1) at room, nitrogen, and helium temperatures has a maximum in the range of alloys containing 22-35 at.% uranium, i.e., in the range of the δ_1 phase; the single-phase (δ_1 phase) alloy of zirconium with 27.7 at.% of uranium has not only the highest resistivity among all the alloys studied but also an anomalous temperature dependence of its electrical resistance (as compared with other metals), in that it rises with falling temperature: ρ_r = 159.5; ρ_n = 162.3; ρ_h = 163.4 $\mu\Omega \cdot$ cm. In the two-phase regions ($\alpha_{Zr} + \delta_1$ and $\delta_1 + \alpha_U$) the resistivity of the alloys varies with composition in a manner corresponding to almost hyperbolic curves; the resistance increases with increasing proportion of the δ_1 phase. The two-phase alloys have a normal (positive) temperature coefficient of electrical resistance, diminishing with increasing amount of the δ_1 phase. Measurements at 4.2°K showed (Fig. 1) that the equilibrium alloys of the uranium–zirconium system were not superconducting.

The results of our present measurements of the resistivity of uranium – zirconium alloys at room temperature agree closely with our earlier results obtained with samples annealed at 580°C for 500 h [3] and also with the results of [4] relating to samples annealed at 500°C for 1000 h.

A study of the electrical resistance, of zirconium alloys containing 26 and 30 at.% uranium [11] showed that the δ-phase of these alloys had a negative temperature coefficient of electrical resistance in the temperature range 90-870°K. There are no data regarding the resistivity of binary uranium – zirconium alloys at very low (under 90°K) temperatures.

Thermo-emf. The curve relating the low-temperature integrated thermo-emf to composition (Fig. 2) is analogous to that representing the electrical resistance: the maximum thermo-emf also corresponds to the region of the δ_1-phase; alloys containing a large proportion of the δ_1-phase have a thermo-emf with a sign differing from that of the original components. Since $\varepsilon \approx (k/e)\Delta T \ln(n_1/n_2)$ (where k is Boltzmann's constant, e is the charge on the electron, ΔT is the temperature gradient, n_1 and n_2 are the numbers of conduction electrons in unit volumes of the metals in contact), the change in the sign of the thermo-emf means, in particular, a change in the concentration of conduction electrons in the alloy under consideration.

Internal Friction. There are no sharp peaks on the temperature dependence of the internal friction of uranium, zirconium, or zirconium alloys containing 14.1; 27.7, and 41.6 at.% uranium (these being the

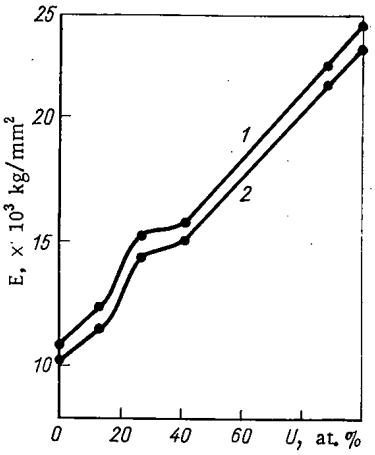

Fig. 4

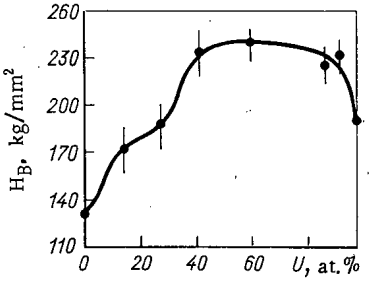

Fig. 5

Fig. 4. Elastic modulus of uranium – zirconium alloys at temperatures: 1) 77.4°K; 2) 295°K.

Fig. 5. Dependence of the hardness on the composition of uranium – zirconium alloys (T = 295°K).

only alloys so studied) between T_n and T_r; however, the background of the internal friction depends very considerably on the composition of the alloy at both low and room temperatures. We see from the curves relating the internal-friction background to the uranium content (Fig. 3) for three temperatures (77.4; 173, and 273°K) that the greatest deviation (in the sense of a reduction) from the law of additivity among all the alloys studied always occurs for those containing 27.7 at.% of uranium, i.e., in the region of the δ_1 phase.

Young's Modulus. On measuring the elastic modulus at 293 and 77.4°K we also found a slight deviation from the law of additivity in the sense of an increase in the Young's modulus of the alloy corresponding in composition to the δ_1-phase (Fig. 4).

Hardness. The curve relating the hardness of uranium – zirconium alloys to composition (Fig. 5) has no sharply-expressed peaks. A flat hardness maximum occurs for alloys containing 40-90 at.% uranium; in the region of the δ_1 phase there is a slight deviation of the hardness values from the smooth curve (in the sense of a reduction), in agreement with the data of [4].

On the basis of the foregoing results we may draw certain conclusions regarding the nature of the chemical bond in the δ_1 phase of uranium – zirconium alloys. This phase cannot be regarded as belonging to the class of ordering solid solutions. The increase in the electrical resistance and the slight reduction in the hardness of annealed δ_1 alloys testify to the accuracy of this assertion.

The high resistivity, the change in the sign of the thermo-emf, and the anomalous (for metals) temperature coefficient of electrical resistance (the slight semiconducting behavior of the conductivity at low temperatures) indicate that some of the electrons in the δ_1 phase are bound. A reduction in the number of free electrons is possible when stronger directional bonds are created. The thermodynamic and diffusion characteristics of uranium – zirconium alloys [1-3] in fact indicate an increase in the strength of the interatomic bond in the δ_1 phase as compared with solid solutions based on uranium and zirconium. This is also indicated by the reduction in the background of internal friction (Fig. 3) and a slight increase in elastic modulus (Fig. 4) in the δ_1 phase relative to the additive law.

Since the appearance of an ionic component is of low probability, owing to the very slight difference between the electronegativities of uranium and zirconium, we may reasonably assume that the interaction between the components in the δ_1 phase is characterized by a mixed metallic – covalent rather than a purely metallic type of chemical bond. When covalent bonds are formed, the concentration of the conduction electrons diminishes and may even pass into the range of "semiconducting" concentrations, which leads to a considerable increase in the resistivity and a change in the sign of the thermo-emf as compared with the original components. It was indicated earlier [12] that compounds with a mixed type of chemical bond were often semiconductors.

Our conclusion as to the existence of a metallic – covalent type of chemical bond in the δ_1 phase of uranium – zirconium alloys in no way contradicts the physical nature of the uranium, for which covalent bonds are quite typical [13], nor the assumption as to the partly ordered, layer-like structure of the δ_1 phase [14-16], since covalent bounds may arise for a partly ordered disposition of the atoms in the crystal lattice. This conclusion is also in accord with the results obtained at high temperatures (outside the range of existence of the δ_1 phase) [1-3], since the extrema there observed on the concentration dependences of the physical properties may be explained by the fact that the rupture of the covalent bonds and the disruption of the partial order take place gradually over a wide range of temperatures.

LITERATURE CITED

1. G. B. Fedorov and E. A. Smirnov, At. Energ., 21, No. 3, 189 (1966).
2. G. B. Fedorov, E. A. Smirnov, and F. I. Zhomov, in Metallurgy and Metallography of Pure Metals, No. 7 [in Russian], Atomizdat, Moscow (1968), p. 116.
3. G. B. Fedorov and E. A. Smirnov, At. Energ., 25, No. 1, 54 (1968).
4. O. S. Ivanov and G. N. Bagrov, in: Structure of Alloys Belonging to Certain Systems Including Uranium and Thorium [in Russian], Gosatomizdat, Moscow (1961), p. 5.
5. J. Duffey and C. A. Bruch, Trans. AIME, 212, 17 (1958).
6. H. Saller and F. Rough, Nucl. Engng., Pt. 1, 56 (1954); Metallurgy of Zirconium [Russian translation], IL, Moscow (1959), p. 269.
7. H. Saller, Second Nucl. Eng. and Sci. Conf. Paper 57-NESC-20 (1957); At. Energ., 3, No. 8, 176 (1957).
8. V. I. Kutaitsev, Alloys of Thorium, Uranium, and Plutonium [in Russian], Gosatomizdat, Moscow (1962), p. 130.
9. M. T. Zuev, Yu. F. Bychkov, and A. N. Rozanov, in: Metallurgy and Metallography of Pure Metals, No. VI [in Russian], Atomizdat, Moscow (1967), p. 75.
10. G. F. Feforov, ibid., p. 68.
11. R. D. Barnard, Pro. Phys. Soc., 78, No. 503, 722 (1961).
12. B. G. Livshits, Physical Properties of Metals and Alloys [in Russian], Mashgiz, Moscow (1959), p. 215.
13. A. N. Holden, Physical Metallurgy of Uranium [Russian translation], Metallurgizdat, Moscow (1962), p. 38.
14. E. Boyko, Acta Cryst., 10, 712 (1957).
15. J. Silcock, Trans. AIME, 209, 521 (1957).
16. Yu. N. Sokurskii, A. Ya. Sterlin, and V. A. Fedorchenko, Uranium and Its Alloys [in Russian], Atomizdat, Moscow (1971), p. 215.

PHASE STRUCTURE OF NIOBIUM-BASED ALLOYS IN THE SYSTEM NIOBIUM — TUNGSTEN — ZIRCONIUM — CARBON

E. M. Savitskii and K. N. Ivanova

UDC 669.293.5

The phase diagram of the system niobium — tungsten — zirconium — carbon has been insufficiently investigated, although the corresponding ternary systems niobium — tungsten — zirconium [1], niobium — tungsten — carbon [2] and niobium — zirconium — carbon [2-5] have been fairly thoroughly researched. However, data on the phase structure of multicomponent niobium alloys containing zirconium (titanium or hafnium), carbon, and up to 30 wt.% tungsten are fragmentary [6, 7] and often based on assumptions.

The system niobium — tungsten — zirconium — carbon is one of the most promising for obtaining high-strength niobium-based alloys with precipitation hardening, which are capable of withstanding considerable stresses at high temperatures. In alloys of this system, solid-solution and carbide hardening can be successfully combined.

We have investigated the phase structure of alloys of the system niobium — tungsten — zirconium — carbon, rich in niobium and containing up to 4 at.% zirconium and 2 at.% carbon (alloys of the cross section with a constant tungsten content of 10 at.% (18 wt.%) were investigated). The solubility of carbon in niobium-based alloys was determined at 1800°C, which is one of the most probable temperatures of strengthening heat treatment of such alloys with precipitation hardening.

TABLE 1. Composition of Niobium-Based Alloys of the System Niobium — Tungsten — Zirconium — Carbon

Admixture							
zirconium		carbon		zirconium		carbon	
at.%	wt.%	at.%	wt.%	at.%	wt.%	at.%	wt.%
0,5	0,46	—	—	1,5	1,34	0,4	0,047
1	0,92	—	—	2,5	2,24	0,4	0,047
1,5	1,35	—	—	0,5	0,45	0,65	0,077
2,5	2,24	—	—	1,0	0,89	0,65	0,077
4,0	3,57	—	—	1,5	1,34	0,65	0,076
—	—	0,2	0,023	2,5	2,4	0,65	0,076
—	—	0,4	0,047	4,0	3,59	0,65	0,076
—	—	0,65	0,077	0,5	0,45	1,0	0,118
—	—	1,0	0,118	1,0	0,90	1,0	0,119
—	—	1,5	0,179	1,5	1,35	1,0	0,119
—	—	2,0	0,23	2,5	2,25	1,0	0,119
0,5	0,44	0,2	0,023	4,0	3,60	1,0	0,119
1,0	0,89	0,2	0,023	1,0	0,9	1,5	0,179
1,5	1,34	0,2	0,023	2,5	2,26	1,5	0,178
2,5	2,22	0,2	0,023	4,0	3,62	1,5	0,178
4,0	3,58	0,2	0,023	1,0	0,90	2,0	0,23
0,5	0,44	0,4	0,047	2,5	2,27	2,0	0,23
1,0	0,89	0,4	0,047	4,0	3,63	2,0	0,23

Note. The tungsten content was constant in all the alloys, namely 10 at.% (18 wt.%).

EXPERIMENTAL METHOD

To study the phase regions of the investigated sector of the phase diagram of the system niobium — tungsten — zirconium — carbon we used the microscopic method, together with color etching, and x-ray analysis (phase analysis and determination of the lattice constant); the hardness and microhardness were also measured.

Weighed amounts (60 g) of the alloys were melted in an arc furnace with a nonconsumable tungsten electrode in an inert atmosphere (purified helium) at 400 torr. To obtain a uniform composition, the bars were inverted five times. The initial materials were niobium, obtained by electron-beam melting (0.005% oxygen, 0.013% nitrogen, 0.015% carbon, and 0.009% hydrogen), zirconium iodide, cermet tungsten, and spectrally pure carbon. Table 1 gives the compositions of the alloys. Most of the alloys were subjected to chemical analysis; this revealed close agreement between the alloy composition and the calculated values. Alloys not doped with carbon contained a small amount of carbon (0.015-0.02 wt.%), which originated from the initial niobium.

Translated from Atomnaya Énergiya, Vol. 34, No. 2, pp. 89-92, February, 1973. Original article submitted February 16, 1972.

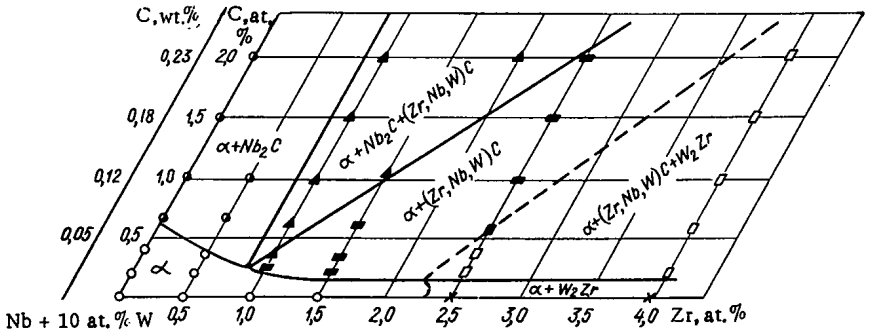

Fig. 1. Isothermal cross section at 1800°C of the niobium vertex of the system niobium – tungsten – zirconium – carbon.

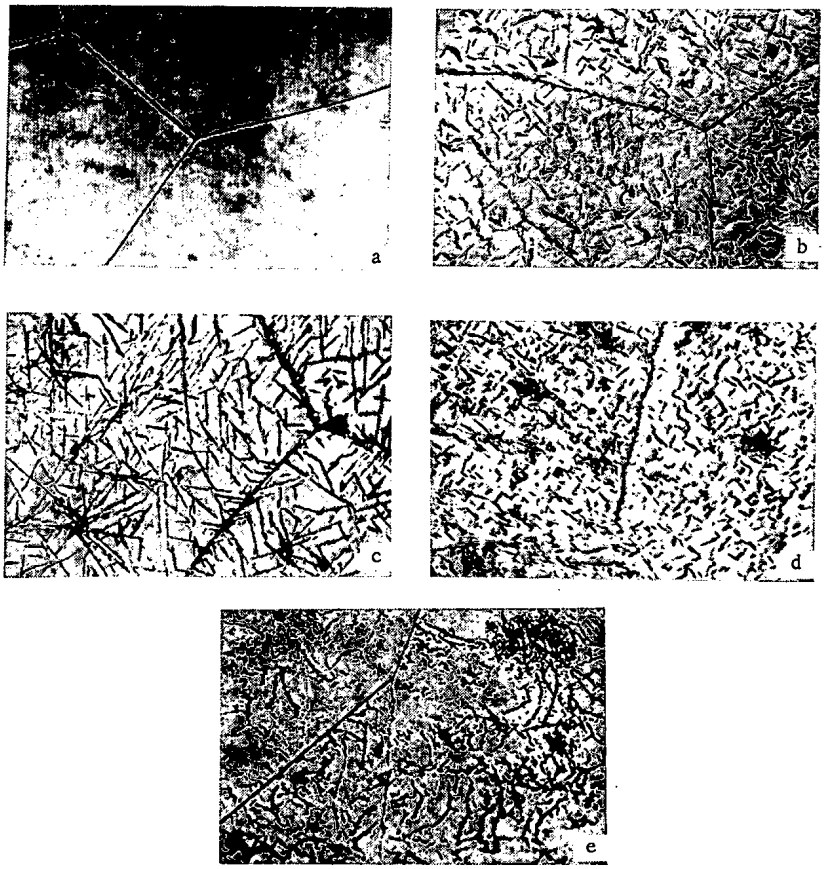

Fig. 2. Microstructure of alloys quenched at 1800°C (× 500): a) Nb – 0.2 at.% C – 10 at.% W(α-solid soln.); b) Nb – 0.6 at.% C – 10 at.% W(α-solid soln. + Nb_2C); c) Nb – 1.5 at.% C – 10 at.% W(α-solid soln. + Nb_2C); d) Nb – 0.5 at.% Zr – 1 at.% C – 10 at.% W(α-solid soln. + Nb_2C); e) Nb – 4 at.% Zr – 10 at.% W(α-solid soln. + W_2Zr).

The cast alloys were forged at 1350°C and then homogenized in a TVV-5 vacuum furnace at a residual pressure of $5 \cdot 10^{-6}$ torr in the following stages: at 1900°C for 4 h and at 1800°C for 6 h.

Quenching was performed in a current of gaseous helium in a vacuum furnace after high-temperature annealing at 1800°C for 1 h in a vacuum of $5 \cdot 10^{-6}$ torr. The cooling rate in the temperature range of possible decomposition of the solid solution was >40 degree/sec.

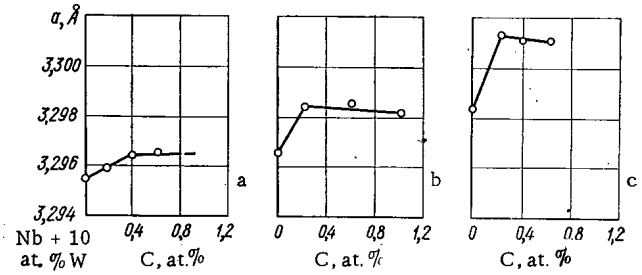

Fig. 3. Lattice constant in alloys of cross sections containing 0.5, 1, and 2.5 at.% zirconium (a, b, c, respectively) as a function of carbon content.

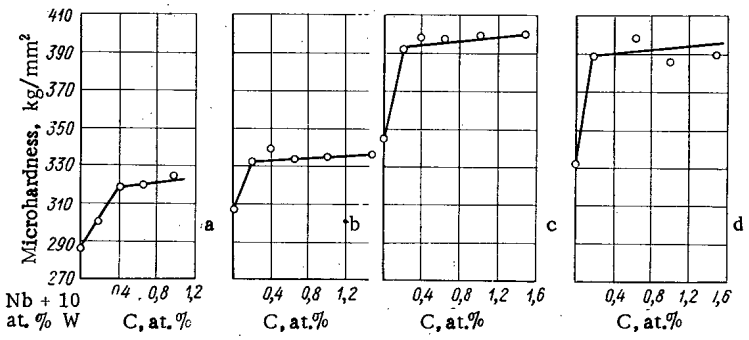

Fig. 4. Microhardness in cross sections of alloys containing 0.5, 1.5, 2.5, and 4 at.% zirconium (a, b, c, and d, respectively) and 10 at.% tungsten as a function of carbon content.

To reveal the microstructure we used an etcher consisting of 2 parts of HF, 2 parts of HNO_3, 1 part of CH_3COOH, and 1.5 parts of H_2O.

The lattice constants were determined by a precision method in Ni K_α-radiation from the (321) line in a black-reflection camera (oscillating flat specimen and rotating film). The exposure was 2 h, the standard was gold. X-ray phase analysis was performed on powders in a Debye camera of diameter 57.4 mm in Cu K_α-radiation (Ni filters, exposure 5 h). Color etching of thin sections was performed in a special apparatus for electropolishing and electroetching at 20V, using the etcher indicated in [8]. The etching time was more then 1 min. The hardness was measured in a Vickers apparatus at load of 30 kg; the microhardness was measured in a PMT-3 durometer at a load of 50 g.

RESULTS

Using the microscopic and x-ray analysis data and the measured values of the hardness and microhardness, we constructed the isothermal cross section of the system niobium – tungsten – zirconium – carbon at 1800°C up to 4 at.% zirconium and 2 at.% carbon and with a constant tungsten content of 10 at.% in the alloys (Fig. 1).

At 1800°C, in these alloys the carbides Nb_2C and (Zr, Nb, W)C and the compound W_2Zr are in equilibrium with the α-solid solution. At this temperature the solubility of carbon in niobium is ~0.55 at.% [9]. According to our data, the solubility of carbon in niobium containing 10 at.% tungsten at 1800°C is also ~0.5 at.% (see Fig. 1). Therefore addition of up to 10 at.% tungsten to niobium has no effect on the solubility of carbon; this agrees with the conclusions drawn by Taylor and Doyle [10]. The microstructure of niobium – tungsten alloys containing up to 0.4 at.% carbon is one-phase (Fig. 2a), but is already two-phase at a carbon content of 0.65 at.% (see Fig. 2b).

The phase which separates as thin elongated plates is niobium carbide Nb_2C. With an increase in the carbon content of the alloy to 1-2 at.%, Nb_2C is obtained in coarser form (see Fig. 2c). The shape and number of the carbide particles are particularly distinct when the material is subjected to color etching: the yellow carbides against the reddish brown background of the solid solution are located at the grains and along the boundaries as acicular plates of the Widmanstatten structure type.

When about 1 at.% or more zirconium is added to niobium – tungsten – carbon alloys, the solubility of carbon decreases (at 1800°C it falls from ~0.5 to ~0.2 at.% (see Fig. 1)).

Determinations of the lattice constant (Fig. 3) and microhardness of the alloys (Fig. 4) confirmed the results of microscopic analysis. The curves plotting the change in the lattice constant and microhardness of these alloys exhibit sharp breaks corresponding to the solubility limit of carbon. For alloys containing 1 at.% or more zirconium, the breaks on these curves correspond to 0.2 at.% carbon (see Fig. 3b-c and Fig. 4 b-d).

Note that addition of zirconium to the alloys leads to marked crushing of the large carbide inclusions and to their more uniform distribution in the base of the matrix. The phases which segregate out are niobium carbide Nb_2C with a hexagonal lattice (see Fig. 2d), and zirconium monocarbide, doped with niobium and tungsten, with an fcc latice: (Zr, Nb, W)C.

The slight decrease in the lattice constant with progressive carburization of alloys containing 1-2.5 at.% zirconium (see Fig. 3b-c) indicates that the niobium-based solid solution loses carbon as a result of removal as the compound (Zr, Nb, W)C. In contrast with the coarse acicular phase, the carbide phase (Zr, Nb, W)C has different and more dispersed segregations.

X-ray phase analysis revealed that the alloys in this part of the system contain the compound W_2Zr, which is a Laves phase with an fcc $MgCu_2$-type lattice [1, 11]. According to [1], this phase appears in niobium alloys at a 4:1 (wt.%) ratio of tungsten to zirconium. The compound W_2Zr is clearly observed in alloys of the system niobium – tungsten – zirconium – carbon. The x-ray diffraction patterns exhibit lines of only two phases: an indium-based α-solid solution with a bcc lattice and a W_2Zr phase with an fcc lattice. Under the microscope this phase appears as elongated and thickened dark veinlets (see Fig. 2e). The W_2Zr phase is not observed in these alloys with a lower zirconium content (1.5 at.%). However, when the alloys simultaneously contain 2.5-4 at.% zirconium and 0.2-2 at.% carbon, the content of this phase is much less owing to combination of zirconium to form the carbide phase (Zr, Nb, W)C.

Note that the rate of segregation of the carbide phases is very great; this makes it difficult to obtain strictly one-phase alloys during quenching [12], despite the high cooling rates.

The solubility of carbon in the alloys of this part of the system niobium – tungsten – zirconium – carbon at 1600°C is no different to that at 1800°C, judging from microstructural and x-ray analyses and determinations of the microhardness.

Of these alloys, those of niobium and tungsten with up to 0.7 at.% carbon and 1% zirconium have the lowest hardness (up to 180-200 kg/mm^2) and maximal technological effectiveness. Alloys containing 0.7-1.5 at.% carbon and 1-2.5 at.% zirconium have a satisfactory plasticity and a hardness of 220-240 kg/mm^2. Incorporation of these components within the above limits reduces the plasticity of the alloys owing to an increase in the number and size of the carbide particles.

The (Zr, Nb, W)C phase may be an effective strengthener in niobium-based alloys of the system niobium – tungsten – zirconium – carbon, particularly if the material is subjected to appropriate heat treatment (accelerated cooling after annealing at 1800-2000°C).

LITERATURE CITED

1. E. M. Savitskii and A. M. Zakharov, Zh. Neorganich. Khim., 7, No. 11 (1962).
2. A. C. Barber and P. H. Morton, High Temperature Refractory, Metals, New-York – London – Paris (1966), p. 391.
3. V. S. Emel'yanov et al., in: Metallurgy and Metallography of Pure Metals [in Russian], No. 6, Atomizdat, Moscow (1967), p. 92,
4. P. Stecher et al., Monatsh. Chem., 95, 1630 (1964).
5. E. Delgrosso et al., J. Less-Common Metals, 12, No. 3 (1967).
6. W. Chang, Columbium-Base Alloys, USA Patent No. 3384479, May 21 (1968).
7. A. Dalton and G. McAdam, Metallography and Heat Treatment (Express Information), No. 27, 34 (1970).
8. M. Picklesimer, US Atomic Energy Commission Oak Ridge Nat. Laboratory, Rept. (1957), p. 2297
9. E. Rudy et al., Planseeberichte fur Pulvermetallurgie, 16, No. 1 (1968).

10. A. Taylor and N. Doyle, J. Less-Common Metals, No. 5, 511 (1967).
11. R. Domogala et al., J. Metals, 5, 73 (1953).
12. F. Ostermann and F. Vollenrat, in: New Refractory Metallic Materials [Russian translation], Mir, Moscow (1971), p. 130.

EXPERIMENTAL FITTING OF DATA RELATING TO THE IRRADIATION OF GRAPHITE IN REACTORS TO A UNIVERSAL SCALE OF DAMAGE-INDUCING FAST NEUTRON FLUX

V. I. Klimenkov and V. G. Dvoretskii

UDC 539.16.04:621.039.512.45

This problem arises in connection with matching the neutron-induced damage in graphite irradiated by neutron fluxes of different parameters [1] (for example, when the irradiation takes place in different reactors or in different parts of the same reactor). The point is that the damage suffered by the graphite as a result of irradiation depends on the intensity and energy spectrum of the neutron flux causing the damage.

The results of neutron irradiation may be meaningfully compared if the dose is measured in units of the integrated fast-neutron flux causing the damage [2]. If we know the intensity and spectrum of the neutron flux, the results may be fitted to this scale by a computational procedure, allowing for the concept of equivalent temperatures [3] and the damaging capacity of neutrons of different energies over the whole spectrum [4, 5]. If the spectrum of the neutron flux is unknown a calibrating experiment differing fundamentaly from experimental matching [6, 7], may be necessary. In the latter case, the neutron flux density is expressed in terms of a known spectrum with a specific lower energy limit (for example, > 0.18 MeV).

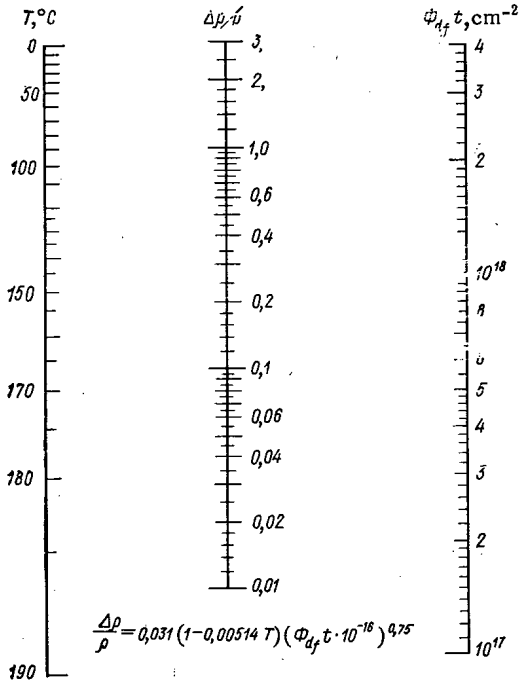

Fig. 1. Nomogram for solving the calibration equation in the case of PGG graphite (perpendicular to the direction of cutting the sample).

Experimental Method. The calibrating experiment is carried out as follows: An ampoule containing a graphite sample and an activation threshold detector (for example, Ni^{58}) is irradiated in a reactor for a time t_{irr}. The irradiation is carried out at that point of the reactor for which matching is required. The ampoule should not seriously affect the parameters of the neutron field.

From the specific activity of the threshold detector the equivalent fission neutron flux Φ^f_{Ni} is determined. For this purpose we use the cross section of the (n, p) threshold reaction averaged over the fission spectrum. The integrated $\Phi^f_{Ni} t_{irr}$ should not deviate very greatly from the range 10^{17}–3.10^{18} neutrons/cm^2, while the graphite irradiation temperature T_{irr} should lie in the range 100–150°C.

In the irradiated graphite sample the residual radiation increment in electrical resistance $\Delta\rho/\rho$ is determined; then from the fall in electrical resistance which occurs on annealing $\Delta\rho = f(T_{ann})$ the graphite irradiation temperature is found [8]. The temperature measurement may be duplicated by using the diamond method [9].

Translated from Atommaya Énergiya, Vol. 34, No. 2, pp. 93–96, February, 1973. Original article submitted January 31, 1972.

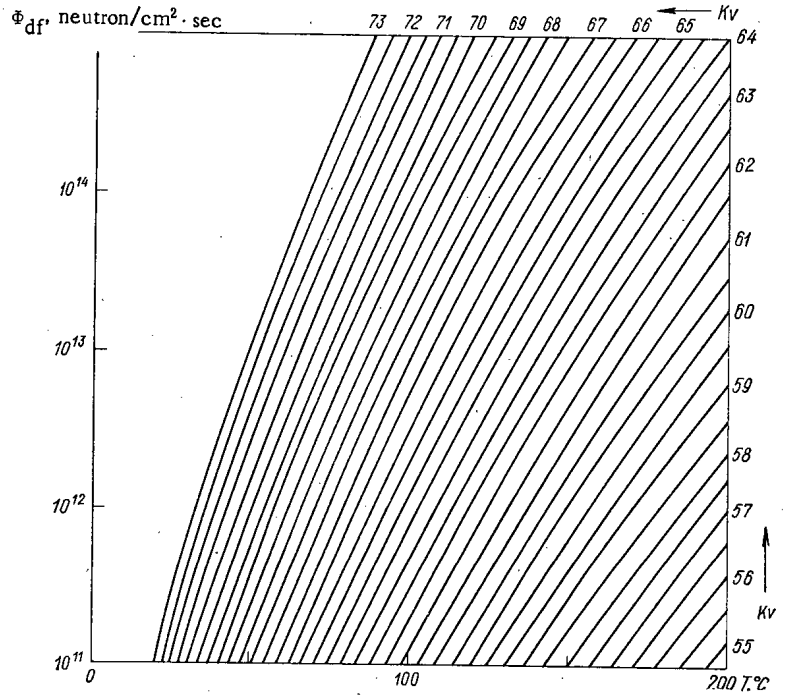

Fig. 2. Cartesian abacus for the irradiation temperature, neutron flux, and graphite irradiation equivalence criterion.

TABLE 1. Results of the Experiments and Analysis

Parameter	Irradiation			
	channel 14			channel 4
	I	II	III	IV
t_{irr} $\times 10^{-5}$ sec	2,55	9,9	4,75	0,155
Φ'_{Ni}, $\times 10^{-12}$ neutrons /cm · sec²	1,3	0,95	1,3	146
Φ^f_{Ni}, 10^{-18} neutrons/cm²	3,32	9,40	6,17	1,68
T_{irr}, °C	100	100	150	100
$\frac{\Delta\rho}{\rho}$	0,64	1,24	0,60	2,40
Φ_{df}, $\times 10^{-12}$ neutrons /cm² · sec	3,84	2,72	3,68	382
T, °C	72	78	120	40
k_{fx}	2,95	2,50	2,83	2,62

From the value of $\Delta\rho/\rho$ and also that of Φ^f_{Ni} determined from the activation threshold detector, with due allowance for the irradiation temperature, we find the conversion factor for converting the equivalent fission neutron fluxes at the points of irradiation in the reactor in question to the universal scale of the fast neutron flux Φ_{df} causing the damage:

$$k_{fx} = \Phi_{df}/\Phi^f_{Ni}. \quad (1)$$

This is done by means of a calibrating formula [2] derived for graphite of the PGG type cut perpendicularly to the axis of formation

$$\Delta\rho/\rho = 0.030\,(1 - 0.00514T)\,(\Phi_{df}t \cdot 10^{-16})^{0.75}, \quad (2)$$

where T is the irradiation temperature in °C.

The relationship described by this formula is valid for the calibrating value of the damage-inducing flux $\Phi_{dfk} = 2.65 \times 10^{11}$ neutrons/cm² · sec. If in any experiment the irradiation is carried out with another value of Φ_{df}, the concept of equivalent temperatures is applied to the ratio Φ_{df}/Φ_{dfk}. However, the problem is complicated by the fact that the quantity Φ_{df} is unkown, and an iteration method is required [1, 2, 10].

Method of Analyzing the Experimental Data. In order to simplify the iterative calculations a nomogram is used (Fig. 1) for solving Eq. (2) with respect to $\Phi_{df}t$. The first value of $\Phi_{df}t$ obtained in the first iteration from the experimental values of $\Delta\rho/\rho_{exp}$ and T_{irr} enables us to determine

$$\Phi_{df1} = \frac{(\Phi_{df}t)_1}{t_{irr}}. \quad (3)$$

to a first approximation.

If this quantity differs from the calibration value of Φ_{dfk} equal to $2.65 \cdot 10^{11}$ neutrons/cm^2 · sec. (it is usually higher than this), the conditions of Eq. (2) are not satisfied. A correction has therefore to be introduced. For this purpose we have to determine the equivalent temperature T_{eq1} (lower than T_{irr}). When irradiating in a flux of Φ_{dfk} this gives the same rate of damage as is obtained on irradiating in a higher flux of Φ_{df1} at a higher temperature T_{irr} [11].

For the resultant values of T_{eq1} and $\Delta\rho/\rho$ a second value of $\Phi_{df}t)_2$ is found by means of the nomogram in a second iteration; as in expression (3), this is then used to determine $\Phi_{df2} = (\Phi_{df}t)_2/t_{irr}$. The whole procedure is then repeated until constant values of T_{eq} and Φ_{dfn} not varying from one iteration to another are obtained. This means that the conditions imposed upon Eq. (2) are finally satisfied. From the resultant value of Φ_{dfn} we then determine the desired conversion factor k_{fx} from Eq. (1). Now all the values of $\Phi^f_{Ni}t$ obtained in experiments relating to the irradiation of graphite at a specified point of one particular reactor X have to be multiplied by this conversion factor in order to obtain the integrated neutron-irradiation dose in universal units of the neutron flux $\Phi_{df}t$ causing the damage.

The application of this concept may be greatly simplified (as compared with the method proposed earlier [11]) if we introduce a continuous dependence on the ratio of the fluxes. On the basis of the same simple principles as were used to initiate the concept [10], we may establish a dimensionless similarity criterion (that of Kurchatov) for equivalent conditions of irradiation with respect to neutron flux and temperature:

$$Kv = \frac{Q}{kT_{irr}} + \frac{\ln \Phi_{df}}{\Phi_0}. \quad (4)$$

In the temperature range T(°K) in which the activation energy of the radiation defects in graphite Q may be regarded as identical, a constant value of the similarity criterion Kv for a number of cases of irradiation with differing values of Φ_{df} and T_{irr} implies equivalence of the conditions of irradiation, giving an identical rate of graphite damage (k is Boltzmann's constant). The Cartesian abacus shown in Fig. 2 easily enables us to select equivalent conditions over a wide range of Φ_{df} (we take $\Phi_0 = 1$ neutron /cm^2 · sec).

Results of Experiment. Irradiation was carried out in channels 4 and 14 of an SM-2 reactor (not at nominal power). The stainless steel ampoules each contained two samples of PGG graphite cut perpendicular of the axis of formation. Threshold indicators 10-20 mg in weight, in the form of discs 2 mm in diameter, cut from nickel and carbonyl iron foil (0.05 mm thick), were placed in a miniature cadmium capsule (wall thickness 1 mm). Diamond powder was placed in a similar capsule made of aluminum.

The activity of the threshold indicators was measured, after irradiation, by a relative method, by comparing the indicator measured with a standard indicator of known activity and identical geometry, the relative error not exceeding ±8%. The electrical resistance of the graphite samples before and after irradiation was measured by the ordinary potentiometric method, by comparing the fall in voltage in a standard resistance and the resistance used for measuring the error was only one in the third decimal point when determining the relative increment in electrical resistance.

Table 1 shows the experimental data and the results obtained on analyzing these in order to determine the conversion factor. The mean experimental value of k_{fx} for channel 14 of the SM-2 reactor (irradiations I-III), equal to 2.75, was quite close to the calculated value of $k_{fx} = 2.86$ [2] obtained from the known spectrum in this channel. We see that the method here described yields perfectly acceptable results. The use of this method is desirable when comparing data relating to the behavior of graphite obtained in different types of reactors [12], in foretelling the behavior of graphite in the piles of uranium – graphite reactors [13], and also when studying the difference in the behavior of the graphite inside individual units of the piles [14], for which it is important to consider the difference not only in the irradiation temperature but also in the neutron spectra. A disadvantage of the method is its limitation to fairly low graphite irradiation temperatures. However, this refers not to the irradiation of graphite in a research program but only to a specific calibration experiment. This limitation is therefore only important when the required (lowish) temperature cannot be achieved in the reactor. As regards the apparent disadvantage arising from the fact that the method is related to a specific type of graphite, we see from Eq. (2) that the problem reduces to one of introducing a correcting factor ρ_x/ρ_{PGG} on the right-hand side of this equation, where ρ_x relates to any type of reactor graphite [2].

LITERATURE CITED

1. D. Reed et al., Radiation Damage in Reactor Materials, Vol. 2, IAEA, Vienna (1969), p. 143.
2. V. I. Klimenkov and V. G. Dvoretskii, Contribution to the Fourth All-Union Coordinating Conference on the Dosimetry of Intensive Fluxes of Ionizing Radiations [in Russian], Mendeleevo (1971).
3. M. Thompson and S. Wright, J. Nucl. Materials, 16, No. 2, 146 (1965).
4. V. I. Klimenkov and V. V. Kirsanov, in: Dosimetry of Intense Fluxes of Ionizing Radiations [in Russian], Fan, Tashkent (1969), p. 76.
5. V. G. Dvoretskii, V. I. Klimenkov, and V. V. Kirsanov, in: Radiation Dosimetry and Spectrometry of Ionizing Radiation [in Russian], Fan, Tashkent (1970), p. 213.
6. V. N. Vikhrov and N. F. Pravdyuk, in: Dosimetry of Large Doses [in Russian], Fan, Tashkent (1966).
7. A. V. Borodin et al., At. Energ., 32, No. 2, 161 (1972).
8. V. I. Klimenkov, in: Radiation Dosimetry and Spectrometry of Ionizing Radiations [in Russian], Fan, Tashkent (1970), p. 210.
9. V. I. Karpukhin and V. A. Nikolaenko, Temperature Measurement by Means of Irradiated Diamond [in Russian], Atomizdat, Moscow (1971).
10. H. Bridge et al., Radiation Damage in Reactor Materials, IAEA, Vienna (1963), p. 531.
11. L. Valette, Radiation Damage in Reactor Materials, Vol. 2, IAEA, (1969), Vienna, p. 97.
12. R. Blackstone et al., ibid., p. 543.
13. V. I. Klimenkov and V. R. Zolotukhin, At. Energ., 30, No. 2, 231 (1971); 31, No. 5, 506 (1971).
14. B. V. Brokhovich et al., Second Geneva Conference, Vol. 2, Contributions of Soviet Scientists [in Russian], Atomizdat, Moscow (1958), p. 319.

UNIFIED INDUSTRIAL SYSTEM OF NUCLEAR INSTRUMENTS FOR INSTRUMENTAL ACTIVATION ANALYSIS

B. G. Egiazarov, V. V. Matveev, and Yu. P. Sel'dyakov

UDC 543.53:539.1.07.543

The progress of technology is indissolubly linked with the production of new materials and the manufacture of objects based on these; it is accordingly vital to create rapid precision methods of monitoring the elemental composition of materials. Analytical methods based on classical approaches (chemical, physicochemical, spectroscopic, mass-spectroscopic, and others) have certain specific advantages; however, not all the problems associated with elemental analysis can be operatively solved by these techniques.

The initiation and development of one of the several nondestructive methods of analyzing the composition of materials, instrumental activation analysis (IAA), which is widely employed in various fields of science and technology, have resulted from this lack. It is therefore desirable to determine the principal requirements laid upon the analytical apparatus and the general approach to the creation of activation complexes.

Necessary Limitations

In solving a problem of this kind we envisage certain basic limitations which enable us to reduce very considerably both the composition of the system and the modification which have to be made to the instruments and equipment. These limitations may naturally be expressed in terms of the basic or common problems and principles involved in IAA.

The most promising and extensively invoked applications of IAA now in existence for scientific and industrial purposes are the methods of neutron and gamma-activation analysis. These methods may be used with various sources of activating radiation derived from various types of nuclear reactions [1]. In our own opinion, industry, in particular, will continue to favor instruments based on relatively simple, compact, and inexpensive controllable radiation sources of the accelerator type, or on isotope sources.

The radioactive isotopes formed as a result of activation emit various forms of radiations: γ quanta, neutrons, and charged particles. The various forms taken by these radiations and their varying energy and space–time parameters necessitate the use of a variety of detection units and systems, which in turn determine the secondary recording apparatus required. On classifying the various methods of activation analysis by reference to the form of the secondary radiation recorded by the apparatus, we readily establish that methods based on the recording of γ radiation have the greatest practical value [2].

In analyzing possible versions of various IAA systems and complexes, we may note the general requirements imposed upon analogous units and instruments [3]. In their functional structure, IAA systems and complexes comprise characteristic units differing as regards design and practical construction. These units include: 1) the source of activating radiation; 2) the transporting system for conveying the samples from the irradiation to the measuring zone and vice versa; 3) induced-activity detection devices; 4) signal-recording tracts, including units of amplitude and time selection, as well as units for the storage and processing of the data; 5) a system for controlling the complex.

Such was the functional approach adopted in setting up the first Soviet unified IAA system.

Translated from Atomnaya Énergiya, Vol. 34, No. 2, pp. 97–104, February, 1973. Original article submitted September 4, 1972.

Unified System

The unification of any system is based on unifying the technical arrangements and practical structures entering into the system of objects envisaged. The first step in unification and compaction is that of choosing the principal constituent units. Then the dimensions of the frames carrying the electronic circuits and the order of their installation have to be established. The next stages take in complete working units, then whole instruments, and so forth. In this sense complexes are the highest stage of unification; their structure, composition, and parameters are determined by the purposes actually in hand, and allow for the specific characteristics of the various IAA applications envisaged. An analysis of the construction of the apparatus in purpose-built IAA systems, allowing for the views of specialists and initial experience in the creation of such systems, showed that in the construction of a unified IAA system the functional approach was the best. The instrumental composition of the system about to be considered was by this method determined.

1. A two-channel pneumatic shuttle (PS-2) (Fig. 1) with a central control desk (CCD) is widely employed in carrying out the simultaneous activation analysis of the sample (containing the material under analysis) and a "standard" (substance with a known content of the element to be determined). Since in this case all the succeeding stages in the analysis are carried out synchronously, there is no need to monitor the neutron flux and introduce corresponding corrections in subequent calculations.

The pneumatic shuttle comprises a two-position pneumatic delivery with corresponding chambers and pneumatic equipment (compressor, storage device, valves, etc.). Each channel of the pneumatic delivery contains chambers for irradiation, measurement, loading, and ejection, connected by a polyethylene specimen conduit 16 mm in diameter. The ampoules for the sample and standard are made of polyethylene and have the following dimensions: external diameter and length 15 and 46 mm, internal diameter and length 10 and 40 mm, maximum weight of the samples ~50 g. For introducing the ampoules into the specimen there is a loading chamber containing a cassette with ten ampoules. The irradiation chamber is designed so as to place the ampoules in the field of ionizing radiation. In order to ensure adequate activation of the sample and "standard", during irradiation these are rotated around their axes in a plane normal to the flux of activating radiation. The measuring chambers serve to fix the ampoules in relation to the units detecting the radiation of the induced activity. During the measurements the ampoules are rotated. The length of each channel of the specimen conduit is up to 25 m. The rate of feeding the samples is no less than 10 m/sec. In order to monitor the position of the samples in the conduit a photorecording system is provided, connected to the pneumatic display on the control desk.

The orders required to control the pneumatic shuttle are sent from the control desk, which contains a pneumatic shuttle control unit and a timer. The pneumatic shuttle may be governed from the desk either manually or automatically. In the automatic control mode the timer independently specifies five time intervals (irradiation, first holding period, first measurement, second holding period, second measurement) between 1 sec and 59 min 59 sec with a step of 1 sec. If necessary up to ten repeated measuring cycles of each sample may be given from the control desk.

2. A single-channel pneumatic shuttle (PS-1) with a central control desk (CCD) delivers the sample to three positions: the irradiation zone, the measuring zone, and the place at which the sample is processed radiochemically. In contrast to the two-channel pneumatic shuttle, this one has the following auxiliary devices: a pointer enabling the direction of delivery of the samples to be reversed, a cooling chamber for holding the samples after irradiation, a final ejection chamber which may be placed in the radiochemical laboratory room. The main technological characteristics of the pneumatic shuttle PS-1 are analogous to the PS-2.

The central control desks of the two systems are unified. In order to convert the CCD from one system to the other it is sufficient to change the control unit for the pneumatic shuttle.

3. An all-wave neutron monitor (ANM). Since the unified system here developed is mainly intended to provide activating radiation in the form of fast neutron fluxes, the control desk contains a neutron recording tract enabling the neutron flux to be regulated. The neutron monitor may operate with two detection units in the irradiation zone. One of these is a "long counter" and the other a scintillation counter. The use of a thin scintillator in the latter unit facilitates control of the energy distribution of the fast neutrons, which is necessary in carrying out certain kinds of analysis. This electronic recording tract of the fast neutron monitor comprises an amplifier, a discriminator, an intensity meter, and a conversion (scaling) unit.

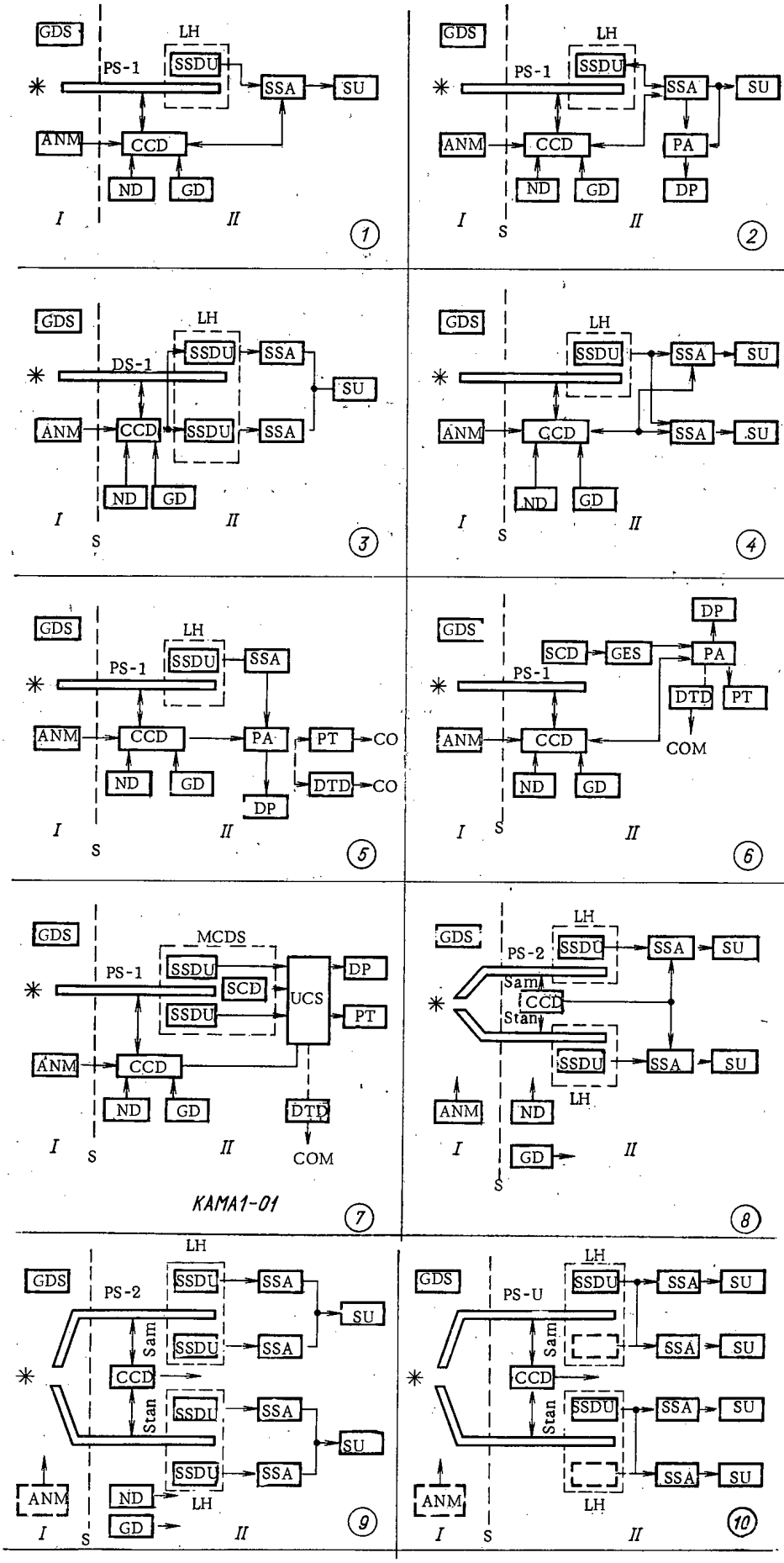

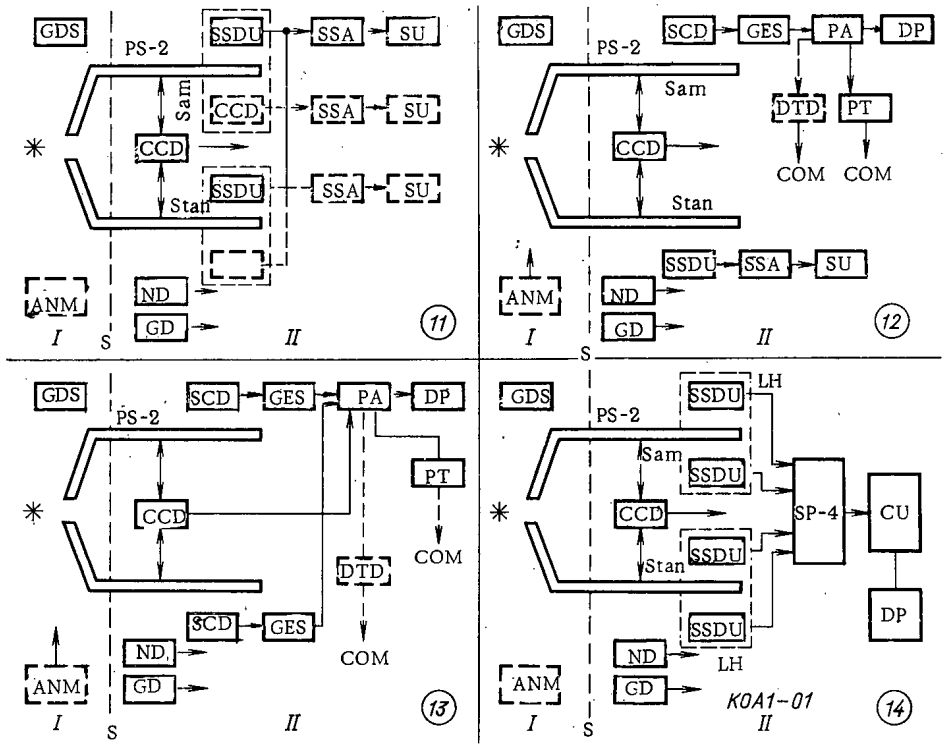

Fig. 1. Block diagrams of various activation devices derived from the unified system of nuclear instruments: 1) Simplest arrangement with a single-channel stabilized pulse analyzer; 2) the same arrangement but with a multichannel pulse analyzer; 3) arrangement with two detection units and the summation of information; 4) arrangement with two channels of amplitude analysis; 5) combined arrangement with information-extracting units; 6) arrangement with a semiconducting γ radiation spectrometer; 7) arrangement with a multicrystal total coincidence spectrometer; 8) arrangement with single-channel analyzers (sample – standard); 9) a similar arrangement but with two tracts of amplitude analysis in the sample and standard channels; 11) arrangement with time-sequential measurements of the sample and standard activity (in one or several channels); 12) combined arrangement with a semiconducting spectrometer (in the sample channel) and a scintillation spectrometer (in the standard channel); 13) arrangement with semiconducting spectrometers in two channels (sample and standard); 14) complex four-channel automated arrangement with a device for processing the results of the analysis. I) Irradiation zone; II) measuring zone; S) arbitrary symbol for biological shielding.

4. The scaling unit with its digital display (SU) is designed for a load of up to 4.10^6 pulses/sec. The information is brought out to gas-discharge digital indicators. The scaling unit may operate under manual or automatic control. In the latter case it may receive "start" and "stop" instructions (for example, from the central control desk timer), corresponding to the beginning and end of a specific time interval.

5. The stabilized scintillation detection unit (SSDU) together with the tract of a single-channel stabilized analyzer (SSA) form a constituent part of the spectrometer with the following parameters: detector – sodium iodide activated with thallium, dimensions $\phi 150 \times 150$ mm; energy resolution – 12% on the 661 keV line; stabilization factor – at least 50; number of levels of discrimination (channels) – 100; width of differential window – 2-35 channels; maximum load – up to $2 \cdot 10^5$ pulses/sec; time instability – no worse than 1%; integrated nonlinearity – no more than 1.5%; dead time of the discriminator 2 μsec. The signals from the output of the SSA may be passed for storage to the SU and for subsequent processing to the time selector.

6. A four-channel spectrometric unit (SP-4) with a set of four detectors (SSDU) and lead housings for siting these (LH); this consists of four identical tracts incorporating single-channel spectrometers (SSA).

In order to broaden its potentialities, the device includes time selectors so as to facilitate any choice of information in conjunction with the amplitude selectors. The resolving time of the "fast" and "slow" coincidence circuits are 0.1 and 1 μsec respectively. The time delay in one of the tracts of the apparatus for recording chance (random) coincidences is 2 ± 0.1 μsec.

The installation also contains intensity-adding units and gating circuits. One feature of the spectrometer circuitry lies in its ability of be used either as four (or less) independent single-channel spectrometers or as two identical spectrometers operating in the 4π measuring mode or in the mode of fast/slow coincidences with due allowance for those of a random nature.

The gating circuits may be controlled from the control desk in such a way as to allow information to be transmitted solely during the "measuring" period. Information from the output units of the installation may be passed to the scaler SU or other devices for storage.

7. A computer (COM) is provided for processing the results of the analysis. This constitutes a specialized electronic computing system containing three arithmetical and two command (order) recording units, an operative memory, and a permanent recording system containing the algorithms for processing the information. The algorithms for processing the results of the measurements enable the concentration of an element to be calculated: a) from one separated γ line, without allowing for contributions from interfering reactions, with a constant background of the matrix (for example, in determining oxygen content); b) as in a) but with a variable matrix background (for example, in determining oxygen in fissile materials); c) as in a) but allowing for interfering reactions (spectral-ratio method); d) from cascade γ lines with a constant matrix background (for example, in determining nitrogen content); e) as in d) but with a variable matrix background (for example, in determining nitrogen in fissile materials).

The concentration of the element to be determined (wt.%) is calculated from the generalized formula

$$\eta = \frac{1}{km_{\text{sam}}}\left[\frac{(N_{\text{sam}^1}-\Phi_1)-\alpha(N_{\text{sam}^2}-\Phi_2)}{(N_{\text{st}}-\Phi_{\text{st}})(1-\alpha\beta)} - A\right] - c\eta_x,$$

where k is a constant, allowing for the mass of the standard, the amount of the element which it contains, the difference in the conditions of recording the sample and standard, and so forth, m_{sam} is the mass of the sample, $N_{\text{sam}1}$, $N_{\text{sam}2}$, N_{st} are the numbers of counts from the sample in two time intervals and from

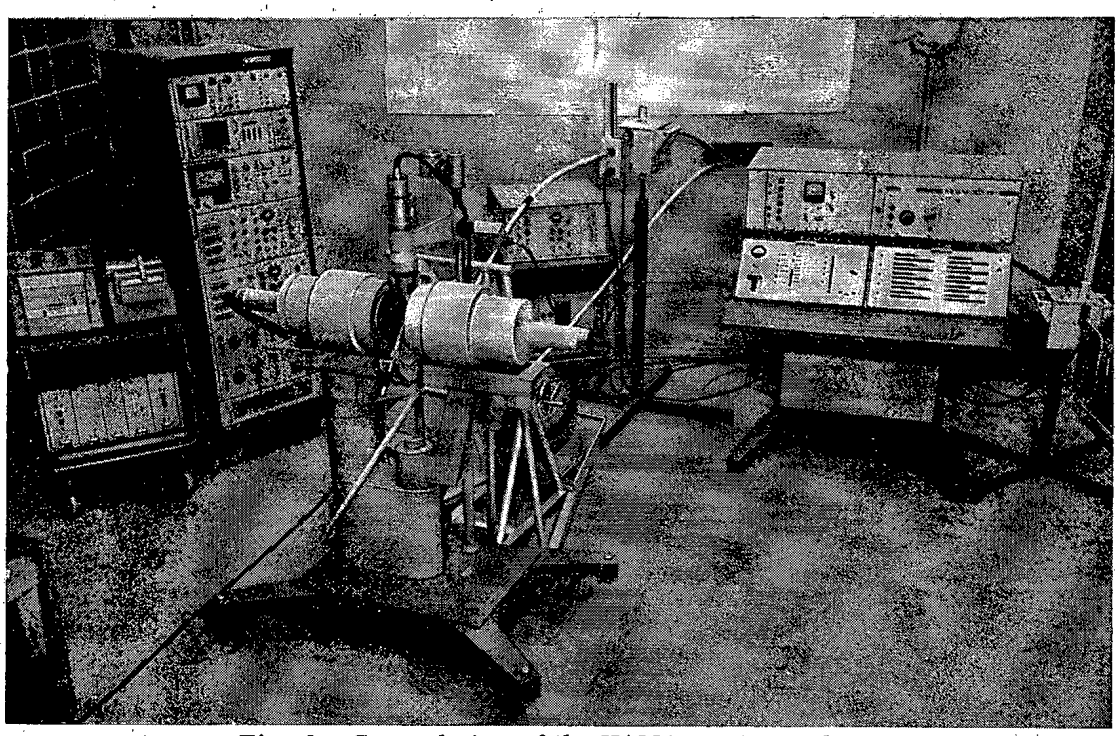

Fig. 2. General view of the KAMA-1-01 complex.

the standard, Φ_1, Φ_2, Φ_{st} are the number of background counts on the sample and standard tract, η_x are the known or independently determined contents of interfering elements in the samples, c is the contribution introduced by the interfering elements when measuring the element to be determined, A is a constant allowing for the presence of the element to be determined in the ampoule material, and α, β are coefficients. The transformation of the generalized formula into a specific expressions for calculating the concentration of the element may be achieved by inserting the corresponding data.

The relative error is calculated by means of the computer using the formula

$$\delta = \sqrt{\frac{(N_1+\Phi_1)+\alpha^2(N_2+\Phi_2)}{[(N_1-\Phi_1)-\alpha(N_2-\Phi_2)]^2}+\frac{N_{st}+\Phi_{st}}{(N_{st}-\Phi_{st})^2}}.$$

In this way the mean and the error of the mean may be deduced as follows

$$\eta_m = \frac{\sum_n^n \eta_i}{n}; \quad \bar{\delta} = \frac{\sqrt{\sum_n^n \eta_i \delta_i}}{\sum_n^n n_i}.$$

The orders specifying the choice of processing algorithm, the initiation of the processing, etc. are directed to the computer from the control desk. The results are brought out to digital displays and a digital printer.

8. A universal total coincidence spectrometer (UCS) with a multicrystal system of detection units (MCDS). The spectrometer incorporates three detection units and amplitude-time selectors. The scintillation tracts of the spectrometer have an amplification-factor stabilization circuit analogous to that used in the one- and four-channel spectrometers of the unified system. The presence of the fast coincidence circuit and the unit for the linear addition of pulse amplitudes facilitates use of the spectrometer under a variety of conditions (4π measurement, separation of cascade γ lines with respect to the peak of the sum, the Compton mode, the pair mode, etc.).

9. A γ emission spectrometer (GES) with a semiconducting detector (SCD). The principal parameters of the spectrometer are: detector – planar and coaxial germanium with a volume of 5-60 cm^3 (to order); energy resolution – 3.0-6.0 keV of the 661 keV line; integrated nonlinearity – no greater than 0.2%.

The use of an SCD spectrometer together with a multichannel pulse analyzer and a VUS-2 instrument enables more complicated γ spectra to be studied.

10. A multichannel pulse-amplitude analyzer (PA) extends the potentialities of activation analysis. In the information-storage tracts the signal amplitude is converted into digital code. Units for stabilizing the conversion process are provided in the spectrometer in order to ensure a high stability of the conversion coefficient during prolonged measurements.

An information-storage unit with 1024 channels and a channel capacity of 10^6 with digital discrimination units enables specific parts of the energy spectrum to be selected, and also recorded in individual groups of the information-storage system. In addition to the storage of information relating to the whole spectrum, the experimental worker is enabled to isolate and store information in individual groups (splitting the store memory into groups 1024×1, 256×4, 128×8, 64×16, 32×32) and also the realize other modes of storage in accordance with specific requirements. The presence of digital discrimination units enables time-correlated information to be stored (when working with two or three detection units). The corresponding problems inculde: seeking and separating cascade lines, ensuring analytical resolution in the presence of cascade transitions, realizing the conditions of a pair spectrometer with three coincidences and control based on an annihilation radiation peak, and so forth. The digital discrimination units are able to record spectra independently (in accordance with specific requirements) in the four groups of the analyzer memory and distinguish up to four subgroups in each of these. These potentialities enable the experimental worker to carry out investigations involving contributions from interfering reactions, investigations based on the method of spectral ratios, and so on.

For the operative control of a set of information, the "zero" channels of the analyzer are used, together with a scaling unit, by means of which the experimental worker may determine the total number

of pulses in the whole spectrum or in any part of the spectrum separated out by the digital discrimination unit. The analyzer enables control operations to be carried out on the basis of the number of counts in any of its channels or "dead-time" counters, and also allows the spectra to be normalized with respect to the area and number of counts in any selected channel.

The information is taken out to the screen of a cathode-ray tube, digital displays, and a digital printer; when using the AP-1 istrument the data obtained from the analyzer may be directly translated to a computer or tape-puncher.

11. A digital printer (DP).

12. A device for passing the results to punched tape (PT) or punched cards (PC).

13. A device for directly transferring the data to a computer (DTD).

14. A γ radiation dosimeter with a signal system (GDS).

15. A γ radiation dosimeter (GD).

16. A neutron dosimeter (ND).

Certain nuclear instruments forming part of the unified system are standard and are already being produced by industry (for example, dosimeters, digital printers, etc.).

Possibilities of synthesizing activation devices of different complexities and with different purposes using the unified system of nuclear instruments and equipment under consideration are illustrated in Fig. 1. Of course, the arrangements illustrated by no means exhaust all possibilities; in Fig. 1 only a few versions are shown. The first arrangements are based on a single-channel pneumatic shuttle system, so that in these the activating radiation flux monitor is designed for normalization of the data. A set of dosimetric instruments is required in all the arrangements. We see from the designs illustrated that, by basing the sets of measuring instruments required for instrumental activation analysis on the unified systems here described, a considerable flexibility may be achieved in the construction of various forms of activation equipment.

In the middle of the sixties two main tendencies became readily discernible in instrumental activation analysis, the measuring equipment required in the two cases being essentially different: The first was associated with the mass analysis of one or a small number of elements in samples of similar composition (problems of this kind are most frequently encountered in the industrial applications of instrumental activation analysis); the second was associated with work of a research and methodical nature as carried out in scientific-research laboratories and centers.

These two spheres of activity embrace a large number of analytical problems. We may demonstrate the potentialities of the unified system under consideration by taking as an example the construction of sets of apparatus satisfying the requirements of these two aspects of investigation.

The KOA-1-01 complex (Fig. 1, 1-14) is designed for the automated analysis of one or a small number of elements in samples with the same (or little varying) matrix (base). In order to ensure high efficiency of the analysis, a method is provided for comparing the induced activity in the sample with a standard. The technical realization of this method is based on a two-channel pneumatic shuttle system for simultaneously moving the sample and standard, and also identical tracts for measuring the induced activity of the sample and standard.

The KOA-1-01 complex consists of three units: 1) A pneumatic shuttle system (PS-2 and CCD); 2) a four-channel stabilized scintillation spectrometer (SP-4 and SSDU); 3) a computer for analyzing the results of the measurements (computing unit CU and digital printer DP). The external view of the KOA-1-01 complex and its main constituents are described in [4, 5].

The KAMA-1-01 complex (Fig. 1, 1-7) is intended for processing various methods of instrumental activation analysis and carrying out analyses for large numbers of elements. The tolerances relating to errors and the reproducibility of the measurements in this system are less stringent than in the KOA-1-01, and only a single-channel pneumatic shuttle is required. The results of the analysis (proportions of the elements) are obtained after normalizing the data with respect to the neutron flux by reference to the readings of a monitor.

Functionally the KAMA-1-01 consists of two subsystems: 1) A pneumatic transportation system (PS-1 and CCD); 2) a universal gamma spectrometer comprising a multipurpose scintillation gamma spectrometer, a semiconductor spectrometer, a device for storing information based on a multichannel analyzer and scaling unit, and also peripheral apparatus for extracting the information.

A general view of the KAMA-1-01 complex in laboratory form is shown in Fig. 2, and individual units in [5].

The sensitivity of the two complexes for analyzing oxygen and nitrogen is 20-400 and 400-600 pulses/mg respectively (the 14 MeV neutron flux equals 10^{10} neutrons/cm^2 · sec).

In order to estimate the reliability of the results of an analysis based on the foregoing complexes, experiments were carried out to determine the apparatus error due to inaccuracy in siting the ampoules in the irradiation and measuring chambers, instability of the electronic systems, etc. Experiments were carried out to determine the reproducibility of the results obtained on measuring the amount of oxgyen in Plexiglas. An analysis of the results of repeated measurements showed that the apparatus error in the measurements (the reproducibility) equalled 0.7% for the KOA-1-01 and 4% for the KAMA-1-01 without allowing for statistical errors. The actual data relating to the results of these analyses are presented in [4, 5].

The unified system described in this paper and the basic complexes derived from it may be supplied to customers on ordering through the V/O "Izotop" trade organization [6].

LITERATURE CITED

1. B. G. Egiazarov, Nuclear Instrumentation, No. 13 [in Russian], Atomizdat, Moscow (1970), p. 124.
2. B. G. Egiazarov, Nuclear Instrumentation, No. 14 [in Russian], Atomizdat, Moscow (1970), p. 83.
3. A. F. Belov et al., Transactions of the Scientific-Technical Conference on Apparatus for Activation Analysis, Budapest, 1968 [in Russian], Izd. SEV, Moscow (1969).
4. S. N. Venkov et al., At. Energ., 31, No. 3, 227 (1971).
5. B. G. Egiazarov et al., Measuring Techniques in Instrumental Neutron-Activation Analysis [in Russian], Atomizdat, Moscow (1972).
6. Catalog of the Trade Organization V/O Izotop, Apparatus for Activation Analysis [in Russian], (1972).

NUCLEAR SPECTROSCOPY AT THE RADIUM INSTITUTE*

B. S. Dzhelepov, N. N. Zhukovskii,
R. B. Ivanov, and V. P. Prikhodtseva

UDC 543.42

In 1945, V. G. Khlopin and P. I. Lukirskii suggested to B. S. Dzhelepov that research on nuclear spectroscopy be initiated at the Radium Institute. The nuclear spectroscopy laboratory came into being some time after that. The laboratory has always been a small one, accommodating never more than a dozen or so physicists and two radiochemists. Nevertheless, while it has been in existence the laboratory staff working there have published a total of 189 research papers, and the Radium Institute has been awarded the "For the best work" prize on eight different occasions.

On three occasions the laboratory has successfully gone beyond the "front lines" of nuclear spectroscopy: the staff has devised instruments which were, in terms of some of their spectral characteristics, the best in existence anywhere in the world, and these instruments have been invaluable in securing especially useful research data. Three groups of research efforts and papers which briefly illustrate the development of nuclear spectroscopy as a whole are mentioned in the text below.

In the first example, magnetic spectrometers for γ-rays were involved: there were the retron machine (built in 1948 [1]) and the electron machine (built in 1953 [2]). During the first decades following the discovery of radioactivity, there were no methods available for the study of the spectra of hard γ-rays. The first paper on γ-ray spectroscopy appeared in 1927, authored by D. V. Skobel'tsyn [3]. The spectrum of Compton electrons knocked out of atoms of a gas by hard γ-quanta was studied in a Wilson cloud chamber immersed in a magnetic field. The source of radiation in that case was radium in equilibrium with its decay products. γ-Ray spectrum of radium obtained by D. V Skobel'tsyn is shown in Fig. 1a.

Research at the Radium Institute also include analysis of the spectra of recoil electrons knocked out of thin polystyrene films. Refined twofold focusing of electrons in a magnetic field, and electrical recording of coincidence events, were utilized in this analysis. From 1950 through 1966, the retron and electron spectrometers were used in the study of γ-ray spectra of over 30 radioactive nuclides [4-9]. These were the best γ-ray spectra obtainable during that time. The spectrum of γ-rays emitted by radium is depicted in Fig. 1b [9].

In recent years, γ-ray spectroscopy has undergone still further development: scintillation spectrometers have made their appearance, and later Ge(Li)-spectrometers. The γ-ray spectrum of radium which was measured in 1969 by Lingeman et al. [10] is shown in Fig. 1c. Thus, the development of γ-spectrometric techniques and hardware over the past 45 years is lucidly mirrored in Fig. 1a, b, c.

The second group of research papers forthcoming from the nuclear spectroscopy laboratory pertained to α-ray spectrometry. Until 1950, analysis of the spectra of α-particles has been performed primarily with the aid of ionization chambers, or in spectrometers with a uniform magnetic field (Rutherford spectrometer). The first group of instruments exhibits large aperture (high luminosity), but poor resolution; the second group exhibits excellent resolution at the cost of low luminosity.

*This report was delivered at the jubilee scientific session devoted to the 50th anniversary of the Radium Institute (January, 1972).

Translated from Atomnaya Énergiya, Vol. 34, No. 2, pp. 105-109, February, 1973. Original article submitted July 14, 1972.

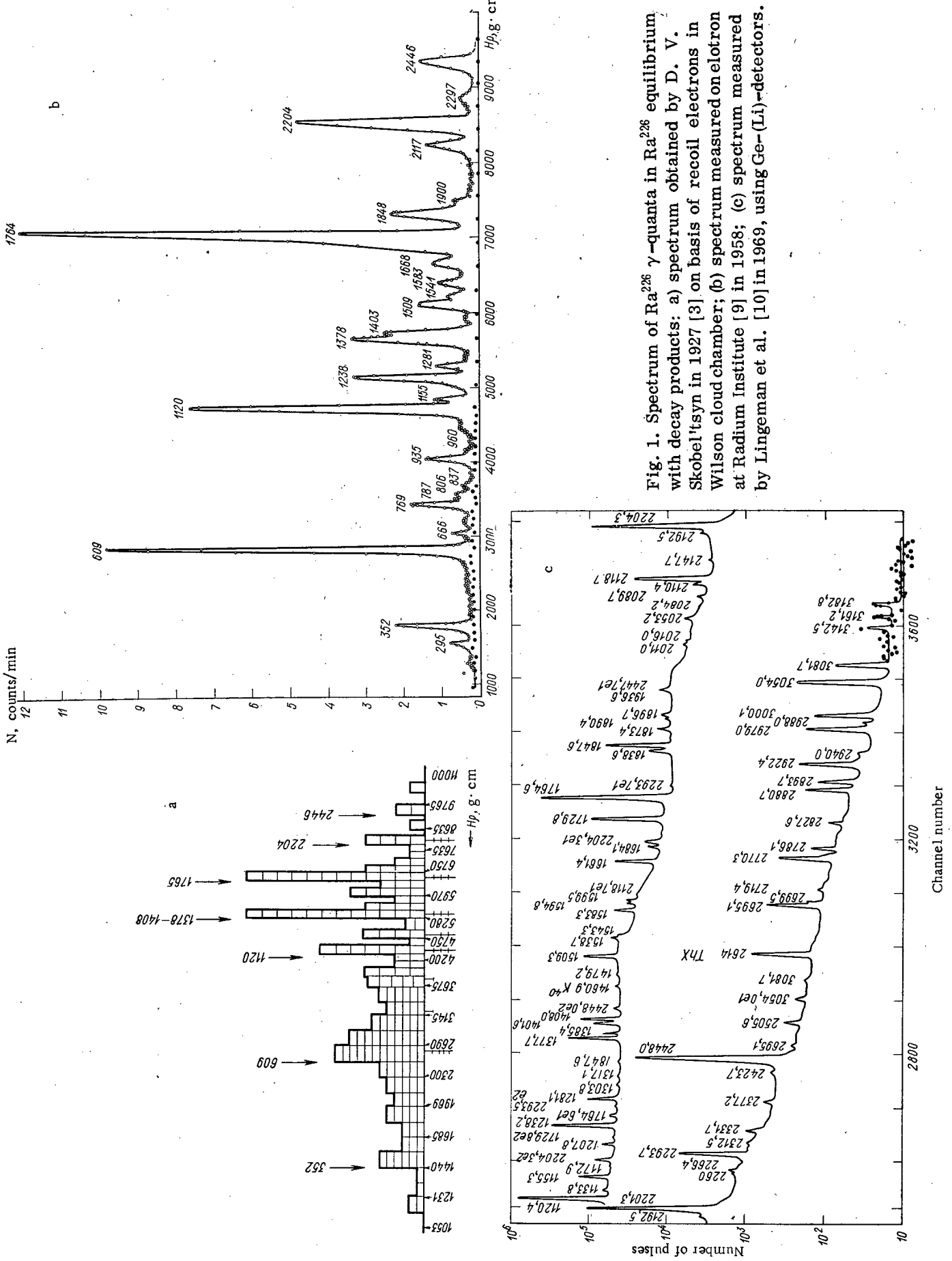

Fig. 1. Spectrum of Ra^{226} γ-quanta in Ra^{226} equilibrium with decay products: a) spectrum obtained by D. V. Skobel'tsyn in 1927 [3] on basis of recoil electrons in Wilson cloud chamber; (b) spectrum measured at Radium Institute [9] in 1958; (c) spectrum measured by Lingeman et al. [10] in 1969, using Ge-(Li)-detectors.

Of course, α-ray spectra exhibit a fine structure with components differing tens of thousands of times in intensity while the concomitant difference in energies is insignificant. Similar cases are encountered most frequently in the decay of nuclei having an odd number of nucleons; the excited states of the daughter nuclei of those nuclides are highly numerous and are situated close together. Under those conditions, investigation of α-decay with the aid of the methods already mentioned has little effect, and it became obvious, after β-ray spectrometry had been converted to the use of nonuniform magnetic fields, that such a conversion was also feasible in α-ray spectrometry. Reliance on the principle of focusing charged particles in a nonuniform magnetic field has made it possible to step up the luminosity of the instruments several tens of times without loss of high resolution.

The first instrument for these studies was built by a team headed up by L. L. Gol'din in 1956 [11]. The instrument proved useful in uncovering a host of interesting results, but the spectrometer luminosity left something to be desired, so that it proved difficult to study faint α-lines with the instrument. This meant that it was still necessary to devise instruments of greater aperture and with greater equilibrium orbit radii.

The α-ray spectrometer built at the Radium Institute in 1959 was designed for maximum luminosity a a line half-width $\approx$7 keV. The radius of the equilibrium orbit was 33.5 cm, the luminosity 0.21% of 4π [12]. This instrument was employed in studies of the spectra of nuclides $Cm^{242-246}$, $Pu^{239-241}$, U^{233}, and Ac^{225}, and its daughters [13, 14, 15].

An α-ray spectrometer such that R $\approx$ 150 cm was built by S. A. Baranov and colleagues in 1959 [16], and later by V. G. Chumin and colleagues in 1967 [17]. These spectrometers featured a resolving power of 1.3-2.0 keV at a luminosity of 0.04-0.09% of 4π. Figure 2 shows, as an example, images of the α-lines obtained by staff members of the Radium Institute and of JINR [18] in studies of Ac^{225} α-ray spectra.

The third instrument devised by the Radium Institute was a β-ray spectrometer with double focusing by a toroidal field (the "double orange") [19]. A schematic arrangement of this device is shown in Fig. 3. The use of a toroidal field provided excellent luminosity, while double focusing and spaced-out counters made for a low background of 4 to 5 coincidences per hour. The instrument can be used to measure spectra of conversion electrons emitted by very weak preparations. In the range Z = 30 and $\Delta E \cong 1$ MeV, the conversion ratios are very low (10^{-5} to 10^{-4}), and instruments of this type are needed for conversion measurements in neutron-deficient isotopes. Figure 4 shows the Ga^{69} lines K-1106 and K-1336. The conversion ratios for those lines are respectively $(2.7 \pm 0.4) \cdot 10^{-4}$ and $(1.6 \pm 0.4) \cdot 10^{-4}$ [20].

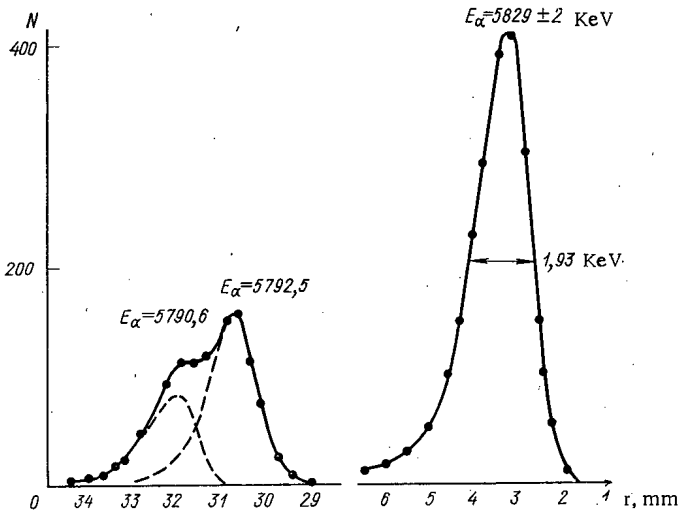

Fig. 2

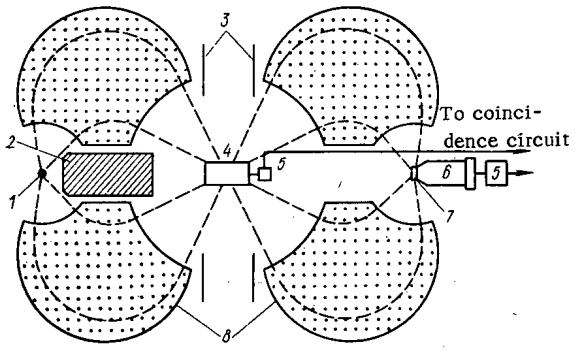

Fig. 3

Fig. 2. Portion of Ac^{225} γ-ray spectrum with α-transitions 5790.6 and 5792.5 keV (here r is the distance on the photographic plate; N is the number of α-tracks in the 400 μ band).

Fig. 3. Schematic design of β-ray spectrometer in plane of pole pieces: 1) source; 2) lead absorber; 3) diaphragm; 4) Geiger counter; 5) cathode follower; 6) photomultiplier; 7) acceptance slits and plastic scintillator; 8) pole pieces.

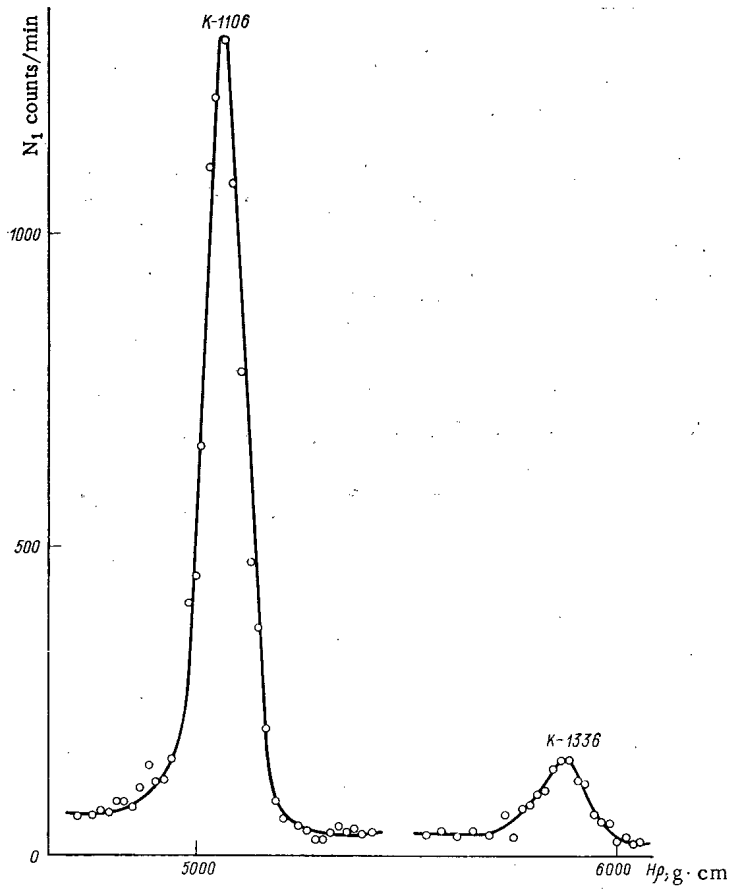

Fig. 4. Conversion spectrum of Ge^{69}.

A lot of other research work has also been done in the nuclear spectroscopy laboratory: investigations of the properties of neutron-deficient nuclides, investigation of annihilation, etc. [21-29].

LITERATURE CITED

1. B. S. Dzhelepov and M. L. Orbeli, Dokl. Akad. Nauk SSSR, 62, 615 (1948).
2. B. S. Dzhelepov, et al., Izv. Akad. Nauk SSSR, Ser. Fiz., 17, 518 (1953).
3. D. Skobelzyn, Z. Phys., 43, 354 (1927).
4. Soviet Research on Nuclear Spectroscopy. Bibliographic Index for 1917-1960 [in Russian], Nos. 976, 1091, 1095, 1103, 1106, 1120, 1127, 1128, 1132, 1160, 1161, 1181, 1208, 1211-1215, 1253, 1255, 1259, 1270, 1278, 1290, 1294, 1372, 1377, 1385, 1422, 1538, 1559, 1561, 1573, 1576, 1587, 1645, 1646, 1678, 1696, Izd. BAN SSSR, Leningrad (1965).
5. Soviet Research on Nuclear Spectroscopy. Bibliographic Index for 1961-1965 [in Russian], Nos. 1400, 1405, 1407, 1455, 1468, 1495, 1535, 1536, 1546, 1555, 1670, 1694, Izd. BAN SSSR, Leningrad (1968).
6. B. S. Dzhelepov, et al., Izv. Akad. Nauk SSSR, Ser. Fiz., 30, 403 (1966).
7. B. S. Dzhelepov, N. N. Zhukovskii, and A. G. Maloyan, Yad. Fiz., 1, 941 (1965); 3, 785 (1966).
8. B. S. Dzhelepov, et al., Izv. Nauk SSSR, Ser. Fiz., 30, 394 (1965).
9. B. S. Dzhelepov, et al., Nucl. Phys., 8, 250 (1958).
10. E. Lingeman et al., Nucl. Phys., A133, 630 (1966).
11. L. L. Gol'din, and E. F. Tret'yakov. Izv. Akad. Nauk SSSR, Ser. Fiz., 20, 859 (1956).
12. B. S. Dzhelepov, et al., Izv. Akad. Nauk SSSR, Ser. Fiz., 23, 782 (1959).
13. Soviet Reserach on Nuclear Spectroscopy. Bibliographic Index for 1917-1960 [in Russian], No. 1717, Izd. BAN SSSR, Leningrad (1965).
14. Soviet Research on Nuclear Spectroscopy. Bibliographic Index for 1961-1965 [in Russian], Nos. 946, 1726, 1748, 1761-1763, Izd. BAN SSSR, Leningrad (1968).
15. B. S. Dzhelepov, et al., Izv. Akad. Nauk SSSR, Ser. Fiz., 31, 151 (1967).

16. S. A. Baranov et al., Izv. Akad. Nauk SSSR, Ser. Fiz., 23, 1402 (1959).
17. N. A. Golovkov et al., JINR Preprint P13-3340 [in Russian], Dubna (1967).
18. N. A. Golovkov et al., Yad. Fiz (1972).
19. B. S. Dzhelepov, P. A. Tishkin, and I. A. Shishelov, Izv. Akad. Nauk SSSR, Ser. Fiz., 29, 2157 (1965).
20. B. S. Dzhelepov et al., Izv. Akad. Nauk SSSR, Ser. Fiz., 34, 1610 (1970).
21. Soviet Research on Nuclear Spectroscopy. Bibliographic Index for 1917-1960 [in Russian], Nos. 2456, 2460, 2462, 2463, Izd. BAN SSSR, Leningrand (1965).
22. Ya. Vrzal et al., Izv. Akad. Nauk SSSR, Ser. Fiz., 31, 1660 (1967).
23. Ya. Vrzal,et al., Izv. Akad. Nauk SSSR, Ser. Fiz., 31, 1647 (1967).
24. B. S. Dzhelepov, A. G. Dmitriev, and N. N. Zhukovskii, Izv. Akad. Nauk SSSR, Ser. Fiz., 33, 14 (1969).
25. B. S. Dzhelepov et al., Izv. Akad. Nauk SSSR, Ser. Fiz., 33, 1650 (1969).
26. Ya. Vrzal et al., Izv. Akad. Nauk SSSR, Ser. Fiz., 33, 7 (1969).
27. B. S. Dzhelepov et al., Izv. Akad. Nauk SSSR, Ser. Fiz., 34, 29 (1970).
28. B. S. Dzhelepov et al., Izv. Akad. Nauk SSSR, Ser. Fiz., 34, 2067 (1970).
29. B. S. Dzhelepov, A. G. Dmitriev, and N. N. Zhukovskii, Izv. Akad. Nauk SSSR, Ser. Fiz., 35, 2257 (1971).

BOOK REVIEWS

NEW BOOKS

E. E. Berlovich, S. S. Vasilenko, and Yu. N. Novikov, Lifetimes of Excited States of Atomic Nuclei*

The book goes into various aspects relating to the study of lifetimes of excited states of nuclei. The place occupied by nuclear transformations, in particular electromagnetic transitions in nuclei, in the time scales of processes occurring in nature is examined. Theoretical relations needed for calculating the partial probabilities of electromagnetic transitions are cited, and the basic theoretical formulas for the probabilities of transitions in the various nuclear models are discused. The principles underlying direct and indirect experimental techniques for measuring the lifetimes of levels are expounded. New aspects and perspectives in research are considered. Experimental data on the lifetimes of levels accumulated up to the beginning of 1970 are reviewed. These data are displayed in tabular form.

The book is written for specialists in nuclear physics.

A. P. Komar, S. P. Kruglov, and I. V. Lopatin, Measurement of Total Energy of Bremsstrahlung Beams from Electron Accelerators†

This monograph is the first in Soviet literature to present a systematic exposition of methods for measuring the total energy of beams of bremsstrahlung emitted by electron accelerators. The comparative characteristics of these methods are presented, and ways of developing and improving those methods still further are discussed. Considerable space is devoted to quantometers as the most promising instruments for absolute measurements of bremsstrahlung beam energy.

An appendix contains the latest tables of attenuation factors for γ-radiation in the energy range from 10 keV to 100 GeV, as well as energy losses and electron path lengths in various materials at energies ranging from 10 keV to 1 GeV.

The book is written for a broad readership of research scientists, engineers, and technicians concerned with bremsstrahlung and electrons, and also for graudate physics students.

Yu. V. Naumov and D. E. Kraft, Isobaric Spin in Nuclear Physics‡

This text offers a presentation of modern concepts on the role played by isobaric spin in nuclear physics. Selection rules on isospin for beta-decay, γ-radiation, and nuclear reactions are discussed. Topics pertaining to isospin impurities in heavy nuclides are covered. Data on excitation of analog states in various nuclear reactions are presented in detail. Special attention is focused on the possibility of securing information on the nuclear structure from experiments designed to study analog states.

The book is written for experimental physicists, instructors in technical colleges, and graduate physics majors.

*Nauka, Leningrad (1972).

†Nauka, Leningrad (1972).

‡Nauka Leningrad (1972).

Translated from Atomnaya Énergiya, Vol. 34, No. 2, pp. 109-110, February, 1973.

Nuclear Geophysics Techniques for Sampling and Assaying, and Processing Minerals*

This book is devoted to one of the new areas of application of nuclear geophysics techniques: sampling and assaying in the mining and ore processing industry. These methods of sampling make it possible to assess the quality of minerals and ores rapidly, at lower costs, and without taking physical samples from the product stream.

The text discusses problems in mining nuclear geophysics, currently familiar experience in applications of nuclear techiques in mines, results of recent work on copper–nickel, apatite, and rare-metal occurrences. Possibilities, opportunities, and the effectiveness of geophysical sampling and assaying under the concrete conditions prevailing in mines and occurrences of distinct types are discussed and evaluated on the basis of those examples. Results of laboratory research on the development of nuclear physics techniques for assaying and sampling minerals and ores are discussed.

The book is written for workers in the mining and ore processing industry involved in assaying and sampling of economic minerals at the point where the minerals are extracted and processes. The text can also prove useful to geophysicists, geologists, and other specialists utilizing nuclear physics methods in ultimate analysis of minerals and ores.

R. E. Krzhizhanovskii and Z. Yu. Shtern, Heat-Transfer of Nonmetallic Materials†

This reference handbook lists data on the physical properties of oxides and carbides over a broad range of temperatures and variation in other parameters. Attention is centered on the heat-transfer properties and thermodynamic properties of these materials. Available factual material serves as a basis for reflecting the effect exerted on those properties by factors such as temperature, heat-treatment history, amount of impurities present, density of material, and the surroundings.

The handbook is designed for a broad range of users including specialists engaged in research, design, and operation of power equipment and other equipment based on thermodynamic principles, and can also be useful to students at college level.

V. N. Andrianov, Fundamentals of Radiative Heat Transfer and Complex Heat Transfer‡

The book provides a systematic exposition of the theory behind radiative heat transfer and complex heat transfer, as well as methods for experimental research on those processes. Theoretical methods for calculations and investigations of radiative and complex heat transfer are also covered. New methods are proposed. An analysis of the similarity of those processes is accompanied by a discussion of experimental research techniques.

The book is written for research scientists, engineers, college instructors, graduate students, and undergraduate majors in heat power, heat transfer, and power plant specialties.

A. D. Smirnov, Refrence Handbook for the Power Industry**

The handbook reflects new rules for the operation of electric power plants and networks, electrical power plants in industrial enterprises, rules for technological design of fossil-fueled electric power generating stations and networks, and standards for basic electrical equipment.

The handbook is written for a broad range of specialists servicing electrical power plants in industrial enterprises.

*Nauka, Leningrad (1972).

†Energiya, Leningrad (1972).

‡Energiya, Moscow (1972).

**Second edition, Energiya, Moscow (1972).

M. L. Fel'dman and A. K. Chernovets, The Electrical Part of Nuclear Electric Power Stations*

The book presents features of the design, construction, and operation of the electrical part of nuclear electric power stations with different types of nuclear power reactors. Special attention is reserved for discussion of reliable operation of electrical power equipment and of the power station as a whole.

This book is the first systematized description of the electrical part of high-output nuclear power stations, and is intended for engineers and technicians involved in the operation, construction, and design of power station equipment, as well as for instructors, and students at graduate and undergraduate levels.

Ya. Vilenkin and E. A. Trakhtengerts, Mathematical Software for Process Control Equipment†

The book outlines the current techniques available for organizing mathematical software for process control computers. Multiprogramming techniques, dynamic memory distribution, buildup of large files of data, and information processing topics, are discussed. The discussion extends to methods for designing translators from programming languages, and mathematical techniques of program optimization.

The book is written for computer technology specialists.

*Energiya, Leningrad (1972).
†Energiya, Moscow (1972).

OPTIMIZATION OF HEAT REMOVAL IN A NUCLEAR-REACTOR CHANNEL AS A PROBLEM IN GAME THEORY

V. S. Ermakov and G. I. Zaluzhnyi

UDC 536.242:621.039.577

The article gives a description of an analytical investigation on the optimization of heat removal in a nuclear-reactor channel using the methods of game theory. In particular, we consider a cooperative bi-matrix game with arbitrary nonzero sum, in which we assume agreement in the compatible selection of parameters in the optimizable variants of heat removal in a reactor channel. The constructed working matrix is of the form

$$K(A, B)=\begin{pmatrix} a_{11}b_{11}, & a_{12}b_{12}, & \ldots, & a_{1m}b_{1m} \\ a_{21}b_{21}, & a_{22}b_{22}, & \ldots, & a_{2m}b_{2m} \\ a_{n1}b_{n1}, & a_{n2}b_{n2}, & \ldots, & a_{nm}b_{nm} \end{pmatrix}, \quad (1)$$

where a_{ij} and b_{ij} are matrix elements that depend linearly on the distributions λ_i and η_i, which characterize the volume occupied maximally and minimally by the thermally stressed packets of fuel elements in the reactor core, respectively. It is shown that the optimal solutions are complex strategies in the form of the vectors $x = \{x_1, x_2, \ldots, x_m\}$ and $y = \{y_1, y_2, \ldots, y_n\}$, which have positive components, and for which the following equality holds:

$$x_1+x_2+\ldots+x_m=y_1+y_2+\ldots+y_n=1.$$

The optimal strategies $x^{(0)}$ and $y^{(0)}$, determining the conditions of equilibrium and the value of the game S are as follows:

$$x^{(0)}=K^*J/K^*J^TJ; \quad (2)$$

$$y^{(0)}=K^*J^T/K^*J^TJ; \quad (3)$$

$$S=\Delta(K)/K^*J^TJ, \quad (4)$$

where K* is a reciprocal matrix consisting of cofactors of the elements of the matrix K; $\Delta(K)$ is the determinant of matrix K; J is a unit row-vector; and J^T is a transposed unit row-vector.

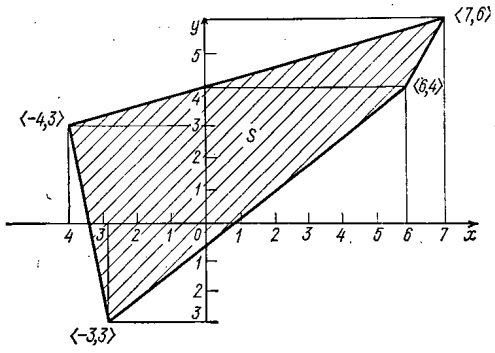

Fig. 1. Admissible region of variation of optimal strategies in the game.

The relation between the distributions λ_i and η_i and the calculated values of the heat removal in the optimizable variants are taken according to the functionals (5) and (6) for the maximal and minimal thermally stressed channels, respectively. The physical possibility of the selected functional relations was verified numerically in [1]:

$$I_i^Q=2\pi R_\Gamma\alpha\lambda_iQ\int_0^{L'}\int_{\tau_0}^{\tau_k}[\bar{t}(z,\tau)-\theta(z,\tau)]\,dz\,d\tau; \quad (5)$$

$$I_i^P=2\pi R_\Gamma\alpha\eta_iP\int_0^{L'}\int_{\tau_0}^{\tau_k}[\bar{t}(z_1,\tau)-\bar{\theta}(z,\tau)]\,dz\,d\tau, \quad (6)$$

Translated from Atomnaya Énergiya, Vol. 34, No. 2, p. 111, February, 1973. Original article submitted October 27, 1971.

where $t(z, \tau)$ is the average temperature of the material medium of the packets; $\theta(z, \tau)$ is the average temperature of the material medium of the coolant; and τ is the time. The total quantities of heat removed from the total volume of the zone G and from the annular subzone g_i are as follows:

$$I_i^g = I_i^Q + I_i^P, \tag{7}$$

$$I^G = (I_i^Q + I_i^P)/N, \tag{8}$$

where N is the number of annular subzones into which the core is divided.

The corresponding functions of transformation from the physical parameters of the core to the distribution parameters are as follows:

$$\text{a) } Q_i = \lambda_i Q; \quad \text{b) } P_i = \eta_i P; \quad \text{c) } G_i = g_i G,$$

where G, Q, and P are the volumes of the core, the maximal, and minimal thermally stressed packets. As an example we consider the simplest numerical case, which by randomization can be reduced to a (2×2)-matrix game. It is shown to be possible to reduce the problem to this simplest form in Fig. 1, in which we represent the admissible set S inside of which all the strategies of the game occur. The set obtained is convex, formed by the four coordinates a_{ij} and b_{ij}, and the two symmetric coordinates [2].

LITERATURE CITED

1. V. S. Ermakov et al., Inzh.-Fiz. Zh., 19, No. 2, 243 (1970).
2. G. Owen, Game Theory, Saunders (1968).

FORMULATION OF BOUNDARY CONDITIONS IN THE METHOD OF SUBGROUPS

M. N. Nikolaev and D. A. Usikov

UDC 621.039.51

The conditions discussed in an earlier paper by M. N. Nikolaev et al. relevant to the "joining" conditions of subgroup fluxes of neutrons on the interfaces between media [1] are not applicable to calculations of cells in heterogeneous lattices. This paper contains derivations of more general boundary conditions. The subgroup equations are derived in sequence from the kinetic equation in integral form.

The first stage involves averaging the equation about each lethargy u with respect to a smoothing interval Δu containing many resonances, and subsequent conversion from Riemann integration with respect to the energy to Lebesgue integration with respect to the total cross section. This results in the Σ-representation of the kinetic equation for the smoothed flux. The distribution function of the cross sections in the averaging interval is then approximated by the finite sums of the weighted delta-functions (δ-representation). The averaging of the resulting equations over the group intervals leads to a system of subgroup equations for each energy group.

It is clear from the derivation that the central focus in the problem of subgroup boundary conditions is the treatment of correlations in the structure of the cross sections of those media the collisionless flight length between which is not neglibibly short (e.g., contiguous media). In the case of a cell in a heterogeneous lattice, the correlations between the structure of cross sections of all media comprising the homogeneous zones of the lattice cell have to be taken into account as a rule.

Translated from Atomnaya Énergiya, Vol. 34, No. 2, p. 112, February, 1973. Original article submitted November 22, 1971.

Two methods have been proposed for the solution of this problem. In the first method (the method of "continuous" or "all-the-way" subgroups), the method of decomposition into subgroups is selected in a manner uniform for all the zones, so that the neutrons belonging to each subgroup have definite cross sections of interaction in each zone. The boundary conditions then assume their customary form and can be used in the solution of the kinetic equation whether in integral form or in integrodifferential form. The disadvantage of this method is that the number of such "all-the-way" subgroups within each group is equal to the product of the number of subgroups for all of the isotopes present in the system in question, that is to say, it can become quite large.

The second method calls for treatment of the subgroup structure of the cross sections individualized for each specific nuclide, and that entails solving a system of integral equations for the subgroup of densities of collisions with each of the isotopes exhibiting a resonant structure of cross sections within that group. Consequently, the total number of subgroups to be considered in this method is equal to the sum of the number of subgroups for the isotopes. This means that, for methods realizing the solution of the integral equation (Monte Carlo method, method of collision probabilities), the individual treatment of the subgroup structure of cross sections of the nuclides is to be preferred.

LITERATURE CITED

1. M. N. Nikolaev et al., At. Energ, 29, 11 (1970), 30, 426 (1971).

EFFECT OF THE STATE OF THE ZIRCONIUM SURFACE ON THE STRUCTURE AND PROTECTIVE PROPERTIES OF OXIDE FILMS FORMING IN A CORROSIVE ENVIRONMENT

I. I. Korobkov

UDC 620.197.5

The effect of the state of a zirconium surface with different degrees of structural and chemical nonuniformity brought about in the process of preparing the specimens (grain size comminution, contamination by oxygen, nitrogen, chlorine, or fluorine) on the phase composition and on the protective properties of oxide films forming when the specimen is heated in oxygen, water, and steam over a range of temperatures from 250° to 500°C was investigated.

The effect of zirconium grain size on the structure of the oxide films was investigated, using the example of oxidation of thin films (to 1000 Å) of the metal obtained by the method of evaporation and vacuum condensation (10^{-7} mm Hg). When the temperature of the substrate changes, a film with a different grain size results. The UEMV-100K electron microscope and the EG-100A electron diffraction camera were employed to measure the size of the original grain and the dimensions of the oxide crystals forming. Oxidation of zirconium films with grain size ≈50 Å in oxygen at temperature 250-270°C at first brings about an "amorphous" structure of oxide with crystalline grain size <10 Å. The oxide crystals are observed to grow with increasing time or temperature of oxidation, and a change ensues in the phase composition of the film. Only cubic ZrO_2 structure is observed in the film at crystalline grain sizes from 40 Å to 150 Å, but tetragonal structures are detected at grain sizes 150-200 Å, a mixture of tetragonal and monoclinic forms of ZrO_2 at grain sizes from 200 Å to 350 Å, and only monoclinic ZrO_2 at grain sizes 350 Å or larger. The sequence of transformations is related to the size of the ZrO_2 crystal grains in the film, which is the principal factor determining the stability of high-temperature modifications in the low-temperature range [1].

Translated from Atomnaya Énergiya, Vol. 34, No. 2, pp. 112-113, February, 1973. Original article submitted December 3, 1971.

When recrystallized zirconium foil <1000 Å in thickness, with an average grain size of the order of 1 μ, is oxidized, an oxide film consisting of a mixture of monoclinic and cubic (tetragonal) modifications of ZrO_2 forms on the surface of the foil; this oxide film eventually goes over slowly to the monoclinic form at 300°C. When a coarse-crystalline foil is oxidized, oriented growth of ZrO_2 single crystals of monoclinic structure is conspicuous. The orientation of the single crystals depends on the plane in the metal on which they nucleated.

After specimens of coarse-crystalline zirconium were treated in nitrogen (at 800°C), chlorine (600°C), or fluorine (300°C), fine ZrO_2 crystal grains, predominantly of a cubic modification with total or partial misorientation, form in response to oxidation. This same effect of reduction in the dimensions of crystal grains combined with misorientation of the crystal grains is observed in an oxide film in the case where oxygen is previously dissolved in the zirconium (over 5 at.%). In those instances, we observe high rates of oxidation of the specimen in the period prior to the transition alluded to above, and a pronounced dependence of the oxidation rate on the oxygen pressure, which is indicative of permeability of the oxide films to molecular oxgyen.

Apparently, the mechanism by which the oxygen, nitrogen, chlorine, and fluorine effect the process of zirconium oxidation exhibits a general physicochemical nature: all of these elements, when present on the surface of the specimen, have the effect of increasing the chemical inhomogeneity of the metal and bringing about nonuniform oxidation of grains, so that coherent bonding between the ZrO_2 crystal grains and the metallic zirconium is impaired and the grain size of the crystals ends up reduced. As the crystal grains undergo reduction in size, they may also experience a change in structure from monoclinic to tetragonal or cubic, accompanied by a corresponding reduction in the specific volume occupied by the ZrO_2. This transformation may well be the reason for the formation of pores sized 10 Å to 15 Å, observed in oxide films on zirconium [2]. When the number of pores in the film is sufficiently great, molecular oxygen becomes capable of penetrating through to the metallic zirconium substrate.

LITERATURE CITED

1. Yu. M. Polezhaev, Zh. Fiz. Khim., 41, No. 11, 2958 (1967).
2. B. Cox, J. Nucl. Materials, 29, No. 1, 50 (1969).

TIME SELECTION IN ACTIVATION ANALYSIS

G. S. Vozzhenikov

UDC 550.835

Activation of materials of complex chemical composition usually results in the formation of several artificially radioactive products including some that hinder quantitative analysis of tracer isotopes. Conditions favoring noise discrimination with the aid of time selection, which plays a role in nondestructive activation analysis similar to that played in radiochemical deactivation, in combined research efforts, are formulated in the text of the article.

If we assume that the disturbing influence exerted by any persistent or long-term noise at the instant when irradiation is terminated is not greater than a specified fraction δ_0 of the activity of the tracer isotope, then we end up with an expression including the time of activation t needed for noise discrimination:

$$\delta_0 i^{-1} = (1 - e^{-\varphi\lambda t})\,(1 - e^{-\lambda t})^{-1}, \qquad (1)$$

where i is the ratio of the saturated activities of the D-noise and the tracer; φ is the ratio of their decay constants; λ is the decay constant of the tracer.

Translated from Atomnaya Energiya, Vol, 34, No. 2, pp. 113-114, February, 1973. Original article submitted February 2, 1972.

As the activation time is shortened, the fraction contributed by any D-noise becomes smaller, relative to the activity of the tracer till it attains a minimum value at an exposure time of zero. For that reason we are confronted with a fundamental limitation in the discrimination of such D-noise, which can be written as the following inequality:

$$\delta_0 > ik. \tag{2}$$

In the case where (2) is observed, numerical solution of Eq. (1) can be used to find each of the m values of the activation time (m being the number of D-noise events in the medium), the minimum of which governs discrimination down to the specified level of what we term the "principal" D-noise. The fraction contributed by each of the remaining D-noise events will be smaller than δ_0.

Discrimination of short-lived noise is achieved by calculating the cooling time, i.e., the pause t_p between the instant when irradiation is terminated and when the induced activity begins to be recorded. Assuming that the disturbing influence of the K-noise does not exceed the specified fraction δ of the tracer activity during the cooling time, we get

$$t_{p, \Delta\lambda^k} = \ln \frac{j}{\delta}, \tag{3}$$

where j is the ratio of the induced activities of the K-noise and of the tracer at the moment the specimen is removed from activation: $\Delta\lambda^k = \lambda^k - \lambda$ (where λ^k is the decay constant of the K-noise).

Equation (3) can be used to determine, with ease, each of the n values of the cooling time (n is the number of K-noise events occurring in the medium), the maximum of which governs the decrease in the "principal" K-noise component down to a specified level. The fraction of each of the remaining K-noise components relative to the tracer activity will be less that δ.

When K-noise and D-noise are present simultaneously, it is more difficult to detect tracer present. In that case, we have to resort to the limiting value t_{max} of the cooling time, at which the ratio of the activities of the principal D-noise and of the tracer attains the maximum permissible level δ_{max}. This state of affairs places restrictions on time selection options, since we must have $t_p < t_{max}$, or

$$\delta_0/\delta_{max} > (j/\delta)^{\tau}, \tag{4}$$

where $\tau = (\lambda - \lambda)/(\lambda^k - \lambda)$ [sic]. Constraint (4) takes into account the ratio of activities of the decay constants, and the required accuracy of the measurements, so that it becomes possible to assess the feasibility of utilizing time selection in the detection of induced tracer activity when K-noise and D-noise are both present at the same time.

CHARACTERISTICS OF POINT ACTIVATION MEASUREMENTS MADE IN BOREHOLES WITH A CONTROLLED NEUTRON SOURCE

V. V. Strel'chenko and K. I. Yakubson

UDC 543.53

On the basis of calculated and experimental data, the authors analyze the relationship between the values of activation effects for pulsed and traditional versions of point activation measurements in boreholes as functions of the activation characteristics, the resulting radioactive isotopes, and the regimes of operation of a controlled neutron source.

Translated from Atomnaya Énergiya, Vol. 34, No. 2, p. 114, February, 1973. Original article submitted March 21, 1972.

They cite specific situations (types of nuclear reactions and half-life periods of radioactive isotopes, dimensions of the probe, time required for analysis, etc.); preference was given to the pulse version of the analysis.

SPECTRAL-ANGULAR DISTRIBUTION OF FAST NEUTRONS EMERGING FROM DIFFERENT SECTIONS OF THE SURFACE OF AN IRON REFLECTOR

D. B. Pozdneev and M. A. Faddeev

UDC 539.125.162.5:539.12.172

The Monte Carlo method is used for calculating the differential energy spectra of neutrons emerging from different sections of the surface of iron reflectors with thicknesses of 2, 4, 6, 10, 20, and 40 cm and the integral neutron characteristics of a 3-MeV isotropic source which is in contact with the material under investigation. The analysis is performed for different reflector sections with the radii r equal to 2, 4, 6, 10, 20, and 40 cm relative to the centrally located source for six ranges of the polar angle θ (0-15, 15-30, 30-45, 45-60, 60-75, 75-90°) and in two azimuthal directions. The contributions of the singly and multiply scattered neutrons to the total albedo were taken into account.

As an example, Fig. 1 shows the differential energy spectra of reflected fast neutrons emerging from different sections of the surface of an iron reflector with a thickness of 40 cm in the range $\theta = 0-15°$.

The results obtained are explained by taking into account the elastic and the inelastic scattering of fast neutrons and the excitation of individual nuclear levels.

Empirical equations suitable for engineering calculations are given.

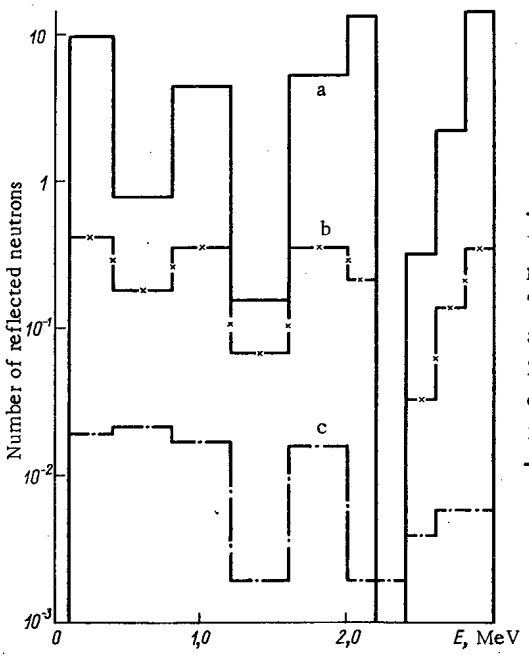

Fig. 1. Differential energy spectra of reflected fast neutrons (iron reflector thickness, 40 cm; $\theta = 0-15°$). The number of reflected neutrons emerging from an area of 1 cm^2 in the ranges of r values 0-2, 6-10, and 20-40 cm (a-c, respectively), calculated on the basis of 10^5 primary neutrons of energy 3 MeV incident at the reflector, is plotted along the ordinate.

Translated from Atomnaya Énergiya, Vol. 34, No. 2, p. 114, February, 1973. Original article submitted July 17, 1972.

LETTERS TO THE EDITOR

THE FREE ENERGY OF FORMATION OF URANYL IONS AT HIGH TEMPERATURES

R. P. Rafal'skii

UDC 541.11:541.135:546.791

In [1, 2] we published the results of the experimental determination of equilibrium concentrations of uranium in a solution in the presence of elementary sulfur at high temperatures. Processing of these data [3] made it possible to calculate the equilibrium constant of the reaction

$$3UO_2SO_4\,(aq) + S\,(l) + 4H_2O\,(l) = 3UO_2\,(s) + 4H^+\,(aq) + 4HSO_4^-\,(aq), \quad (1)$$

and then the equilibrium constant of the reaction

$$2UO_2^{2+}\,(aq) + 2H_2O\,(l) = 2UO_2\,(s) + 4H^+\,(aq) + O_2\,(r), \quad (2)$$

which is important in estimating the role of different complexes of hexavalent uranium in processes involving the transfer and deposition of this metal by natural hydrothermal solutions.

The present communication gives corrected values of the equilibrium constant of reaction (2), as well as values of the free energy of uranyl-ion formation in the solution at high temeratures, calculated on the basis of this constant.

The method of determination of the equilibrium constants of reactions (1) and (2) has been described in [3]. Here, however, we do not give the results of the calculation of the constant at 100°C, since we were not certain that we had achieved equilibrium in the corresponding experiments [2]. To clear up this question, we used the results of experiments on the reduction of hexavalent uranium in uranyl sulfate solutions by hydrogen sulfide [4]. As in the experiments involving $UO_2SO_4 + S + H_2O$, we calculated the equilibrium activities of the main components in the solution (H^+, HSO_4, H_2S, H_2SO_3) and the concentrations in the gaseous phase (H_2S; SO_2). The calculation method was the same as had been described earlier [3, 5]. In the calculation we made use of the balance equation

$$4a_U^0 q - \frac{n^0_{H_2S}}{V_{amp}} + [a_{H_2S}\,(aq) - 2a_{H_2SO_3}\,(aq) - 3a_{HSO_4^-}\,(aq)]q + [C_{H_2S}\,(g) - 2C_{SO_2}\,(g)](1-q) = 0,$$

where a_U^0 is the activity of uranium in the original UO_2SO_4 solution, which is taken to be equal to the initial concentration ($y_{UO_2SO_4} \approx 1$); $n^0_{H_2S}$ is the molar quantity of H_2S introduced into the ampule before the experiment; V_{amp} is the volume of the ampule; $q = V_{(aq)}/V_{tot}$ is a coefficient showing what fraction of the ampule has been filled.

From the results of our determination of the equilibrium activities (concentrations) of the components in the experiments involving $UO_2SO_4 + H_2S + H_2O$, conducted at three temperatures and for three values of $n^0_{H_2S}$, we found the corresponding values of K_1. When the latter were calculated from data obtained for the experiments with the smallest amount of H_2S ($V_{H_2S} = 5.6$ cm^3) they were found to be very close to the K_1 values found from the results of experiments involving $UO_2SO_4 + S + H_2O$ (Fig. 1). This indicates that we achieved equlibrium, or at least a near-equilibrium condition, in the experiments with sulfur at 100°C.

Translated from Atomnaya Énergiya, Vol. 34, No. 2, pp. 115-116, February, 1973. Original article submitted June 9, 1972.

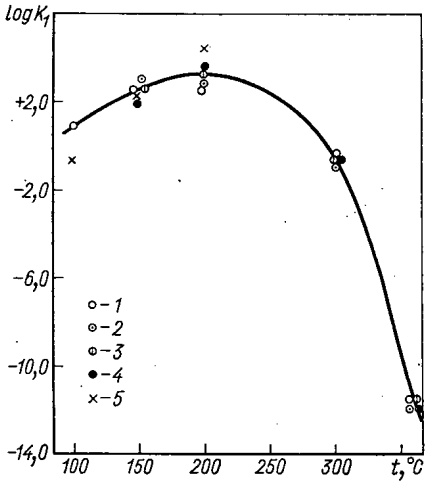

Fig. 1

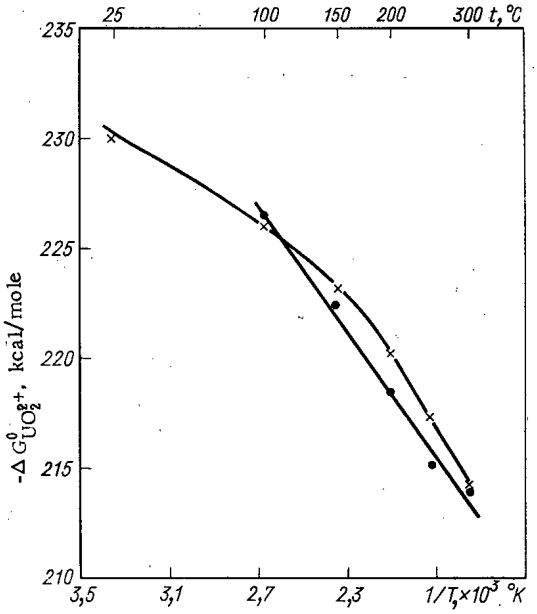

Fig. 2

Fig. 1. Values of log K_1 calculated from experimental data. The curve is drawn through the average values of log K_1 calculated from the results of the experiments involving $UO_2SO_4 + S + H_2O$; 1-4) from the results of experiments involving $UO_2SO_4 + S + H_2O$ conducted with original uranium concentrations of 2.5, 5, 10, and 20 g/liter, respectively (25 at 360°C); 5) from the results of experiments involving $UO_2SO_4 + H_2S + H_2O$ conducted with C^0_U = 9.8 g/liter and V_{H_2S} = 5.6 cm^3).

Fig. 2. Values of $\Delta G^0_{UO_2^{2+}}$ calculated on the basis of average experimental values of K_1 (⊜) and calculated from the data of [8] (×).

We found completely different results when we formally calculated K_1 from the data of experiments involving $UO_2SO_4 + H_2S + H_2O$ which were conducted for V_{H_2S} values of 16 and 32 cm^3. In this case the values of the equilibrium constant did not agree with each other at all, nor with the quantities shown in Fig. 1. For example, the value of log K_1 calculated for 150°C from the results of experiments conducted with V_{H_2S} = 5.6, 16, and 32 cm^3 are, respectively, 2.1, −17.9, and −26.4. Obviously, at high H_2S activity values the reactions taking place in the system are different from those taking place at low values of a_{H_2S}; this is also shown by the experimentally determined increase in the equilibrium constant of uranium in a solution with increased V_{H_2S} [4].

In calculating the equilibrium constant of reaction (2), we used the values of the constant of instability of uranyl monosulfate, UO_2SO_4, which was different from those used earlier. The later values were determined from an equation describing the variation as a function of temperature [6]. We give below the values of the equilibrium constant of reaction (2) which were calculated using the average experimental values of K_1*:

t, °C	100	150	200	250	300
log K^0_2	−42,8	−33,9	−26,9	−21,8	−19,0

Having determined the constant of equilibrium of reaction (2), we used the well-known relation

$$\Delta G^0 = -RT \ln K,$$

to find the value of ΔG^0 for this reaction at different temperatures, after which we calculated the free energy of formation of UO_2^{2+}:

$$\Delta G^0_{UO_2^{2+}(aq)} = \Delta G^0_{UO_2(s)} - \Delta G^0_{H_2O(l)} - \frac{1}{2}\Delta G^0_{reac} \qquad (3)$$

*The values of log K_1 for 250 and 350°C were obtained by graphical interpolation.

The values of $\Delta G^0_{H_2O(l)}$ at high temperatures, needed for calculating the free energy of formation of the uranyl ion, were taken from a handbook [7]. In order to calculate $\Delta G^0_{VO_2(s)}$ from the equation

$$\Delta G^0_T = \Delta H^0_{298} - T\Delta S^0_{298} + \int_{298}^{T} \Delta C^0_p dT - T\int_{298}^{T} \frac{\Delta C^0_p}{T} dT \qquad (4)$$

we used thermodynamic data from the same handbook.

The resulting values of $\Delta G^0_{UO_2^{2+}}$ are in good agreement with the values given in [8] (Fig. 2). However, according to our data, the graph of $\Delta G^0_{UO_2^{2+}}$ as a function of 1/T°K in the 100-300°C temperature range is nearly a straight line and may be described by the equation

$$\Delta G^0_{UO_2^{2+}} = -189{,}72 - 13{,}618 \cdot 10^3\, T^{-1}. \qquad (5)$$

The differences between the values of $\Delta G^0_{UO_2^{2+}}$ found from Eq. (5) and from Eq. (3) do not exceed 0.5 kcal/mole, which is evidently within the limits of experimental error.

LITERATURE CITED

1. R. P. Rafal'skii, A. D. Vlasov, and I. V. Nikol'skaya, Dokl. Akad. Nauk SSSR, 151, No. 2, 432 (1963).
2. A. D. Vlasov and R. P. Rafal'skii, Zh. Neorg, Khimi., 9, No. 9, 2222 (1964).
3. R. P. Rafal'skii, Dokl. Akad. Nauk SSSR, 199, No. 2, 448 (1971).
4. R. P. Rafal'skii and B. S. Osipov, At. Energ., 30, No. 1, 52 (1971).
5. R. P. Rafal'skii and A. I. Zarubin, Dokl. Akad. Nauk SSSR, 187, No. 3, 658 (1969).
6. N. M. Nikolaev, Izv. Sibirsk. Otd. Akad. Nauk SSSR, Ser. Khim. Nauk, No. 7, Part 3, 61 (1971).
7. G. B. Naumov, B. N. Ryzhenko, and I. L. Khodakovskii, Handbook of Thermodynamic Quantities [in Russian], Atomizdat, Moscow (1971).
8. A. A. Nikitin et al., Geokhimiya, No. 3, 297 (1972).

EXPERIMENTAL DATA ON THE THERMAL NEUTRON SPECTRUM IN WATER-MODERATED REACTORS

S. S. Lomakin and G. G. Panfilov

UDC 621.039.512.4

Calculation of the energy distribution of thermal neutrons shows that a complete description of the thermalization process requires taking account of the chemical binding and the crystal structure of the moderator.

A commonly used quantity for comparing calculation and experiment is the spectral index $I^r_{1/v}$:

$$I^r_{1/v} = \left(\frac{Cr}{C_{1/v}}\right)_x \Big/ \left(\frac{Cr}{C_{1/v}}\right)_0,$$

where the quantities in parentheses are the ratios of the saturated activities of the detectors. The activation cross section of one of the detectors has a resonance in the thermal neutron region and the cross section of the other is proportional to $1/v$. The detectors are irradiated at a point where the neutron spectrum is unknown and at a point where it is known. The experimentally determined spectral parameter $I^r_{1/v}$ is also used to reconstruct the thermal neutron spectrum by a method based on the Westcott formalism [1] and the representation of the neutron energy distribution function by polynomials [2].

We have measured the neutron energy distribution parameters by using activation detectors in certain types of water-moderated reactors. We measured the spectral indices and the cadmium ratios with Lu^{176}, Mn^{55}, Cu^{63} detectors.

Since Lu^{176} has a strong resonance at 0.142 eV the value of $I^{Lu}_{1/v}$ is very sensitive to a change in the thermal neutron spectrum. Depending on the experimental conditions manganese or copper was used as a $1/v$ detector.

Table 1 shows the results of our measurements of the spectral indices and cadmium ratios in the VVR and MR reactors [3] and the VVER [4]. In the latter case the detectors were irradiated in a reactor of the second unit of the Novo-Voronezh Atomic Power Plant in instrument channels passing through fuel assemblies with various U^{235} enrichments. The measurements of the parameters mentioned were made in the moderator.

TABLE 1. Spectral Indices and Cadmium Ratios in Water-Moderated Reactors

Reactor	U^{235} enrichment, %	Detector	Content of element, mg/cm²	Thickness of cadmium shield, mm	$I^{Lu}_{1/v}$	$R^{1/v}_{Cd}$
VVR	10	Lutecium	40	1,00	1,310±0,026	9,1±0,3
		Manganese	40			
MR	90	Lutecium	20	0,55	1,035±0,025	9,7±0,3
		Copper	18			
VVER	2	Lutecium	20	0,55	1,008±0,025	5,33±0,16
		Copper	45			
	1,5	Lutecium	20	0,55	1,000±0,025	6,50±0,20
		Copper	45			

TABLE 2. Neutron Temperature in Water-Moderated Reactors

Reactor	U^{235} enrichment, %	$\frac{\Sigma_a(kT_m)}{\Sigma_s}$	T_n, °K *	A *
VVR	10	0,137	400±12	2,02
MR	90	0,178 †	390±12	2,04
VVER	2	0,159	396±12	1,92
	1,5	0,126	375±11	1,85
RFR	10	0,138	394	2,11
MELUSINE	20	0,130	375	1,92

* Corrected experimental values.

† The value of $\Sigma_a(kT_m)/\Sigma_s$ for the fuel element assembly of the MR reactor was calculated by neglecting the effect of beryllium on the neutron spectrum inside the assembly.

Translated from Atomnaya Énergiya, Vol. 34, No. 2, pp. 117-118, February, 1973. Original article submitted May 20, 1971; revision submitted September 22, 1972.

The quantity $(C^{Lu}/C^{1/v})$ for detectors irradiated in the VVR reactor was measured in the graphite prism of the F-1 reactor [5], and at the core center in the MR and VVER reactors.

If the Westcott model of the neutron spectrum [1] is used the effective neutron temperature can be determined from the above data. For detectors of finite thickness the Westcott ratios have the form

$$\left(\frac{C^{Lu}}{C^{1/v}}\right)_x = B\,\frac{g^{Lu}(T_n)\,G_{th}^{Lu}(T_n)+rS^{Lu}(T_n)\,G_{epi}^{Lu}}{g^{1/v}(T_n)\,G_{th}^{1/v}+rS^{1/v}(T_n)\,G_{epi}^{1/v}};$$

$$R_{Cd}^{1/v}=\frac{g^{1/v}(T_n)\,G_{th}^{1/v}+rS^{1/v}(T_n)\,G_{epi}^{1/v}}{rS^{1/v}(T_n)\,G_{epi}^{1/v}+\frac{r}{k}\sqrt{T_n/T_0}},$$

where $g(T_n)$ and $S(T_n)$ are functions of the neutron energy and are tabulated in [6] for the most important detectors; T_n is the neutron temperature, G_{th} and G_{epi} are the self-shielding factors for thermal and epithermal neutrons, r is the Westcott parameter characterizing the fraction of epithermal neutrons, k is a factor taking account of the thickness of the cadmium shield and the isotropic nature of the neutron flux [1]. The values of r and T_n can be obtained by solving this system of equations; the constant B is determined from calibration measurements of $(C^{Lu}/C^{1/v})_0$.

The Westcott formalism should be used for weakly absorbing media when the thermal neutron spectrum can be adequately approximated by a Maxwellian distribution. According to Westcott [6] the ratio of the absorption cross section to the slowing down power $\Sigma_a/\xi\Sigma_s$ should not exceed 0.1, although he assumed that it could be larger. In [7, 8] a limit of 0.2 is established for $\Sigma_a/\xi\Sigma_s$.

Table 2 shows our measured values of the effective neutron temperature for water-moderated reactors, and data for the RFR and MELUSINE reactors obtained from [9, 10], based on the Westcott model. Table 2 shows $\Sigma_a(kT_m)/\Sigma_s$ calculated for a homogenized cell of the specific reactor. The value of σ_s was taken as 20 b per hydrogen atom and the disadvantage factor as 1.1. The experimental values of A were used to calculate the neutron temperature in the moderator from the relation

$$T_n = T_m\left[1+A\,\frac{\Sigma_a(kT_m)}{\Sigma_s}\right]$$

where T_m is the temperature of the moderator, °K.

Our experimental values of A for cells with various U^{235} enrichments and various uranium-to-water volume ratios are in good agreement with one another and with the results of other experimenters for the RFR and MELUSINE reactors.

The above results for water reactors and earlier data on graphite-moderated reactors [11] show that a first approximation to the neutron temperature in the moderator can be determined from the Coveyou formula or similar formulas of other authors [12-15] by using a value of A_{eff} appropriate to the kind of moderator, i.e.,

$$T_n = T_m\left[1+A_{eff}\,\frac{\Sigma_a(kT_m)}{\Sigma_s}\right].$$

For water reactors $A_{eff} = 1.98 \pm 0.08$ (the average of the A values given in Table 2).

LITERATURE CITED

1. C. Westcott et al., Second Geneva Conference, Paper 15/P202 (Canada) (1958).
2. G. Dixon and R. Sher, Nucl. Sci. and Engng., 41, 357 (1970).
3. V. V. Goncharov et al., Third Geneva Conference, Paper 323 (USSR) (1964).
4. A. Ya. Kramerov et al., Third Geneva Conferrence, Paper 304 (USSR) (1964).
5. S. S. Lomakin et al., Nuclear Instrument Making , Proceedings of the All-Union Scientific-Research Institute of Instrument Making, No. 12, [in Russian], Moscow (1970), p. 230.
6. C. Westcott, AECL-1101 (1960).
7. R. V. Meghreblian and D. Holmes, Reactor Analysis, McGraw-Hill, New York (1960).
8. D. Albert, Kernenergie, 10, No. 2 (1967).

9. D. Albert, ZFK-RN-13 (1961).
10. Neutron Fluence Measurements, Vienna, IAEA (1970).
11. S. S. Lomakin et al., At. Dnergiya, 29, No. 1, 36 (1970).
12. R. Coveyou et al., Nucl. Energy, 2, 153 (1956).
13. S. Kobayashi, J. Nucl. Sci. and Technol., 4, No. 9, 451 (1967).
14. E. Cohen, First Geneva Conference, Paper 611 (USA) (1955).
15. K. Beckurts and K. Wirtz, Neutron Physics, Springer, New York (1964).

EVALUATION OF NEUTRON SENSITIVITY FOR A PERSONNEL DOSIMETER USING TYPE-K NUCLEAR EMULSION

M. G. Gelev, M. M. Komochkov,
I. T. Mishev, and M. I. Salatskaya

UDC 539.12.08:621.386.82

During the past ten years at JINR, type-K nuclear emulsion 20 μ thick deposited on triacetate film and enclosed in a correcting holder [1, 2] has been used to measure the individual neutron doses received by staff members when working near radiation sources. In [1, 2] this method was verified for the measurement of the dose from fast neutrons ($0.5 \leq E < 15$ MeV); it allows dose measurement in the range 0.02–15 rem. However, in order to determine the total personnel dose from neutrons when working outside the thick shielding of reactors and accelerators, it is insufficient to know the fast neutron dose alone. As has been shown [3, 4], the contribution from thermal neutrons ($E < 0.4$ eV) in such cases to the total dose may amount to 10%, and to 60% or more for intermediate neutrons (0.4 eV $< E <$ 0.5 MeV). Consequently, personnel monitoring dosimeters must record with sufficient accuracy the dose not only from fast neutrons but also the dose from thermal and intermediate neutrons. This paper presents a calculated estimate of the sensitivity of a personnel neutron dosimeter using type-K emulsion to thermal and intermediate neutrons and an experimental verification of the sensitivity of such a dosimeter to thermal neutrons.

In the composition of the type-K emulsion used in personnel neutron dosimetry, nitrogen [5] appears along with other elements. Through the action of thermal neutrons, the reaction $N^{14}(n, p)C^{14}$ takes place in the emulsion with the emission of protons having an energy in the neighborhood of 6 MeV. The range of these protons in the emulsion is approximately 6μ. The number of protons, N(E), created per cm^2 of emulsion during its irradiation by neutrons with an energy E can be determined from

$$N(E) = \Phi(E)\,\sigma(E)\,A,$$

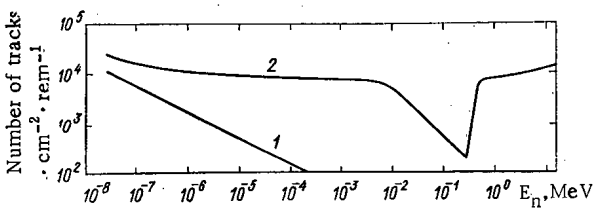

Fig. 1

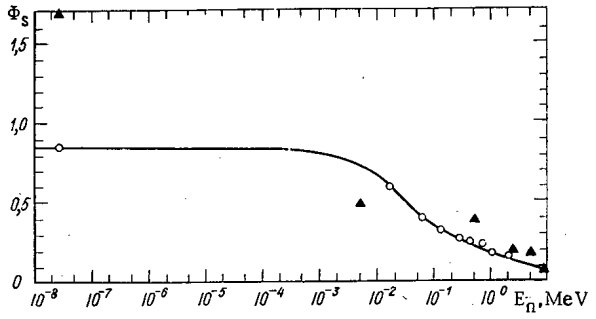

Fig. 2

Fig. 1. Dependence of calculated sensitivity of personnel dosimeter using type-K nuclear emulsion on neutron energy: 1) irradiation without phantom; 2) irradiation with phantom.

Fig. 2. Dependence of thermal neutron flux Φ_s scattered "backward" from a phantom for incidence of unit flux with energy E (data from [7]): ○) experiment; ▲) calculation.

Physics Institute, Bulgarian Academy of Sciences, Sofia, Bulgaria. Translated from Atomnaya Énergiya, Vol. 34, No. 2, pp. 118–121, February, 1973. Original article submitted February 7, 1972.

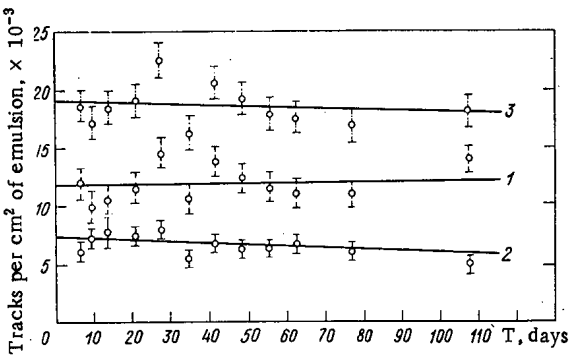

Fig. 3

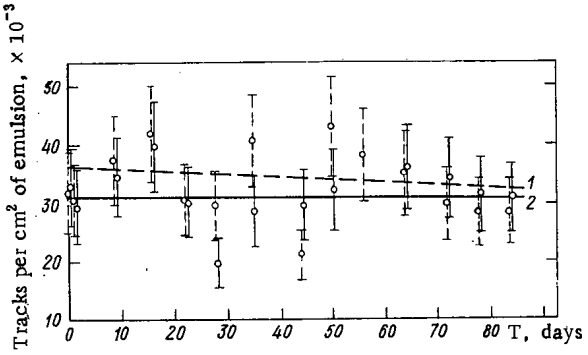

Fig. 4

Fig. 3. Dependence of emulsion track number on time between irradiation and processing (for constant absorbed dose): 1) number of tracks $\leq 6\mu$; 2) number of tracks $>6\mu$; 3) total number of tracks in emulsion.

Fig. 4. Dependence of emulsion track number on time between irradiation and processing (for constant absorbed dose): 1) number of tracks in films stored in refrigerator at 6°C; 2) number of tracks in films stored at room temperature.

TABLE 1. Neutron Sensitivity of Personnel Dosimeter Containing Type-K Emulsion Located on the Body

Neutron energy range	Sensitivity × 10^{-4}, tracks · cm^{-2} · rem^{-1}
Thermal neutrons (E < 0.4 eV)	1,6
0.4 eV-0.5 MeV (1/E spectrum)	0,16
0.5-0.15 MeV (Po-Be source)	0,92

where $\Phi(E)$ is the fluence of neutrons with energy E, $n \cdot cm^2$; $\sigma(E)$ is the cross section for the reaction N^{14} (n, p)C^{14}, cm^2; A is the number of nitrogen atoms per cm^2 of emulsion. For a type-K emulsion $20 \pm 3\mu$ thick, the value of A is $(7 \pm 1) \times 10^{18}$ cm^{-2}.

We assume that the detection efficiency for protons is 100% and that there is no fading in the emulsion; then the number of protons emitted from a nitrogen nucleus is equal to the number of recorded tracks formed by those protons. In Fig. 1, curve 1 shows the dependence of sensitivity on neutron energy as calculated under the above assumptions. Here and in the following, the sensitivity is expressed by the number of tracks per cm^2 of emulsion per rem of neutrons; the value of the quality factor (QF) for neutrons is taken from [6]. For neutrons with an energy of 0.025 eV, the cross section is taken to be 1.76×10^{-24} cm^2 and the variation of cross section with increase in neutron energy is assumed to be inversely proportional to velocity. As is clear from Fig. 1 (curve 1), a film with type-K emulsion cannot be used as a dosimeter for intermediate neutrons because of the steep drop in its sensitivity with increasing neutron energy. However, the use of such a film in a dosimeter which is worn on the body is possible for a broader range of neutron energies. As has been shown [7], the flux of thermal neutrons scattered from a phantom during its irradiation by intermediate neutrons depends weakly on energy up to 7 keV and is approximately 0.8 neutrons per incident neutron (Fig. 2). From data in [8], this quantity is about 0.5 neutrons per incident. The flux of thermal neutrons scattered from the phantom decreases markedly as the neutron energy increases. On the basis of data in [7], the energy dependence of the sensitivity of type-K emulsion (20 μ) to thermal and intermediate neutrons was calculated with the inclusion of emulsion registration of thermal neutrons scattered "backwards" from the phantom. The results are shown in Fig. 1 (curve 2). The portion of curve 2 for neutron energies above 0.3 MeV gives the dependence of the sensitivity to fast neutrons for an emulsion in a correcting holder [1]. As is clear from this data, emulsion in a correcting holder can be used as a personnel neutron dosimeter for neutrons with energies from thermal to 7 keV and from 0.5 to 15 MeV. In the neutron energy region 7-500 keV, the sensitivity of such a dosimeter varies markedly; therefore it cannot be used as a neutron dosimeter in that energy region.

To verify experimentally the sensitivity of personnel dosimeters using type-K emulsion (20μ) deposited on triacetate film to thermal neutrons, dosimeters were irradiated in the thermal column of an IRT-2000 reactor (Physical Institute, Bulgarian Academy of Sciences, Sofia). The cadmium ratio in the neutron beam was greater than 1000. The thermal neutron flux was measured with indium detectors and the error of the determination was ±20%. Under such conditions, it was found that the sensitivity of the dosimeter to thermal neutrons without a phantom was $(0.84 \pm 0.19) \times 10^4$ tracks · cm^{-2} · rem^{-1}. As was already pointed

TABLE 2. Dose Contributions from Various Neutron Groups at JINR Installations and Corresponding Dosimeter Sensitivities

Installation	Dose contribution, %			Dosimeter sensitivity, tracks·cm^{-2}·rem^{-1}	Correction factor
	Thermal neutrons E < 0.4eV	Intermediate neutrons, 0.4 < E < 0.5 MeV	Fast neutrons, 0.5 < E < 15 MeV		
Synchrocyclotron	5	55	40	$0,56 \cdot 10^4$	1,65
Proton synchrotoron	5	15	80	$0,84 \cdot 10^4$	1,1
IBR	10	55	35	$0,59 \cdot 10^4$	1,56
Cyclotron	3	37	60	$0,67 \cdot 10^4$	1,37

out (see Fig. 1, curve 1), the calculated sensitivity is $(1.23 \pm 0.18) \times 10^4$ tracks·cm^{-2} ·rem^{-1}. Actually, according to estimates, approximately 10% of the tracks contributing to the calculated values will not be counted in a microscopic examination because of short track length (less than 3μ) for protons escaping from the emulsion and because of large angles between the track and emulsion surface (more than 77°). Thus the calculated and experimental values of the sensitivity agree within the limits of error.

The sensitivity to thermal neutrons of a personnel dosimeter located on the body was determined from data in [7] by multiplying its sensitivity without a phantom by 1.86. The results are given in Table 1.

To estimate the sensitivity of a dosimeter to intermediate neutrons outside the thick concrete shield of a reactor or accelerator, one can assume the neutron spectrum is inversely proportional to energy (particularly at a reactor). The dosimeter sensitivity obtained under this assumption, including back-scatter of thermal neutrons from a phantom, and the experimentally determined sensitivity to thermal neutrons without a phantom are shown in Table 1. Also shown is the dosimeter sensitivity to fast neutrons according to [1].

The dosimeter sensitivity for fast neutrons is used in the method presently employed at JINR for measuring personnel neutron dose. However, this is not correct because there are thermal and intermediate neutrons in controlled areas. The relative dose contributions from neutrons of various energies in working areas outside the shielding of nuclear physics installations at JINR are shown in Table 2 [9]. The same table gives the neutron sensitivity of the personnel dosimeter calculated in accordance with this data and the correction factors K by which one should multiply the dose recorded in accordance with the method of [1] in order to obtain the total personnel dose from neutrons with energies from thermal to 15 MeV.

Thus the neutron dose recorded with a personnel dosimeter containing nuclear emulsion is underestimated by 10-65% for work in areas outside a shield; the degree of underestimation depends on the radiation source and the shield. Furthermore, the contribution of particles with energy above 20 MeV to the total dose outside a shield should not be greater than 5% [10]. A greater contribution to the dose by particles of high energy can lead to an overestimate of the recorded personnel dose.

Because the tracks of protons from nitrogen are short, it is of interest to study the dependence of track fading in the emulsion on the time between irradiation and emulsion processing. The results of the experiments are shown in Figs. 3 and 4. The figures indicate that fading can be neglected over a period of 100 days after irradiation since its magnitude remains with the limits of error, which is approximately 20%. In addition, reduction in the number of tracks in the film was not observed when the films were stored in a refrigerator or under room conditions similar to the working conditions under which staff members wear or store personnel dosimeters.

Thus, the measured value of the personnel dose for fast neutrons measured by means of the method employed at JINR is overestimated by 10-80% because of the thermal neutron sensitivity of type-K nuclear emulsion. However, if a correction factor of 1.5 is introduced, one can assume that a personnel dosimeter records the total dose from neutrons with energies from thermal to 15 MeV under the working conditions of staff members at the IBR and cyclotron. For staff memebers working at the synchrocyclotron and the proton synchrotron, the introduction of such a factor is permissible only in those cases where the contribution of ultrafast nucleons to the dose does not exceed 5%.

The authors are grateful to L. B. Smirnova and G. P. Korableva for scanning the films under a microscope and to S. Pshone and V. E. Aleinikov for help with the film irradiations.

LITERATURE CITED

1. L. S. Zolin, V. N. Lebedev, and M. I. Salatskaya, At. Energ., 13, No. 5, 467 (1962).
2. M. I. Salatskaya, V. N. Lebedev, and L. S. Zolin, in: Radiation Physics [in Russian], T. P. 5, Riga (1964), p. 107.
3. D. Nachtigall, Neutron Monitoring, IAEA, Vienna (1967), p. 333.
4. V. A. Knyazev et al., At. Energ., 27, 210 (1969).
5. M. F. Rodicheva, Zh. Nauchn. i Prikl. Fotografii i Kinematografii, 5, No. 3, 221 (1960).
6. Basic Safety Standards for Radiation Shielding. Safety Series No. 9, IAEA, Vienna (1968).
7. J. Dennis et al., Neutron Monitoring, IAEA, Vienna (1967), p. 537.
8. P. Nagarajan and D. Krishnan, Health Phys., 17, 323 (1969).
9. V. E. Aleinikov et al., JINR Publication B1-2759 (1966).
10. V. E. Aleinikov et al., Proceedings of International Congress on Protection against Accelerator and Space Radiation, Vol. I, CERN, Geneva (1971), p. 282.

EVALUATION OF SILICON SEMICONDUCTOR DETECTOR EFFICIENCY FOR 0.661 AND 1.25 MeV GAMMA RAYS

M. L. Gol'din, K. R. Pater-Razumovskii, and F. V. Virnik

UDC 539.1.074

One of the important problems in the field of radioisotopic instrument manufacture is the calculation of a gamma emitter from the known counting efficiency ξ of a detector. There is interest in obtaining a formula for the calculation of the quantity ξ for silicon semiconductor detectors (SSD), which are finding ever increasing application in technology.

A silicon p–i–n detector can be considered as a layer of semiconductor of thickness W (depth of the compensated region) which does not depend on the bias voltage U_b. The detection efficiency of such a model for a parallel flux of gamma rays can be determined from

$$\xi = 1 - \exp(-\mu W), \quad (1)$$

where μ is the linear attenuation coefficient. Interaction of the radiation with the "dead" layer is not taken into account because the thickness of the latter is considerably less than W in most cases.

The Compton interaction predominates in silicon for gamma ray energies of 0.661 and 1.25 MeV [1] (values widely used in radioisotopic instrument manufacture). One need consider only single interactions [2] because the mean free path of gamma rays with the energies mentioned is greater than the quantity W of detectors suitable for commercial application. The Compton electron spectrum will be reproduced by the

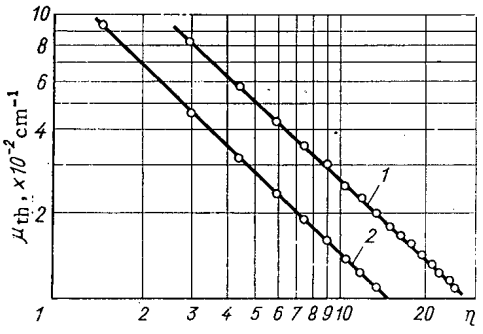

Fig. 1

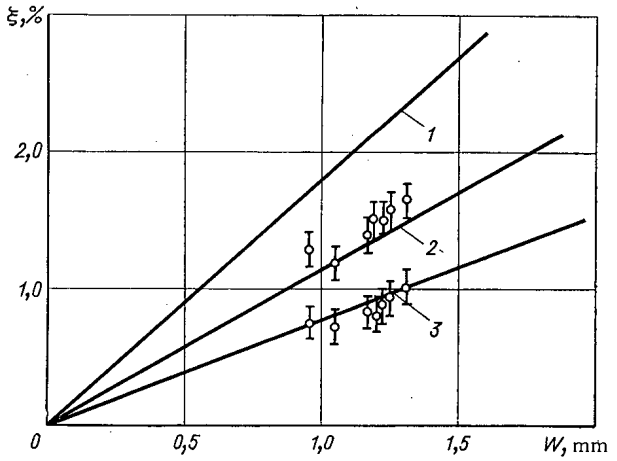

Fig. 2

Fig. 1. Dependence of μ_{th} on the ratio of primary gamma ray energy and detection threshold: 1) Cs^{137}, E_γ = 0.661 MeV; 2) Co^{60}, E_γ = 1.25 MeV; ○) calculated values of μ_{th}.

Fig. 2. Dependence of counting efficiency of silicon p–i–n detectors on detection threshold and sensitive layer thickness for Cs^{137}: 1) $E_{th} \to 0$; 2) E_{th} = 200 keV; 3) E_{th} = 300 keV; –) theoretical lines; ○) experimental points.

Translated from Atomnaya Énergiya, Vol. 34, No. 2, pp. 121-122, February, 1973. Original article submitted March 24, 1972.

detector in the form of a pulse height spectrum. Therefore the number of recorded gamma rays, and consequently the counting efficiency of the detector also, will depend on the detection threshold E_{th}, which is usually determined by the noise level in the detector – preamplifier system. However, the detection of gamma rays with energies $E_k < E_{th}$ is associated with certain difficulties because their energy value is commensurate with the noise. Therefore Eq. (1) for the case under consideration should be rewritten as

$$\xi = 1 - \exp[-(\mu - \mu_{th})W], \tag{2}$$

where μ_{th} is a linear attenuation coefficient which takes into account the loss of energy by gamma rays with $E_k < E_{th}$. The energy of scattered quanta is given by the expression

$$E' = \frac{E_\gamma}{1 + \frac{E_\gamma}{m_0 c^2}(1 - \cos\theta_{th}} = E_\gamma - E_{th} \tag{3}$$

whence

$$\cos\theta_{th} = 1 - \frac{1}{\alpha(\eta - 1)}, \tag{4}$$

where

$$\alpha = \frac{E_\gamma}{m_0 c^2}; \quad \eta = \frac{E_\gamma}{E_{th}};$$

E_γ is the energy of gamma rays incident on the detector.

From well-known formulas [3], one can calculate the quantity μ_{th} and plot the relationship $\mu_{th} = f(\eta)$ (Fig. 1). Using the method of "stretched strings" [4], empirical formulas were obtained for Cs^{137} and Co^{60} respectively:

$$\mu_{th} = 0.24\eta^{-0,95}; \quad \xi = 1 - \exp[(-0.186 - 0.24\eta^{-0,95})W], \tag{5}$$

$$\mu_{th} = 0.14\eta^{-0,98}; \quad \xi = 1 - \exp[(-0.133 - 0.14\eta^{-0,98})W]. \tag{6}$$

Standard sources were used for an experimental check of Eqs. (5) and (6). The system for detection of gamma rays consisted of DKD-0 and DDR 12/2 detectors [5], a transistorized charge-sensitive preamplifier [6], a UIS-2 main amplifier, and an ADD-1 discriminator. Pulses from the integral output of the discriminator were recorded with a pp-15 instrument. The system was calibrated by means of the Compton edge of the electron spectrum. The experimental results are shown in Fig. 2.

If $W \leq 5$ mm, one can use linear approximations to Eqs. (5) and (6) with an accuracy of 5% which are for Cs^{137} and Co^{60} respectively

$$\xi = (0.186 - 0.24\eta^{-0.95})W; \tag{7}$$

$$\xi = (0.133 - 0.14\eta^{-0.98})W. \tag{8}$$

LITERATURE CITED

1. G. Dearnaley and D. C. Northrop, Semiconductor Detectors for Nuclear Radiations [Russian translation], Mir, Moscow (1966).
2. O. I. Leipunskii, Gamma Radiation from an Atomic Explosion [in Russian], Atomizdat, Moscow (1959).
3. K. Sieghahn (editior), Alpha, Beta, and Gamma Spectroscopy [Russian translation], Atomizdat, Moscow (1968).
4. R. S. Guter and B. V. Ovchinskii, Elements of Numerical Analysis and the Mathematical Treatment of Experimental Results [in Russian], Nauka, Moscow (1969).
5. Silicon Surface-Barrier and Diffusion-Drift Semiconductor Detectors for Nuclear Radiations [in Russian], V/O Isotop, Moscow (1968).
6. M. L. Gol'din et al., Izv. Vuz. Priborostroenie, No. 7, 16 (1971).

DETECTOR CHARACTERISTICS OF A SILICON CARBIDE DETECTOR PREPARED BY THE DIFFUSION OF BERYLLIUM

V. A. Tikhomirova, O. P. Fedoseeva, and G. F. Kholuyarov

UDC 539.1.074

For some time past interest has been shown in nuclear particle detectors based on a single hexagonal crystal of silicon carbide which can be used at temperatures of 600°C [1-3]. The radiation stability of these detectors is essentially greater than that of silicon. The present work deals with their investigation.

The detectors are prepared by making a p–n transistor by a diffusion method at 1900-2000°C from gaseous aluminum [1] or boron [2] and a single crystal of n-type silicon carbide with a specific resistance of 1-2 ohm · cm. The size of the sensitive area in the detector is 1-3 μ. It is difficult to obtain a larger sensitive area with a comparable energy detection range in SiC due to the low diffusion coefficient of this dopant in SiC. Detectors so made are characterized by an energy resolution in the range of 15-20% and low efficiency of the sensitive area.

In the present work SiC detectors were made by diffusing beryllium which has a diffusion coefficient in SiC of two to three times that of boron or aluminum [4]. The depth of the p–n transistor region is 10-20μ; this was achieved by diffusing beryllium into n-SiC at a temperature of 1600-1700°C for 20-30 min.

The ohmic contact to the n side was a thermoresistant alloy of tungsten with nickel, imbedded in vacuo at 1600°C, and the contact to the p side (detector window) was metallic chromium, diffused by vacuum sputtering to a thickness of 400 to 500 Å.

The energy resolution of the detector was studied using alpha particles from U^{235} (4.8 MeV) and fission fragments obtained in a reactor by irradiation of U^{235} (90% enriched) under a 6 mg/cm^2 cover.

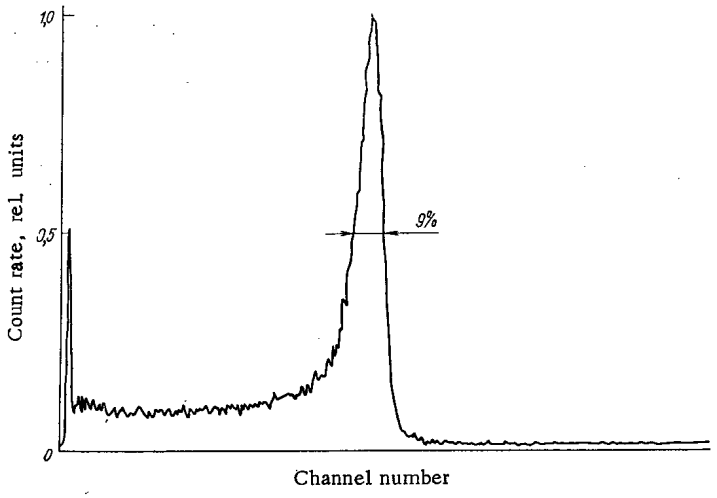

Fig. 1. Energy spectrum of alpha particles, obtained with a SiC detector, biased at 60 V.

Translated from Atomnaya Énergiya, Vol. 34, No. 2, pp. 122-124, February, 1973. Original article submitted May 18, 1972.

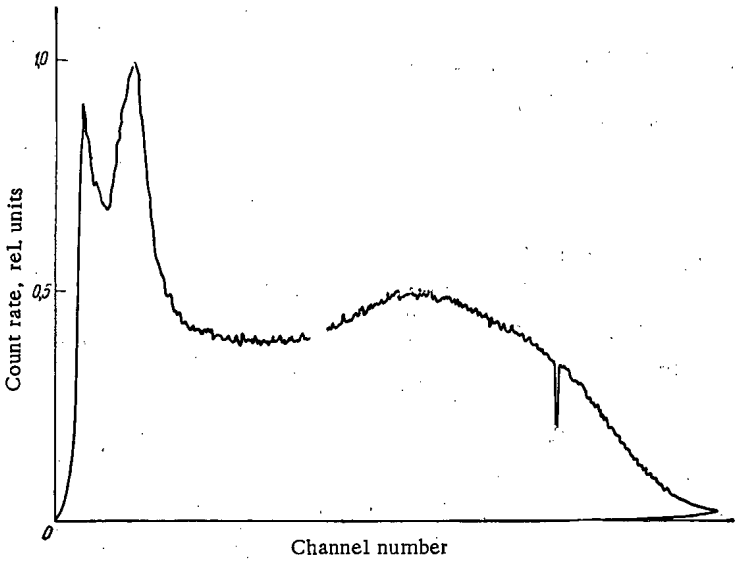

Fig. 2

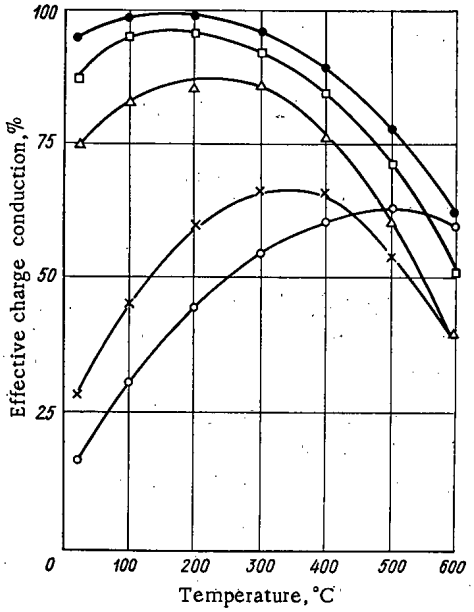

Fig. 3

Fig. 2. Spectrum of U^{235} fission fragments, obtained with a SiC detector.

Fig. 3. Dependence of the effective charge conduction of SiC detectors on temperature (dependence plotted at 60V bias).

In Figs. 1 and 2 typical energy spectra for alpha particles and fission fragments are shown. The energy resolution for alpha particles is 9%, and the effective detection of the alpha particles is 100%, which is substantially greater than that obtained with the SiC detectors used.

Figure 2 shows that the pulses produced by fission fragments are satisfactorily resolved from the noise and uranium alpha particle pulses; this ensures the assignment of the pulses to the fission fragments.

Detectors based on silicon carbide will detect particles to 600°C [3]. The typical dependence of effective charge collection on temperature in SiC detectors with "berylliated" p–n junctions is shown in Fig. 3.

The effective charge conduction of the apparatus was determined by calibration of the alpha particle source with a surface barrier detector of ~10% resolution and using the known average energy created by an electron/hole pair in silicon and silicon carbide.

Comparative studies of the radiation stability of SiC detectors show that they are slightly dependent on the nature of the acceptor and unknown details of how the detector was made.

For examination of the detectors it is possible to use a highly thermalized neutron flux in a fuel-element reactor. Application of radiation with different threshold energy divisions allows estimation of the neutron spectra.

The authors express appreciation to K. A. Konoplev, N. Ya. Semenov, and V. V. Bolshakor for assistance in the reactor experiments.

LITERATURE CITED

1. R. Babcock and H. Chang, Symposium on Neutron Dosimetry, Harwell, England (1962).
2. G. N. Violina et al., Proceedings of the Second Conference on Dosimetry at Large Doses [in Russian], FAN, Tashkent (1966), p. 140.
3. R. Sapera et al., IEEE, No. 5 (1964).
4. Yu. A. Vodakov, Author's Abstract of Candidate's Dissertation [in Russian], Leningrad (1968).

RADIATION STABILITY OF SCINTILLATING PLASTICS

E. D. Beregovenko, V. M. Gorbachev,
and N. A. Uvarov

UDC 539.373.1

Changes in the light yield of scintillating plastics based on polystyrene (PS) in the case of irradiation on static radiation sources were discussed in [1-4]. This work presents the results of an experimental evaluation of changes in the light yield of PS under the influence of pulsed x-radiation.

The radiation source was a pulsed MIG-5000 x-ray tube [5]. In the case of a pulse duration of 1/μsec and an average quantum energy ~0.7 MeV, the maximum dose in the pulse was $2 \cdot 10^4$ R. The dose was measured with glass dosimeters.

The relative losses of the light yield of the scintillator for various time intervals after irradiation, T_{meas}, was determined by two methods: 1) for $T_{meas} \approx (2\text{-}12) \cdot 10^{-6}$ sec according to the change in the transparency of the scintillator for the light radiation of a flash lamp of the IFK type, measured with a photocell; 2) for $T_{meas} \geq 1$ min, the investigated PS was set up on a photomultiplier and a determination was made of the relative change in the value of the exit curve of the FEU during irradiation of the PS with γ quanta of a Co^{60} source before and after the pulse of x-radiation.

If we assume that the concentration of centers of absorption of light is proportional to the dose, then the change in the transparency of the scintillator during its radioscopy with a pulsed flash lamp can be estimated by the ratio

$$I_D/I_0 = e^{-\alpha Dh}, \quad (1)$$

where I_0 and I_D are the currents at the exit of the photoreceiver for PS nonirradiated and irradiated with an x-ray pulse with a dose D, respectively; h is the thickness of the scintillator, cm; α is the coefficient of radiation rarefaction, $R^{-1} \cdot cm^{-1}$.

The change in the light yield of an irradiated scintillator after volume excitation of luminescence with γ quanta is determined by the ratio [6]

$$\frac{I_D}{I_0} = \frac{1 - e^{-\alpha Dh}}{\alpha Dh}. \quad (2)$$

For scintillating plastics based on polystyrene containing 2% paraterphenyl and 0.06% POPOP (cylindrical samples 40-50 mm in diameter and 5-100 mm high were used), we performed 16 irradiations. From the oscillograns obtained, the ratio of the areas under the envelopes of current pulses of the photocell from the flash of the IFK lamp before and after irradiation, which determines the average change in the transparency for the time interval 2-12 μsec after irradiation, was found. The average value of I_D/I_0 was

$$\alpha = (6.44 \pm 0.54) \cdot 10^{-5} \ R^{-1} \cdot cm^{-1},$$

which corresponds to a ~10% loss of transparency at the dose 300 R for a scintillator 50 mm high.

The measurement of the transparency of PS at the moment of time 1, 2, and 10 min after pulsed irradiation was performed under the influence of the γ quanta of Co^{60}. Treatment of the results of these measurements according to formula (2) yielded the following values: for 1 min, $\alpha = 1.34 \cdot 10^{-5}$ $R^{-1} \cdot cm^{-1}$; for 2 min, $\alpha = 1.28 \cdot 10^{-5} R^{-1} \cdot cm^{-1}$; for 10 min, $\alpha = 1.0 \cdot 10^{-5} R^{-1} \cdot cm^{-1}$. The experimentally observable decrease in α with time is evidence of the existence of an effect of restoration of transparency of the scintillator.

Translated from Atomnaya Énergiya, Vol. 34, No. 2, p. 124, February, 1973. Original article submitted June 7, 1972.

During a period of 10 min after irradiation, the value of α decreased sixfold, which corresponds to an absolute restoration of transparency of the scintillator of approximately 400-fold.

The value of the coefficient of radiation damage α in the microsecond region significantly exceeds (by approximately 1000-fold) the previously known values [1-4] and is evidence of the incorrectness of an extension of data obtained on sources of constant intensity to the case of pulsed irradiation.

LITERATURE CITED

1. I. M. Rozman and K. G. Tsimmer, At. Energ., 1, 54 (1957).
2. I. M. Rozman, Izv. Akad. Nauk SSSR, Ser. Fiz., 22, No. 1, 60 (1958).
3. V. D. Bezuglyi and L. L. Nagornaya, At. Energ., 17, 67 (1964).
4. C. Hammon, Kernenergie, 5, No. 12, 845 (1962).
5. K. F. Zelenskii et al., Pribory i Tekhnika Eksperimenta, No. 4, 177 (1969).
6. V. M. Gorbachev and N. A. Uvarov, ibid., No. 3, 123 (1970).

A LOW-BACKGROUND GAMMA SPECTROMETER

Yu. A. Surkov and O. P. Sobornov

UDC 535.853

The scintillation gamma spectrometer is intended for studying low contents of radioactive isotopes in samples of various material compositions. The operating principles were considered in [1]. The possibility of replacing the analyzing detectors (NaI/Tl single crystals) enables the research worker to use the most convenient geometry in order to carry out various types of measurement. The background of the apparatus is reduced by means of a massive lead, steel, and copper screen (total thickness 160 mm) and by a special choice of construction materials and active shielding using a plastic scintillator. The block diagram of the apparatus is shown in Fig. 1.

The shield detector has the shape of a cylinder 400 × 410 mm in size with a well (dimensions ϕ120 × 270 mm) perpendicular to the axis. At the conical ends it is provided with two FEU-49 photomultipliers. The scintillator is covered with a white titanium enamel. In the well is a stainless steel vessel with sides 0.3 mm thick containing the analyzing detector, which is capable of being moved horizontally and vertically by means of a special mechanism, so enabling the samples and crystals to be replaced. In the working position the detector lies in the center of the plastic scintillator. The sides of the shielding structure are set rails and may be moved by means of horizontal displacement mechanisms allowing access to the structural elements of the active shielding. When studying samples 5-50 cm^3 in size the main analyzing detector is an NaI/Tl crystal ϕ100 × 100 mm in size with a well (size ϕ 33 × 60 mm). The resolution of this detector with respect to Cs^{137} (using an FEU-52M) is 9.0%. The crystal is set in a container made of oxygen-free copper with a quartz light-guide window 18 mm thick. In measuring samples up to 500 cm^3 a scintillation unit with an NaI/Tl crystal ϕ 76 × 76 mm in size is employed; this has a resolution of 8.4%. In this case the specimen is placed in a special container around the crystal in the form of a layer 12 mm thick. The apparatus is situated below ground level. A concrete cover some 300 g/cm^2 thick placed above the apparatus further reduces the contribution of cosmic rays to the background spectrum. In order to reduce the contribution from emanations, a blower system is incorproated, and the analyzing detector is automatically made airtight in the working position. As a result of the shielding, the background level in the range 150-3600 keV is reduced by a factor of 80-100 times. The limiting reduction is governed by the intrinsic radioactivity [2].

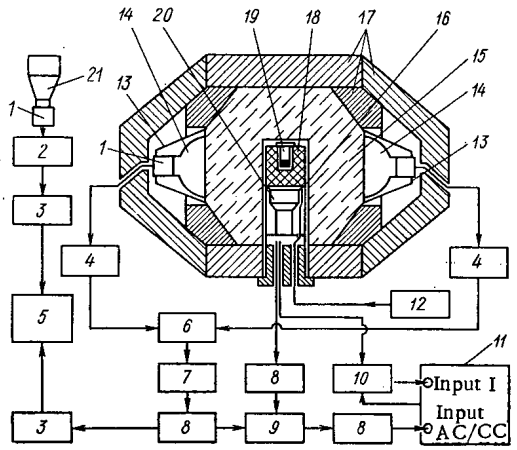

Fig. 1. Block diagram of the apparatus: 1) emitter follower; 2) amplifier-discriminator; 3) intensity meter; 4) amplifier; 5) automatic recording potentiometer (EPP-09M1); 6) adder; 7) delay line; 8) amplifier-shaper; 9) coincidence circuit; 10) digital stabilizer; 11) pulse amplitude analyzer; 12) generator; 13) light-shield screens; 14) FEU-49 photomultiplier; 15) plastic scintillator; 16) light diode; 17) structural elements of shielding; 18) NaI/Tl analyzing detector; 19) Teflon vessel holding the substance under analysis; 20) FEU-52M photomultiplier; 21) sensor for testing external background.

Translated from Atomnaya Énergiya, Vol. 34, No. 2, pp. 125-127, February, 1973. Original article submitted June 22, 1972.

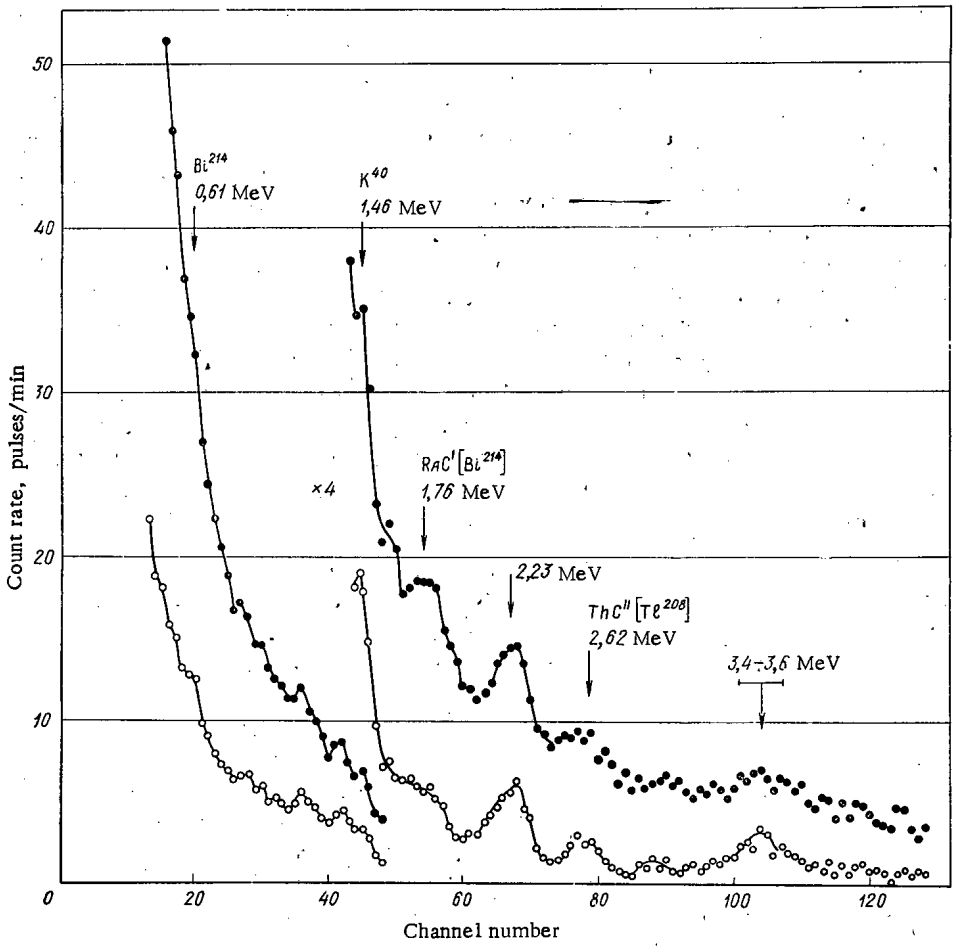

Fig. 2. Background spectra of a gamma-spectrometric system ●) without anticoincidences; ○) with anticoincidences.

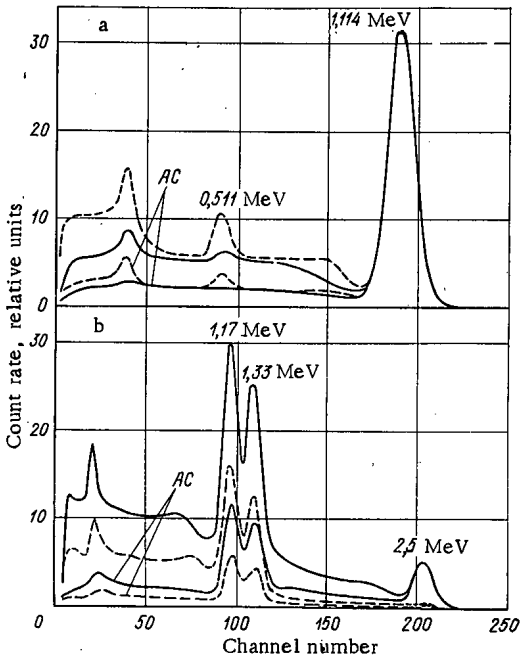

Fig. 3. Spectra of gamma sources in two operating modes of the apparatus (NaI/Tl crystal $\phi 100 \times 100$ mm in size with a well of $\phi 33 \times 60$ mm): a) Zn^{65} (spectra normalized with respect to the maximum of the photo-peak at an energy of E_γ = 1114 keV); b) Co^{60} (spectra normalized with respect to the "live" time of analysis); —) source in well; – –) source out of well.

An amplitude analyzer with 1024 channels collects information simultaneously in two memory groups of 256 channels each, with the apparatus working in two principal modes, viz., with and without anticoincidence shielding (AC). By operating a gating circuit the spectrometer may be converted into the operating condition with coincidence selection (coincidence counter or CC). The use of a light diode (attached to the photomultiplier and triggered from a precise amplitude generator) as reference source, together with the incorporation of a digital peak stabilizer, eliminates the necessity of carrying out an intermediate verification of the energy range with the aid of gamma sources. By virtue of the high stability of the energy range of the system (1% in 30 days) and the use of two spectra (obtained simultaneously and analyzed in an electronic computer) for interpretation, high accuracy of the measurements is assured. By efficiently suppressing the Compton distribution, the cosmic component of the background, and the scattered radiation of the external medium, the anticoincidence system reduces the background in the energy range 150-3600 keV by a factor of 2.5-3 times (depending on the intrinsic background of the detector). The background spectra of a spectrometer with an NaI/Tl detector ϕ 100 × 100 mm in size (well size ϕ 33 × 60 mm) are shown in Fig. 2. Apart from inevitable contributions from natural radioactive elements, the spectra contain a peak evidently due to the H (n, γ)D reaction in the hydrogen of the plastic scintillator involving the development of capture γ radiation with an energy of 2.23 MeV. The peak in the range 3.4-3.6 MeV is due to the presence of contaminating impurities of α-emitters in the actual NaI and its packing [2].

On using crystals with wells there is a reduction in the magnitude of the effective layer, but the increase in the solid angles with which the specimen is "viewed" by the detector (up to 95% of 4π) leads to a considerable rise in efficiency. Thus, for example, depending on the energy of the γ radiation, the gain in photoefficiency fluctuates from 3.5 to 2.1 times in the range 300-1500 keV. An estimate was made by measuring three-dimensional sources of Hg^{203}, Cs^{137}, Zn^{65}, Mn^{54} and K^{40} (weight in steps of 10 g) in the well (ϕ 35 × 50 mm) of an NaI/Tl crystal (ϕ 80 × 80 mm) and in a solid crystal of the same dimensions. The specimens were placed in containers of size ϕ 30 × 60 mm and 60 × 8 mm respectively. Measurements made with crystals of different sizes, with and without wells, showed that the suppression of the Compton effect in the AC mode at a γ ray energy of over 0.5 MeV mainly depended, not on the crystal dimensions, but on the geometry of measurement, reaching a factor of 2.7. The use of a detector with a well enables the activities of such "cascade" emitters as Co^{60}, Sc^{46}, Al^{26}, Na^{22}, Tl^{208} etc. to be determined (relative to the lower background characteristic of the hard region of the spectrum) from the areas of the total peaks, which are not suppressed in the AC mode. The complication of the spectra by the total peaks is also characteristic of solid crystals. This effect can only be neglected when measuring distance point sources. Thus, for an NaI/Tl detector of size ϕ 76 × 76 mm with a Co^{60} point source at a distance of 10 cm, the effect amounts to 2%. Crystals with a well are characterized by smoothing of the edge of the Compton distribution, as a result of which the form of the spectra is simplified (Fig. 3).

When studying samples of lunar soil recovered by the automatic space ships Luna 16 and Luna 20, the activities of natural (U – Ra Th, and K) and long-lived (Al^{26}, Na^{22}, Mn^{54}) cosmogenic radioactive isotopes were determined in this way in [3]. Samples of weight 10 g were analyzed in the well (ϕ 33 × 60 mm) of an NaI/Tl crystal (ϕ 100 × 100 mm). The measurements were carried out continuously for 30 days.

LITERATURE CITED

1. N. A. Vartanov and P. S. Samoilov, Applied Scintillation Gamma Spectrometry [in Russian], Atomizdat, Moscow (1969).
2. O. P. Sobornov and G. A. Fedoseev, "Analysis of the background spectra of scintillation gamma spectrometers," Summaries of Reports to the Sixth All-Union Conference on the Synthesis, Production, and Use of Scintillators [in Russian], Khar'kov (1971).
3. Yu. A. Surkov et al., "Gamma-spectrometric analysis of lunar soil taken by the automatic space ship Luna 16," Transactions of the KOSPAR Symposium, Madrid (1972).

A DIGITAL RECORDING METHOD FOR THE RESULTS OF RADIOMETRIC MEASUREMENTS

V. P. Bovin, K. M. Volodin,
A. A. Eremin, and A. A. Lintser

UDC 550.835.08

In connection with the preparation of designs for automatic control systems (ACS) by geological prospecting and mining enterprises (particularly at uranium mines), a problem of special importance is that of automatically recording and coding geophysical information (data from gamma logging or the testing of ore in a pillar, or results of rapid gamma analysis of excavated ore).

The main requirements for instruments used for geological prospecting work in quarries and pit mines are that the instruments must be portable and must have self-contained power supplies. With these requirements in mind, a system has been worked out for the automatic recording and coding of data from radiometric measurements in such a way that the data can be fed directly into electronic digital computers of the Minsk 22, Minsk 32, and Mir types. The system is designed to present in digital form either continuous measurements (gamma logging of vertical and inclined boreholes) or discrete measurements (gamma logging of horizontal and ascending underground boreholes, gamma sampling of mine output, and rapid gamma analysis of excavated ore directly in mine cars or other transport containers).

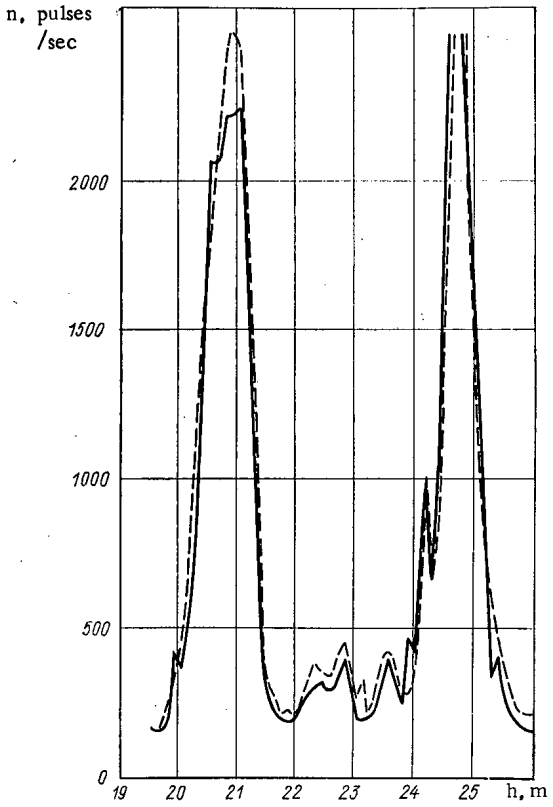

Fig. 1. Diagrams for gamma logging of an ore borehole, obtained by pointwise recording using the PRKS-2 radiometer (—) and by digital recording for ΔZ = 10 cm and v = 75 m/h (– – –).

The recording method considered here consists in measuring the number of pulses emitted by the sensor of the borehole instrument during the time it takes the instrument to traverse a borehole of given length ΔZ (ΔZ is a quantized unit of depth where Z is the depth coordinate). The information carrier transmits two numbers: the number of pulses N corresponding to the number of gamma quanta recorded in the time $\Delta t = \Delta Z / v$ required for the sensor to traverse the distance ΔZ (v is the logging velocity) and the time Δt itself, which is also expressed by a number of pulses. Then the desired quantity — the average counting rate over the borehole length ΔZ — can be defined as $n = N/\Delta t$. The calculation of the counting rate and the interpretation of the resulting values in terms of depth are carried out when the coded information is processed on the electronic digital computer.

Unlike the apparatus described in [1, 2], the apparatus used for representing the data of continuous gamma logging in digital form consists of two

Translated from Atomnaya Énergiya, Vol. 34, No. 2, pp. 127–128, February, 1973. Original article submitted April 10, 1972; revision submitted August 2, 1972.

units: a portable unit and a stationary unit. The portable unit is an intermediate-memory device which contains an ordinary mass-produced tape recorder with self-contained power supply and a special device for converting the angle of rotation of the measuring roller of the hoist into a series of electrical pulses which are used in interpreting the recorded information in terms of depth.

In the logging process, one track of the magnetic tape records in a unitary code the pulses received from the internal converter of the logging radiometer and the pulse commands ("marks") which show the times at which the sensor has traversed a specified interval (2.5 cm, 5 cm, 10 cm) along the borehole.

The recording density along the magnetic tape is of the order of 50 pulses/mm. In order to minimize counting errors, the recording unit of the tape recorder includes a smoothing device. This makes it possible, for a tape speed of 9.5 cm/sec, to record with practically no losses, information corresponding to a equilibrium uranium concentration in the ore of up to 1%.

The information recorded on the magnetic tape is reproduced under stationary conditions and converted by a coder into a digital code to be fed into the computer. The coder consists of two counters which record the pulses, a control apparatus, and a key-punch machine. The counting of pulses from the detection unit and the time counter is continued either until the next "mark" is reached or until one of the counters overflows.

By means of the control apparatus, the number generated in the counter is punched into paper in the form of a machine word consisting of six lines, with the first five lines giving digital information and the last line representing the end of the word. The number on the punched tape is represented in a binary-decimal code, which makes it easier to comprehend the information in visual form. If necessary, the tape is also punched with coded information on the measurement conditions, for use in the interpretation of the gamma logging data: the diameter of the logging instrument, the diameter of the borehole at various depths (from cavernometric data), the density of the drilling mud, and the thickness of the casings. The corresponding numbers, in binary-decimal code, are punched into the tape by a key-punch machine.

When information is recorded in the measuring mode, the points on the magnetic tape serve only for recording the signals for the beginning and end of the counting of a given number of pulses transmitted from the output of the logging instrument. In this case the distance between marks on the magnetic tape is proportional to the measuring time. This method of coding the informatiom makes it possible to reduce the speed of the magnetic tape in the recording mode.

Mockup models of this equipment were tested under operational conditions in 1970 and 1971. The tests were conducted in a number of exploratory boreholes drilled in a quarry. The results (see Fig. 1) show that the logging curves plotted by the digital recording method satisfy the precision requirements for the quantitative interpretation of gamma logging data.

LITERATURE CITED

1. Yu. P. Koloskov, Radiometry (Methods of Ore Geophysics) [in Russian], No. 9, Nedra, Leningrad (1970), p. 131.
2. Yu. P. Koloskov, in: Geophysical Apparatus [in Russian], No. 42, Nedra, Leningrad (1970), p. 173.

GAMMA-RAY BUILDUP FACTOR FOR A SPHERICAL SHIELD

V. A. Zharkov, A. A. Chudotvorov, and A. F. Kolesnikov

UDC 539.122:539.121.72

There are well-known papers which point out the rather strong dependence of gamma-ray buildup factor on shielding – detector distance for plane shields [1].

In this work, we measured the gamma-ray dose buildup factor at the surface of a spherical shield and investigated the dependence of the buildup factor on detector – shield distance. The experiments were performed with two aluminum spheres 25 and 12 cm in diameter at the centers of which a practically point source of Cs^{137} was placed. The gamma ray detectors were a scintillation spectrometer with stilbene crystal and SBM-10 halogen counter with filters which eliminated the energy dependence in the region of low-energy gamma rays. Appropriate corrections for "dead" time were applied to the measurements.

Measurements were carried out with the two detectors for the 25 cm diameter sphere. In this case, good agreement of the results was observed; therefore only the SBM-10 detector was used for measurements with the 12 cm diameter sphere, which facilitated the analysis of experimental results and decreased the error in measurments at small distances from the surface of the shield.

The background from radiation scattered in air was measured with the help of a lead cone which provided an attenuation of not less than 10^5. In the worst case, the background did not exceed 3%. Systematic error in the measurement of the absolute value of the buildup factor resulted mainly from errors in the determination of shield thickness and was 3%. It should be noted that because of the finite dimensions of the detectors, it was impossible to make measurements of the buildup factor directly at the surface of the shield.

In this work, the buildup factor at the surface of the sphere, B_R, was obtained by plotting a smooth experimental curve for $B_r - 1$ as a function of R/r by the method of least squares and subsequent

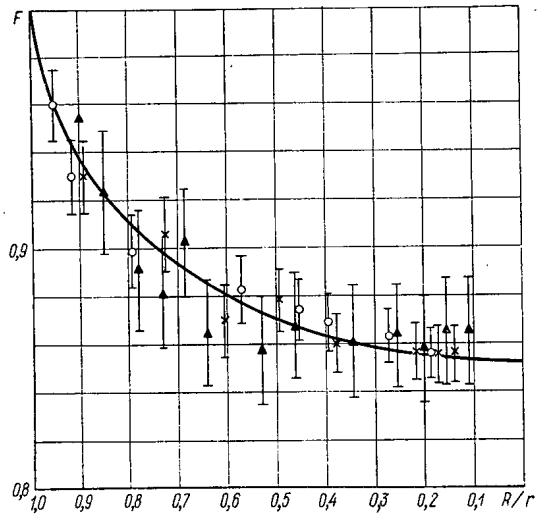

Fig. 1. F as a function of R/r: ○, ×) respectively the SBM-10 and stilbene measurements for a sphere with a wall thickness of 2.4 mean free paths; ▲) SBM-10 measurements for sphere with a wall thickness of 1.1 mean free paths; —) calculated from Eq. (1).

Translated from Atomnaya Énergiya, Vol. 34, No. 2, pp. 128-130, February, 1973. Original article submitted April 17, 1972.

extrapolation of this curve to the values (R/r) = 1 (R is the radius of the sphere, r is the distance from the center of the sphere to the detector, B_r is the buildup factor at the distance r). For the smoothing procedure, we used a dependence of the type const F(R/r), where F is a specially determined theoretical function (see below).

After renormalization, the experimental results were in the form of the dependence of $F(R/r) \equiv (B_r - 1)/(B_R - 1)$ on R/r. As is clear from Fig. 1, the theoretical curve in both cases considered is a good description of the set of experimental points, which confirms the possibility of using this curve for the smoothing procedure.

The experimental values of B_R and their measurement error were determined with the help of an expression obtained by least squares

$$B_R - 1 = \frac{\sum_{i=1}^{n} \left[B_R \left(\frac{r_i}{R} \right) - 1 \right] F \left(\frac{r_i}{R} \right)}{\sum_{i=1}^{n} F^2 \left(\frac{r_i}{R} \right)},$$

where r_i/R are the distances (in relative units) at which measurements of the buildup factor were made; n is the number of such measurements.

For spheres with wall thicknesses of 12 and 5.5 cm (2.4 and 1.1 mean free paths), the values of the buildup factor at the surface of the shield were 3.65 ± 0.13 and 1.88 ± 0.07 respectively. These values agree within the limits of experimental error with the corresponding values for plane shields: 3.7 and 1.9 [2].

For the analysis and interpretation of the experimental data on the dependence of the buildup factor in this work, an analytic relation was obtained in the derivation of which the single assumption was made that the angular distribution of the intensity of scattered radiation with respect to the propagation vector of the primary radiation at a given point on the surface of a spherical shield was similar to the corresponding distribution for a plane shield. The comparative study in [3] of the angular distributions of the intensity of scattered radiation at the surface of spherical and plane shields established there was an insignificant difference in the distributions which was only observed in the region of large angles θ.

Assuming the angular distribution of the intensity is described by

$$\frac{dI^s}{d\Omega} = \frac{e^{-\theta/\theta_0}}{\sin\theta},$$

(θ_0 is a constant which depends on source energy, shielding material, and weakly on shield thickness), we obtain

$$F = \frac{B_r - 1}{B_R - 1} =$$

$$= \frac{1}{\theta_0 (1 + e^{\pi/2\theta_0})} \int_0^{\pi/2} \frac{e^{-\theta/\theta_0} \cos\theta \, d\theta}{\sqrt{1 - \left(\frac{R}{r}\right)^2 \sin^2\theta}}. \qquad (1)$$

With decrease in R/r, the function F falls monotonically from 1

$$\left(\text{at } \frac{R}{r} = 1 \right) \text{ to } \frac{1}{1+\theta_0^2} \cdot \frac{1 + \theta_0 e^{-\pi/2\theta_0}}{1 - e^{-\pi/2\theta_0}} \left(\text{at } \frac{R}{r} \to 0 \right).$$

It is interesting that the limiting minimal value of F is easily obtained from simple physical considerations by using the fact that for any $r \geq R$, the energy flux passing through a sphere of radius r is constant and the current at the surface of a sphere with $r \geq R$ is practically equal to the flux at the surface; in this case, $\lim_{\frac{R}{r} \to 0} = J_R/\Phi_R$, where J_R and Φ_R are the values of the current and flux at the surface of the sphere.

The function F was calculated on the Minsk-22 computer for a Cs^{137} source located at the center of a spherical aluminum shield. In the calculations, the constant θ_0 was assumed to be 0.506 [4]. The maximum deviation of the function F from unity did not exceed 20% (the buildup factors B_r and B_R differed even less).

At energies greater than that of Cs^{137}, and for materials heavier than aluminum, the differences in buildup factors for spherical and plane geometries will obviously decrease because of the reduction in shielding effect, and the values of F (and consequently of B_r/B_R also) will be closer to one, which may explain the high directionality of scattered radiation with respect to the propagation direction of the primary radiation.

LITERATURE CITED

1. Yu. A. Kazanskii et al., At. Energ., 20, 424 (1966).
2. L. R. Kimel' and V. P. Mashkovich, Protection against Ionizing Radiations [in Russian], Atomizdat, Moscow (1966).
3. A. V. Larichev et al., At. Energ., 23, 155 (1967).
4. N. G. Gusev et al., Protection against Ionizing Radiations [in Russian], Atomizdat, Moscow (1969).

FLUORESCENCE OF AIR UNDER THE ACTION OF RELATIVISTIC ELECTRONS

V. D. Volovik, V. I. Kobizskoi,
V. V. Petrenko, G. F. Popov,
and G. L. Fursov

UDC 539.124.17

When charged particles pass through matter, part of their energy goes to ionization and excitation of atoms and molecules of the medium. In gaseous media the energy lost appears in the form of electromagnetic radiation. Some of the ionization radiation lies in the visible and can be recorded by photodetectors.

The mechanism for the generation of ionization radiation by relativistic electrons can be represented as follows. Fast electrons passing through a medium generate secondary or δ-electrons which have a continuous energy spectrum, so that the majority of their energies are in the low-energy region. Secondary electrons can also be formed by bremsstrahlung photons which eject electrons from other atoms by virtue of the photoelectric and Compton effects. The excitation cross section decreases as the incident electron energy increases, so that the luminosity arises in the main from collisions of slow secondary electrons with atoms or molecules of the medium [1].

An investigation has been made of the dependence of ionization luminosity of air on relativistic electron energy, under good geometrical conditions ($6 \cdot 10^{-4}$ ster $\cdot$ cm^2). The investigation was done in electron beams of linear accelerators at the Physicotechnical Institute of the Academy of Sciences of the Ukrainian SSR Khar'kov, in the energy range 20 to 1400 MeV. The accelerators were pulsed at a frequency of 50 Hz. The electron beam passed through a chamber with blackened walls, filled with air at normal pressure and room temperature. The light generated by the electron beam passed along an air-filled light pipe to a FEU-79 photomultiplier which, had lead shielding on all sides, apart from the inlet. To eliminate possible recording of Cerenkov and transitional radiation the radiation recording direction was chosen to be perpendicular to the electron beam, so that the radiation from the side walls could not fall within the photomultiplier field of view. The signal from the photomultiplier anode load went through a preamplifier, a main amplifier, and then to an oscilloscope the sweep of which was triggered by a synchronous pulse from the accelerator.

The light recorded was not that from individual electrons but that from all the electrons in a pulse. For this purpose the photomultiplier output has an integrating RC network with an integrating time constant greater than the current pulse length. Then during attenuation of a pulse the entire cluster of electrons passes through the test volume, and the amplitudes from all the electrons are summed.

The energy dependence of the luminous intensity was measured on different accelerators in the energy range 20 to 1400 MeV. All readings were referred to a single current (0.2 μA) and a single pulse duration (1.5 μsec). The measurement accuracy was ±10%. The experimental points are shown in Fig. 1; it appears that as the incident electron energy increases the light intensity falls off slightly, and does not coincide with the ionization loss curve. Figure 1 also shows the theoretical curve 1, calculated from the Moller formula

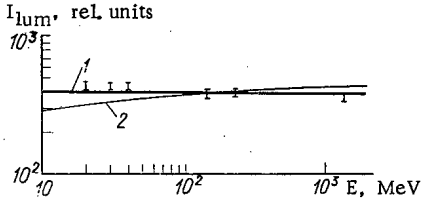

Fig. 1. Ionization emission as a function of primary electron energy: 1) theory for the dependence of energy imparted to δ-electrons in the vicinity of the maximum excitation cross section on the primary electron energy; 2) ionization losses of electrons in air.

Translated from Atomnaya Énergiya, Vol. 34, No. 2, pp. 130-131, February, 1973. Original article submitted December 2, 1971.

for the dependence of the energy imparted to secondary electrons near the maximum cross section for atom excitation on the primary electron energy. If the luminosity is mainly due to slow secondary electrons, the luminous intensity should be proportional to the energy imparted to the secondary electrons near the maximum cross section for excitation of luminosity.

The energy dependence of the ionization luminosity of air was also investigated in [2], but in a very small energy range (1 to 4 MeV) where the luminous intensity does not depend on energy, since the ionization losses in this range also depend very little on energy.

We take the view that our experimental data are in good agreement with curve 1 of Fig. 1. These data will be useful for developing monitors for low and very high charged particle fluxes, and for producing a non-solid-path dosimeter based on gaseous ionization luminosity.

We thank A. A. Grishaev and I. I. Zalyubovskii for their constant interest in this work.

LITERATURE CITED

1. A. Bunner, Detection of Cosmic Rays by Atmospheric Fluorescence, Thesis, New York (1964).
2. Yu. P. Vagin et al., At. Energ, 28, 177 (1970).

FOCUSING OF SUPERCONDUCTING SOLENOIDS IN HIGH-ENERGY LINEAR PROTON ACCELERATORS

B. I. Bondarev, V. V. Kushin,
B. P. Murin, L. Yu. Solov'ev
and A. P. Fedotov

UDC 621.384.643

The principal energy increment (from 100 to 600-1000 MeV) in linear proton accelerators energizing particles to 600-1000 MeV (meson factories [1, 2]) is brought about by resonator cavities operating at frequencies of 800-1000 MHz. Protons are focused by magnetic quadrupole doublets positioned between the resonator cavities and the sections comprising the resonators. This type of quadrupole focusing does not facilitate the effective inscribing of the beam in the accelerator aperture, because of the axial asymmetry resulting. The aperture diameter must be selected in the range of centimeters, so that the effective use of the radio-frequency power establishing the accelerating field in the resonator cavities is curtailed.

To date, the development of superconducting solenoids has attained a level such that they can be employed in accelerators now under construction. The reliance on axially symmetric focusing by a longitudinal magnetic field established by superconducting solenoids has made it possible to narrow the aperture of the focusing channel and to reduce drastically the radio-frequency power required. Moreover, tolerances in the installation and stability of the components in the focusing channel can be relaxed appreciably.

Particle Dynamics

The transverse motion executed by particles in a longitudinal magnetic field is given by the equation

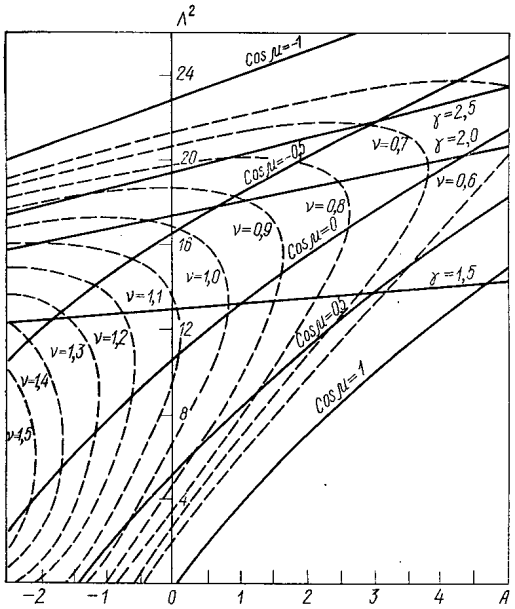

Fig. 1. Stability diagram plotted for ε = 0.8.

$$\frac{d^2r}{dt^2}+\Omega^2 r-\frac{M}{r^3}=0. \tag{1}$$

The beam dimensions are determined by the size of the phase volume occupied by the particles having no initial rotation (M = 0) [3]. Equation (1) then becomes simplified, and in the dimensionless coordinates ρ, z, where

$$\rho=\sqrt{\frac{p_s}{p_{s0}L_0L}}\,r; \quad dz=\frac{\beta_s c\,dt}{L},$$

the equation becomes

$$\frac{d^2\rho}{dz^2}+p(z)\,\rho=0. \tag{2}$$

Here β_S is the velocity of a synchronous particle divided by the speed of light c. The subscript "0" refers to values of the momentum p_S of the synchronous particle and of the focusing period L at the beginning of the accelerator section in question. In the new coordinates, the focusing period is unity, and the function p(z) becomes, within the confines of the accelerating section,

Translated from Atomnaya Énergiya, Vol. 34, No. 2, pp. 131-133, February, 1973. Original article submitted April 17, 1972.

$$p(z) = -A = -\frac{\pi e E_m (1-\beta_s^2)^{3/2} L^2}{m_0 c^2 \beta_s^2 \lambda} \sin\varphi, \tag{3}$$

and in the lenses

$$p(z) = \Lambda^2 = \frac{e^2 H_z^2 (1-\beta_s^2) L^2}{4 m_0^2 c^4 \beta_s^2}, \tag{4}$$

where e, m_0 are the charge and mass of the proton; E_m is the amplitude of the accelerating wave; φ is the phase of the particle with respect to the accelerating wave as reckoned from the peak of the wave; and H_z is the magnetic field intensity.

The stability diagram of Eq. (2), plotted in (A, Λ^2) coordinates, is reminiscent of the stability diagram in quadrupole focusing [3]. In both instances, A is the focusing parameter and Λ is the instantaneous (dimensionless) frequency of transverse oscillations within the confines of the lens. In contrast to quadrupole focusing, where Λ^2 reverses sign periodically, here this parameter is always positive. Figure 1 shows a stability diagram plotted for the case $\varepsilon = 0.8$, where ε is the fraction of the focusing period taken up by the accelerating section. The diagram shows curves of the characteristic parameters $\cos\mu$, ν_{min}, and γ, which are interrelated with the parameters Λ and A by the following formulas:

$$\begin{aligned}
\cos\mu &= \cos\Lambda(1-\varepsilon)\operatorname{ch}\sqrt{A}\varepsilon - \frac{\Lambda^2 - A}{2\Lambda\sqrt{A}}\sin\Lambda(1-\varepsilon)\operatorname{sh}\sqrt{A}\varepsilon; \\
\nu_{min} &= \Lambda\sqrt{\frac{2\sqrt{A}\Lambda\sin\Lambda(1-\varepsilon)\operatorname{ch}\sqrt{A}\varepsilon - [\Lambda^2+A) - (\Lambda^2-A)\cos\Lambda(1-\varepsilon)]\operatorname{sh}\sqrt{A}\varepsilon}{2\sqrt{A}\Lambda\sin\Lambda(1-\varepsilon)\operatorname{ch}\sqrt{A}\varepsilon + [(\Lambda^2+A) + (\Lambda^2-A)\cos\Lambda(1-\varepsilon)]\operatorname{sh}\sqrt{A}\varepsilon}}; \\
\nu_{max} &= \sqrt{A\frac{-2\Lambda\sqrt{A}\cos\Lambda(1-\varepsilon)\operatorname{sh}\sqrt{A}\varepsilon + [(\Lambda^2+A) + (\Lambda^2-A)\operatorname{ch}\sqrt{A}\varepsilon]\sin\Lambda(1-\varepsilon)}{2\Lambda\sqrt{A}\cos\Lambda(1-\varepsilon)\operatorname{sh}\sqrt{A}\varepsilon + [(\Lambda^2+A) - (\Lambda^2-A)\operatorname{ch}\sqrt{A}\varepsilon]\sin\Lambda(1-\varepsilon)}}.
\end{aligned} \tag{5}$$

The thin-lens approximation may be used for estimates. In that approximation, the point on the stability diagram corresponding to the values A = 0 and $\cos\mu = 0$ will be characterized by the dependence of the parameters Λ, ν_{min}, and γ on ε:

$$\begin{aligned}
\Lambda &= \sqrt{\frac{2}{1-\varepsilon}}; \\
\nu_{min} &= \sqrt{2-\varepsilon}; \\
\gamma &= \sqrt[4]{\frac{1}{\left(1-\frac{\varepsilon}{2}\right)\left[1-\frac{\varepsilon^2}{2}-\frac{2\varepsilon(1-\varepsilon)}{3}\right]}}.
\end{aligned} \tag{6}$$

In contrast to quadrupole focusing, the amplitude coefficient γ_{min}, and with it the channel handling capacity, vary inversely with ε. The amplitude coefficient ν_{min} covers the range 1.0–1.4 over a broad range of variation in ε. That means that the channel capacity will be 1.5 to 2 times greater in focusing by a longitudinal magnetic field than in quadrupole focusing, where ν_{min} = 0.6 to 0.8. The values $\varepsilon = 0.8$ and $\nu_{min} = 0.6$ were assigned in the design of a 600 MeV meson factory [2]. At that value of ε, focusing by a longitudinal magnetic field can bring about $\nu_{min} = 1.0$. A 70% increase in ν_{min} at a specified beam emittance decreases the beam radius and the aperture radius by 30%, which accounts for about 20% savings in high-frequency power.

Consequently, radial motion of particles with no initial rotation imparted to them, in a channel with solenoids spaced far apart in terms of their parameters μ, ν_{min}, and ε, is reminiscent of particle motion along one of the transverse axes in a hard focusing channel. The frequency of radial oscillations is much greater than the frequency of longitudinal oscillations, and focusing by the longitudinal magnetic field can no longer be properly referred to as "soft" focusing.

From Eq. (4) it follows that

$$H_z = \frac{m_0 c^2}{e}\frac{2\Lambda\beta_s}{L\sqrt{1-\beta^2}}. \tag{7}$$

The magnetic field strength increases in proportion to the momentum of the synchronous particle, with Λ and L constant. When $\varepsilon = 0.8$, and with the acceleration paced as in [2], the parameter A = 0.8 at 100 MeV.

As the energy is brought up to 600 MeV, this parameter decreases tenfold. At the values of Λ and A referred to, and at $\nu_{min} = 1.0$, the parameter $\Lambda = 3.3$ at 100 MeV and $\Lambda = 2.7$ at 600 MeV. The length of the focusing period varies along the second part of the meson factory from 220 cm to 350 cm. Substituting these values of the set of parameters into Eq. (7), we find that the magnetic field strength at the beginning of the second part is 44 kOe, but increases to 63 as acceleration proceeds.

Tolerances on Parameters of Focusing Channel

Perturbations of the transverse oscillations are caused by the inclinations of the solenoids and by random departures of the fields generated in the solenoids from the rated values.

The random inclinations of the solenoids bring about a displacement Δr of the beam axis, the rms value of which is

$$\sqrt{\overline{(\Delta r)^2}} = \frac{\Lambda^2 (1-\varepsilon)}{\nu_{min}} \sqrt{nD(\Delta)}, \tag{8}$$

where n is the number of focusing periods, and $D(\Delta)$ is the variance of Δ, equal to half the product of the solenoid angle of inclination and the solenoid length. When $\varepsilon = 0.8$, $\nu_{min} = 1$, $\Lambda = 3$ (the average of the above values), and $D(\Delta) = 0.15$ mm, we end up with 2.9 mm as the rms displacement of the beam. The same displacements are observed in the case of quadrupole focusing when more stringent tolerances are imposed on the mounting of the quadrupole lenses.

By following the procedure outlined in [4], we find that, because of focusing fields, the beam dimensions increase θ times on the average, where

$$\bar{\theta} = \sqrt{\left(\frac{\overline{S_p M}}{2}\right)^n + \sqrt{\left(\frac{\overline{S_p M}}{2}\right)^{2n} - 1}}; \qquad \frac{\overline{S_p M}}{2} = 1 + \frac{2\Lambda^4 (1-\varepsilon)^2}{\nu_{min}^2} \left(\frac{\overline{\Delta H_z}}{H_z}\right)^2. \tag{9}$$

If $\sqrt{(\Delta \overline{H}_z / H_z)^2} = 2\%$, then we obtain $\bar{\theta} = 1.5$ for $\varepsilon = 0.8$, $\Lambda = 3$, $\nu_{min} = 1.0$, and n = 110. The coefficient $\bar{\theta}$ is brought down to 1.1 when adiabatic damping is taken into account. Approximately the same $\bar{\theta}$ value is arrived at in quadrupole focusing, when fairly stringent rms tolerances are imposed: the precision in mounting and the stability of the magnetic field are to within 0.1%, the rotation angle of the median planes to within 20'.

Comparative Estimate of Focusing Systems

For superconducting solenoids with magnetic field strength 50-60 kOe, we can make use of NTB-1 grade multicore Nb – Ti superconductors. In an experimental solenoid [5] made from that type of superconductor, at field strength 50 kOe and temperature 4.2°K, the effective current density (taken over the cross section of the winding) is $\approx 2 \cdot 10^4$ A/cm^2. About 5 kg of Nb – Ti alloy is required, at that current density, per solenoid with average characteristics (magnetic field strength 55 kOe, length 60 cm, I.D. 4.5 cm, O.D. 9.2 cm). The cost of such a solenoid plus cryostat is 2.5 to 3 times greater than the cost of a standard magnetic quadrupole doublet. But the cost of a superconducting focusing system, including the refrigerating system and the helium leads, and with ten years of accelerator service taken into account in the calculations, is approximately equal to, or slightly below, the cost of a focusing system based on standard magnetic quadrupoles. If the substantial savings in radio-frequency power are taken into consideration, then the use of superconducting solenoids for focusing in linear proton accelerators is well justified.

LITERATURE CITED

1. L. Rosen, Proceedings of the Sixth Scientific Conference on High-Energy Accelerators, Cambridge, (1967), p. 237, B-36.
2. B. P. Murin, Linear Proton Accelerators [in Russian], Report Presented at the Eighth International Conference on High-Energy Accelerators, Geneva (1971).
3. A. D. Vlasov, Theory of Linear Accelerators [in Russian], Atomizdat, Moscow (1965).
4. B. I. Bondarev, A. P. Durkin, and L. Yu. Solov'ev, Tr. Radiotekhn. Inst. AN SSSR, No. 9, 3 (1971).
5. E. M. Savitskii et al., Pribory i Tekh. Eksperim., No. 5, 270 (1971).

MEASUREMENT OF THE ENERGY DISTRIBUTIONS OF THE FRAGMENTS DERIVED FROM THE FISSION OF PREACTINIDE NUCLEI BY ALPHA PARTICLES, USING THE "TRACK METHOD"

M. G. Itkis, V. N. Okolovich,
A. F. Pavlov, and G. Ya. Rus'kina

UDC 539.173.8.164

Great experimental difficulties arise in measuring the fragment spectra arising from the fission of nuclei with atomic numbers $Z \leq 84$ by charged particles at excitation energies of $E_x < 35$ MeV. On measuring the energies of the fragments with semiconducting counters, the ordinary method cannot be used, owing to the small values of the fission cross sections ($\sigma_f < 0.1$ mb) and the high background of scattered α particles encountered in achieving the required statistical accuracy of the measurements.

An analysis of the energy spectra of fission fragments arising from compound nuclei at the saddle point with fairly low excitation energies is of considerable scientific interest both from the point of view of verifying the existing relationship between the mean kinetic energy of the fragments $\overline{E_K}$ and $Z^2/A^{1/3}$ obtained for fairly large E_x and considerable angular momenta [1], and also from that of verifying Halpern's hypothesis [2] as to the possible increase in the asymmetrical modes of fission of preactinide nuclei for fairly

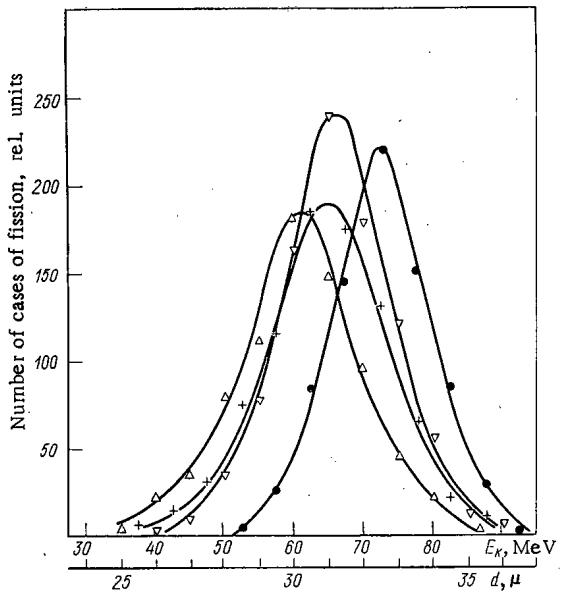

Fig. 1

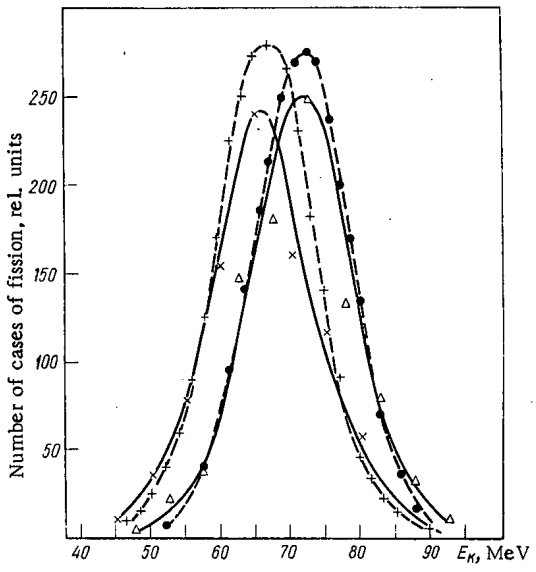

Fig. 2

Fig. 1. Energy distributions of the fission fragments of Ir^{189} (Δ), Pt^{192} (+), Tl^{201} (∇) and At^{213} (●) measured by the track method.

Fig. 2. Comparison between the energy spectra of the fission fragments of At^{213} (●, Δ) and Tl^{201} (+, ×) measured with semiconducting detectors (– – –) and glass detectors (———).

Translated from Atomnaya Énergiya, Vol. 34, No. 2, pp. 133-135, February, 1973. Original article submitted May 18, 1972.

TABLE 1. Results of Measurements of the Energy Distributions of Fission Fragments

Compound nucleus	E_x, MeV	$\bar{E}_K$, MeV: present investigation	$\bar{E}_K$, MeV: data of others	$\sigma(E_K)$, MeV^2	E_K calc, MeV*
$_{77}Ir^{189}$	34,2	127,9±4	—	58,2±7	129,7
$_{78}Pt^{192}$	34,9	135,9±3	—	64,7±5	132,6
$_{81}Tl^{201}$	35,7	139,4±2	138±4 [7]	51,6±4	139,3
$_{85}At^{213}$	27,9	151,5±2	146±4 [6]	45,8±8	149,0

* Results of [1]

low values of E_x. In addition to this, if we can measure the energy distributions of fragments close to the fission barrier, then the degree of purity of the test targets ($Z \leq 84$) with respect to strongly fissile impurities (uranium, thorium) may easily be monitored, which is a necessary condition for obtaining reliable data as to the fission barriers and effective moments of inertia of the nuclei.

The possibility of measuring the energy distributions of fragments by means of glass detectors was discussed in [3, 4] for the case of the spontaneously fissile nuclei Cm^{244} and Cf^{252}. The results indicate a certain nonlinearity in the dependence of the diameters of the craters in the glass on the energy of the fragments, which casts doubts upon the possibility of obtaining reasonably accurate mean kinetic energies of the fragments $\bar{E}_K$ by direct calculations based on the track method.

The track method is more promising for measuring $\bar{E}_K$ in the case of nuclei undergoing fission in a mainly symmetrical manner, for which the energy range of the fragments is considerably narrower and the nonlinearity of the relationship between the diameters of the tracks and the energy of the fragments should have a less noticeable effect.

The present investigation is aimed at verifying the use of this method of the fission of Re^{185}, Os^{188}, Au^{197}, Bi^{209} by α particles with an energy of 38 MeV. In the experiments we used layers of the isotopes in question 100–200 $\mu g/cm^2$ thick; photoemulsion glasses acted as fission-fragment detectors. The irradiated glasses were etched simultaneously in hydrofluoric acid (concentration ~48%) for 170 sec. In order to calibrate the energy scale we measured the fragment spectra for the fission of Au and Bi by 38 MeV α particles and that of Th^{232} by 27 MeV α particles with semiconducting counters. (In the latter case the position of the peaks corresponding to the light and heavy fragments was already well known.) The fragment spectra were measured with glasses and semiconducting counters using exactly the same geometry — at an angle of 90° relative to the axis of the incident particle beam. We made two series of measurements with different batches of glasses and different etching conditions. The irradiated glasses were inspected under an MIRE-2 microscope, with automatic recording of the results of the measurements on punched tape. Control measurements were carried out under a KSM microscope, the reading accuracy of which was about 0.1 μ. The final analysis of the results of our measurements of the fragment spectra was carried out in a BESM-4m computer. For each element we measured up 3000–6000 tracks. Corrections of the kind usual in experiments of this type were introduced into the measured values of $\bar{E}_K$ [5, 6].

The results of an analysis of two independent series of measurements coincided, within the range of errors indicated in Table 1. Table 1 gives the measured values of $\bar{E}_K$, the dispersion of E_K, and also the results of calculations of $\bar{E}_K$ based on [1]. Figures 1 and 2 show the energy distributions of the fragments of the compound nuclei studied and the E_K distributions of the isotopes Tl^{201} and At^{213} obtained by means of semiconducting counters and glasses.

The measured energy distributions of the fragments of the elements under consideration presented in Table 1 and Figs. 1 and 2 indicate a real possibility of making direct measurements of $\bar{E}_K$ by the "track method" and achieving a fair accuracy in so doing. The results of our measurements, coinciding with the calculated values of $\bar{E}_K$ [1] within the limits of experimental error, lead to the conclusion that the angular momentum introduced into the nucleus by the particles and the excitation energy of the compound nuclei have relatively little effect on the mean kinetic energy $\bar{E}_K$.

Our own measurements of $\bar{E}_K$ agree with the theoretical calculations of [8] and with the experimentally measured values of the kinetic energies of the elements under consideration obtained by means of semiconducting counters in earlier investigations [6, 7].

LITERATURE CITED

1. V. Viola and T. Sikkeland, Phys. Rev., 130, 2044 (1962).
2. I. Halpern, Ann. Rev. Nuc. Sci., 9, 245 (1959).
3. V. K. Gorshkov, L. N. L'vov, and G. A. Khruleva, At. Energ., 28, 73 (1970).

4. U. Hoppner et al., Nucl. Instrum. and Methods, 74, 285 (1969).
5. V. N. Okolovich, G. I. Smirenkin, and I. I. Bondarenko, At. Energ., 12, 461 (1962).
6. F. Plasil et al., Phys. Rev., 142, 697 (1966).
7. R. Vandenbosch and J. Huizenga, Phys. Rev., 127, 212 (1962).
8. J. Nix and W. Swiatecki, Nucl. Phys., 71, 1 (1965).

THE AVERAGE NUMBER OF NEUTRONS EMITTED IN THE SPONTANEOUS FISSION OF Cm^{244}, Cm^{246}, AND Cm^{248}

V. V. Golushko, K. D. Zhuravlev,
Yu. S. Zamyatnin, N. I. Kroshkin,
and V. N. Nefedov

UDC 539.173.7

Until the present experiments on the measurement of $\bar{\nu}_p$ – the average number of prompt neutrons emitted per fission – were formulated, the only even–even isotope of curium for which a substantial number of measurements had been made was Cm^{244}; on the basis of the Cm^{244} measurements, Konshin's survey report recommended a value of $\bar{\nu}_p = 2.691 \pm 0.032$. Only one measurement was known for Cm^{246} [2] and one for Cm^{238} [3], and these had been made with relatively low accuracy (3-7%). We therefore thought it desirable to measure $\bar{\nu}_p$ for all the nuclei listed above, under identical conditions and in the same experimental setup, in order to ascertain how $\bar{\nu}_p$ varies with mass number in the fission curium isotopes. Similar measurements were conducted in parallel by G. N. Smirenkin et al. [4].

The fission neutrons were recorded by 48 SNM-18 proportional counters placed in a paraffin moderator 500 mm in diameter and 500 mm in length, with a transverse central channel (diameter 90 mm) for installing the fragment detector. In order to reduce the scattered-neutron background, the neutron detector was placed inside a boron carbide shield 50 mm thick. The recording efficiency for neutrons from the spontaneous fission of Cf^{252} was 29%. We used a neutron detector similar to that described in [5], with resolution time of 3 μsec. The fission fragments were recorded by means of gas-type scintillation detector. The fissionable substance was spread on a stainless-steel substrate. The target spot diameter did not exceed 10 mm. The isotope composition of the targets is shown in Table 1.

In the measurement of $\bar{\nu}_p$, the fragment pulses opened the gate circuit for a period of 180 μsec, during which the neutron pulses were recorded. The reference used in measuring $\bar{\nu}_p$ for the isotopes under investigation was Cf^{252}, for which the $\bar{\nu}_p$ value was taken to be 3.756 ± 0.010 [1]. We made ten series of measurements for each of the investigated isotopes. From the Cf^{252} calibration target we recorded 12 dis/sec, whereas the values for the curium targets ranged from 1.5 to 3 dis/sec.

The experimental results obtained were corrected for the background of random coincidences and for the isotope composition of the targets. As in [5], we introduced a correction for the coincidence of pulses produced by neutrons from a single fission. The role of the variation in neutron-detector efficiency as a function of energy was estimated by comparing the $\bar{\nu}_p$ value for Cm^{244} obtained in the present study with the value recommended in [1]. The values are in good agreement, which shows that the correction for

TABLE 1. Isotope Composition of the Targets

Target	Isotope percentages				
	242	244	245	246	248
Cm^{244}	0,03	99,24	0,42	0,31	—
Cm^{246}	—	0,25	0,29	99,46	—
Cm^{248}	—	5,57	—	1,85	92,58

TABLE 2. Values of $\bar{\nu}_p$ for Curium Isotopes

Isotope	Present study	[4]	Data obtained in 1970-1971
Cm^{244}	2,680±0,027	2,700±0,014	2,691±0,032 [1]
Cm^{246}	2,927±0,027	2,950±0,015	3,20±0,22 [2]
Cm^{248}	3,173±0,022	3,157±0,015	3,11±0,09 [3]

Translated from Atomnaya Énergiya, Vol. 34, No. 2, pp. 135-136, February, 1973. Original article submitted July 31, 1972.

the variation in efficiency as a function of energy does not exceed the limits of measurement error. The maximum value of the other corrections discussed in [5] was no more than 0.1% under the conditions of our experiment.

Table 2 shows, for comparison purposes, the results of the measurements made in the present study and the data of other authors. It can be seen that the results of the present study are in good agreement with the data of [4] and indicate that $\overline{\nu}_p$ for even isotopes of curium increases linearly as the mass number A increases. This result may be regarded as an experimental coinfirmation of the calculations made in [6] for the function $\overline{\nu}_p(Z, A)$.

In conclusion, the authors wish to thank L. I. Prokhorova and G. N. Smirenkin for their valuable advice in the construction of the neutron detector, and also to thank A. P. Druzhnov for his help with the measurements.

LITERATURE CITED

1. V. Konshin and F. Manero, Energy-Dependent $\overline{\nu}$ Values for U^{235}, Pu^{239}, U^{233}, Pu^{240}, Pu^{241} and the Status of $\overline{\nu}$ for Spontaneous-Fission Isotopes, Vienna, IAEA (1970).
2. Major C. Thompson, Phys. Rev., C2, 763 (1970).
3. C. Orth, Nucl. Sci. and Engng., 43, 54 (1971).
4. L. I. Prokhorova et al., At. Energ., 33, 767 (1972).
5. L. I. Prokhorova et al., At. Energ., 30, 250 (1971).
6. I. I. Bondarenko et al., Second Geneva Conference, 1958 [in Russian], Vol. 1, Atomizdat, Moscow (1959), p. 438.

COLLABORATION DAYBOOK

The 15th session of the PKIAE SEV work group on reactor science and engineering and nuclear power was held September 26-29, 1972 at Marianske Lazen (Czechoslovakia). Specialists from Bulgaria, Hungary, East Germany, Poland, Rumania, the USSR, and Czechoslovakia participated in this session, as well as a staff member of the COMECON Secretariat.

The positions originally taken in forecasting calculations were approved in the course of discussions on the development of an updated prognosis of nuclear power development in the COMECON member nations.

The work team discussed proposals on the program of collaboration in the field of research reactors, and concluded that it is now feasible to set up a KNTS body on research reactors. A draft plan for the Commission's work in the field of reactor science and engineering and nuclear power was approved, and various other topics in the organization of collaborative efforts were also discussed.

The first session of the KNTS on water management for nuclear power stations was held at Magdeburg (German Democratic Republic) September 26-29, 1972. Participating were specialists from Hungary, East Germany, Poland, Rumania, the USSR, and Czechoslovakia, as well as a staff member of the COMECON Secretariat.

On the basis of an analysis of research carried out in the COMECON member nations on water management at nuclear power stations, results of which were discussed at a symposium in May 1972, this KNTS worked out proposals on the basic trends in scientific-research work, and proposals on improving the program of collaboration in this domain. Particular emphasis was placed on the fact that construction of nuclear power stations in areas with differing water supply facilities must be accompanied by improvements and refinements in the technology of water treatment, with due attention given to geographical and seasonal conditions. It is important that sufficient attention be given to those aspects of water management in the initial design stage of nuclear power stations.

The fourth session of the KNTS on radiation engineering and technology was held in Budapest, October 5-7, 1972. Members of the council participated alongside experts from Bulgaria, Hungary, East Germany, Poland, Rumania, the USSR, Czechoslovakia, staff members of the COMECON Secretariat, and a representative of the Interatominstrument international economic association on nuclear instrumentation. The agenda specified 12 topics, including a summary of the conference of specialists of COMECON member nations recently held on implementation of high-level radiation facilities and radiation technology in industry.

The council discussed and approved a report on industrial realization of processes designed for radiation fabrication of wood and plastic materials (E. Plander, Czechoslovakia), and accepted this report as a basis for working out measures on the industrial acceptance of processes for radiation modification of wood in the national economies of interested nations. The following points were noted.

1. Wood and plastics can be used in shipbuilding, in the chemical process industry, in the production of textiles, in civil engineering and construction work, and in other areas of modern technology, and can partially replace materials made from more expensive hardwoods (oak, etc.).

2. In some capitalist countries (USA, France, Finland, etc.), industrial production of commodities (predominantly parquet flooring) from radiation-modified wood has been organized. Despite the comparatively high cost of those commodities, they are in great demand because of their excellent service qualities.

Translated from Atomnaya Énergiya, Vol. 34, No. 2, pp. 137-138, February, 1973.

3. In COMECON countries, radiation modification of wood is in the pilot plant and testing stage. In the Soviet Union, for example, the basic parameters of a technological process for production of some commodities from radiation-modified wood have been worked out, full-scale tests of flooring made of modified parquet have been staged, and the prerequisites for instituting a new method in industrial production have been created; experiments designed to study a technology for impregnation by monomers and radiation modification of furniture plywood, parquet flooring, and curing of paint and varnish coatings for wood materials were carried out.

A report presented by a KNTS member, B. Gratu of Rumania, on training of specialists in radiation engineering and technology was approved, and such forms of training and skills upgrading of specialists as mutual exchange of instructors and guest lecturers, organization of special courses, and seminar schools, etc., which are the forms most popular and most widely practiced, were approved and recommended. In particular, the KNTS voted a resolution on the feasibility of organizing, to begin with, a series of lectures on technological dosimetry of radiation processes, and took into consideration a declaration by the Rumanian delegation to the effect that, at any time later than 1973, such courses can be organized in Rumania.

The topical structure of the symposium on radiation processing of foodstuffs and agricultural products (Bulgaria, October 1973) was worked out, and arrangements for further preparatory work on the symposium were approved.

The Council approved plans for the development of unitized assemblies in radiation facilities, for scientific forecasting of the development of basic trends in radiation technology, unified public-health rules and regulations on radiation devices and operation of radiation facilities, unified procedures of dosimetric monitoring of radiation technological processes.

The 1973 work plan was discussed and the agenda of the fifth session of the Council (scheduled for East Germany, April 1973) was discussed.

The session took place in a businesslike and comradely atmosphere. The participants took favorable note of the excellent organization of the session, and the work done by the Hungarian delegation in expediting the session.

The third KNTS session on radioactive wastes and deactivation was held October 8-11, 1972, at Kolobrzeg (Poland). Specialists from Bulgaria, Hungary, East Germany, Poland, Rumania, the USSR, and Czechoslovakia, as well as COMECON Secretariat staff members, participated in the work of the conference.

Assessments of the results of work done with existing facilities designed for reprocessing of low-level and medium-level radioactive wastes, and a "Procedure for geological, hydrogeological, and physico-chemical research in prospecting, exploration, and validation of the suitability of geological structures for safe burial of radioactive wastes," were discussed, as well as criteria for selecting appropriate techniques for the immobilization of nuclear power station radioactive process wastes in relation to the properties of the wastes and the natural disposal conditions.

The 24th session of the work group on nuclear instrumentation met October 10-13, 1972 in Sofiya. Delegations of specialists from Bulgaria, Hungary, East Germany, Poland, Rumania, the USSR, and Czechoslovakia, took part in the session, and representatives of the international association Interatominstrument were also in attendance. Scientific and technical collaboration between COMECON member nations in the field of nuclear instrumentation were discussed.

The specialists discussed the design of a thesaurus suggested by the German Democratic Republic delegation for organization of centralized coverage and searches of the worldwide patent literature on the class of nuclear instruments, and decided to request that PKIAE SEV recommend this design for use in COMECON member nations over a three-year period with subsequent refinements and supplements.

The work group heard a report by Soviet specialists on the general concept of setting up systems of modules and instruments based on integrated circuitry, and suggested that a detailed concept be worked out with subsequent preparations of recommendation on standardization. A broad exchange of information on the status of developments and production of nuclear physics equipment based on integrated circuitry in the COMECON member nations was arranged. A project submitted by the Polish delegation incorporating plants for preparing and holding a symposium on the topic "Development of integrated-circuit nuclear equipment," was discussed and approved (scheduled for April 1973, in Poland).

The specialists discussed topics related to the work plan on the topic "Development of instruments and equipment for scramming and control systems, dosimetric monitoring and radiometric monitoring of VVER reactors," and accepted an informational report by the Polish delegation on the status of preparations for the conference on "Monitoring and control of nuclear reactors and nuclear power stations" (to be held in October 1973, in Poland).

A report prepared by the Hungarian delegation on the progress of work on the topic "Development of procedures and instruments for nuclear medicine," was discussed and approved. A program for the forthcoming April 1973 coordination conference on nuclear medicine was prepared and approved.

The work group discussed 13 draft recommendations on standardization on basic parameters, technical specifications, and techniques for testing various nuclear instrumentation products, and adopted appropriate resolutions. Proposals for the 1973 work plan and a draft resolution for PKIAE SEV on nuclear instrumentation were agreed upon.

A seminar on exchange of experience accumulated to date on the building and acceptance of power plants incorporating fast reactors, specifically the BOR-60 reactor, was held October 25-28, 1972 at Dimitrovgrad (USSR), following the PKIAE SEV guidelines. The seminar attracted about 70 specialists from East Germany, Poland, Rumania, the USSR, and Czechoslovakia. Nineteen reports were heard and discussed, with Soviet specialists presenting results of scientific-research based on the BOR-60 reactor power plant.

The participants of the seminar visited the BOR-60 power plant and were familiarized with its performance and history.

The seminar contributed to the further development of collaboration between COMECON member nations in the field of scientific-research and design and development work concerned with high-output fast power reactors.

THE ALL-UNION CONFERENCE ON THE USE OF RADIATION TECHNIQUES IN AGRICULTURE

D. A. Kaushanskii

The All-Union Conference on the Use of Radiation Techniques in Agriculture was held at Kishinev, October 2-5, 1972. Scientists and agricultural workers participated in the work of the Conference. About 25 reports were presented in plenary meeting. The Conference dealt with: general problems of agricultural radiobiology; irradiation of seeds before planting; radiation genetics and selection; isotopes and radiation in plant protection; isotopes and radiation in plant physiology; and the use of radiation in the storage and technological processing of agricultural products. The Conference was opened by G. Ya. Rud', Corresponding Member of the Academy of Sciences of the Moldavian SSR, who observed that the Conference was being held at a time when the use of radiation techniques in the fields of Moldavia was becoming a significant reality, and the results of many years of research by radiobiologists were being corroborated in practice.

In his welcoming speech, I. N. Berezhnoi, Agriculture Minister of the Moldavian SSR, discussed the results of the use of Kolos industrial mobile gamma units in the Republic over a five-year period, as well as some results of the irradiation of seeds before planting, including corn, sunflowers, and sugar beets, which are crops of great importance to the Republic. The Ministry of Agriculture of the Moldavian SSR is studying the problems involved in further incorporating into agricultural practice the method of preplanting irradiation of seeds by means of Kolos units. It was noteworthy that the preplanting irradiation of corn, a crop which occupies approximately 380,000 ha of the Republic, with an average yield of 3,800 kg /ha (weighted average for 1968-1971), made possible an additional output of about 150,000 tons. This is done by using 15 to 20 Kolos units, costing approximately 1 million rubles. The economic benefit of this measure is about nine times as high as the cost price of the Kolos units.

A. M. Kuzin, N. F. Batygin, K. I. Sukach, N. M. Berezina, and D. A. Kaushanskii spoke in plenary meeting; they discussed the trends and levels of present-day theoretical investigation and also gave an estimate of the results achieved by production testing of the method of preplanting irradiation and of the radiation technology developed for this purpose. Reports on the use of atomic energy in various branches of agricultural science and in production were presented by V. N. Lysikov (radiation mutagenesis in agricultural plants), S. V. Andreev (the struggle against agricultural plant pests), and others.

A. M. Kuzin gave a general discussion of the theoretical prerequisites and experimental studies on the effects of ionizing radiation and pointed out the role of free radicals and changes in the permeability of biological membranes in the acceleration of metabolism, and the role of other factors in the development of the theoretical foundations of preplanting irradiation. In addition, he spoke of a possible sequence of processes taking place in the preplanting irradiation of seeds which will ensure their more rapid germination development, and tillering, earlier blooming, and increased yields.

Advances in radiobiology and their practical utilization in agriculture were discussed by N. F. Batygin (Agrophysical Institute, Leningrad). He noted that radiation can be used successfully as part of a general system of agricultural measures designed to increase yields, and he pointed out the need for broader investigations into the theoretical foundations of mutagenesis and radioselection, as well as the use of radiation protectors and radiation sensitizers in plant protection. The results of extensive production tests and the incorporation of preplanting irradiation and Kolos gamma units into Moldavian agriculture were discussed by K. I. Sukach (Kishinev Agricultural Institute). Kolos mobile gamma units, industrially produced and having a capacity of about 1 ton/h, made it possible in 1968-1972 to conduct tests of this new agricultural

Translated from Atomnaya Énergiya, Vol. 34, No. 2, pp. 139-140, February, 1973.

method. It is sufficient to point out that the weighted-average increase in the corn harvest for the 1968-1971 period was 400 kg/ha (or 12%). In 1972, when over 50,000 ha were planted, 550 tons of seed were irradiated during the spring planting season in 12 different areas of the Republic. The report pointed out that, in the light of planting norms and of the price of commercial seed corn, operation of the Kolos unit for 1 h will bring a farm more than 1,000 rubles of profit, and by the end of the first season the unit will have paid for itself. There are five Kolos units operating in Moldavia today. The conclusion of the report indicated the prospects for further incorporating this method into Moldavian agriculture starting in 1973, using, as examples, corn, sunflowers, and sugar beets.

The level of present investigations on the preplanting irradiation of seeds was discussed by N. M. Berezina (Institute of Biophysics of the Academy of Sciences of the USSR). In her survey of Soviet and foreign studies, she spoke of the role of various factors influencing the reproducibility of the stimulation effect and noted that the existence of a radiation technique that ensures uniform irradiation conditions (dose rate, temperature, degree of nonuniformity of irradiation), together with the modifying factors that have been studied and a number of environmental factors, determines the reproducibility of the results. She pointed out that the preplanting irradiation of seeds, as an agricultural method which does not preclude the utilization of a whole complex of agrotechnical measures, may be regarded as an additional reserve technique for increasing the output of agricultural crops. The data obtained by Soviet researchers are now being confirmed by foreign authors.

In a report by D. A. Kaushanskii (Moscow) entitled "The development of a new radiation technique for agricultural production," it was stated that, at the initiative of the State Committee on the Utilization of Atomic Energy, a number of gamma irradiating units (MRKh-γ-100, RKh-γ-30, Issledovatel' units, RKhM-γ-20 multichamber units, and others) had gone into industrial production and were being delivered to organizations by the All-Union Isotope Society. The author discussed in detail the problems involved in establishing a complex of industrially produced mobile gamma units for the preplanting irradiation of seeds (Kolos, Universal, Kolos-5, and Stimulyator). The resulting complex will make it possible in the near future not only to carry out extensive production tests of this new agricultural technique over large areas, under various soil and climate conditions, for different kinds of seeds (both loose-grained and non-loose-grained) at seeding norms of 0.1-300 kg/ha, but also to begin immediately to incorporate it into agriculture. The report also gave data on the Genetik experimental-industrial gamma unit, designed for sexually sterilizing insect pests at various stages of their development under the conditions prevailing in biofactories, and on the Dezinsektor mobile gamma unit. The possibilities of using the Sterilizator unit (volume 60 liters, dose rate 1.6-1.7 Mrad/h) in agricultural production (for increasing the storage life of fruits and berries and for the sterilization of feed, hides, wool, etc.) were considered. The report discussed some characteristics of the developments of radiation technology in the USSR and elsewhere and noted that today the scientific groundwork is being laid for the establishment of a new field of agricultural machine design – the design of agricultural radiation machinery.

A report on the results of the use of Kolos units in 1970-1972 in the Pavlodar region of the Kazakh SSR was delivered by Yu. A. Martem'yanov. He noted that under the conditions of the Pavlodar region, preplanting irradiation of seeds makes it possible to increase wheat yields by 10%, buckwheat by 16-17%, millet by 15%, sunflowers by 15-20%, and corn silage by 10-12%. In 1971 the profit resulting from the use of a single Kolos unit was 84,000 rubles, and it was expected that the use of two units in 1972 would bring a profit of about 200,000 to 250,000 rubles. The Pavlodar region is the site of the country's first radiation-technology station (RTS), designed to provide the collective farms and state farms of the region with radiation-technique services.

A number of reports were devoted to the results of seed irradiation in the Kirgiz SSR (A. S. Sultanbaev, L. A. Sergeeva), the Belorussian SSR (Yu. M. Vaninskaya), the Latvian SSR (A. T. Miller), the Leningrad region, and other areas of the country.

The use of atomic energy in various fields of agriculture was discussed in survey reports in the section headed by D. M. Grodzinskii (general problems of agricultural radiobiology), A. T. Miller (preplanting irradiation of seeds), V. G. Semin (radiation and genetics selection), V. V. Rachinskii (radiation methods, instruments, and irradiation technology), A. A. Nichiporovich (isotopes and irradiation in plant physiology), and others.

The participants in the Conference familiarized themselves with the new radiation technology used at the M. V. Frunze Agricultural Institute of Kishinev (industrially produced Kolos LMB-γ-IM, and GUBE-4000 units) and also visited the Moldavian Institute of Irrigated Agriculture.

FIFTH ALL-UNION CONFERENCE ON THE PHYSICS OF ELECTRON AND ATOM COLLISIONS

V. B. Leonas

The regularly scheduled All-Union conference on the physics of electron and atom collisions was held at Uzhgorod, September 19-23, 1972. A numerous group of scientists from the socialist countries took part in the deliberations of the conference. The conference paid homage to the memory of the recently deceased Professor N. V. Fedorenko, with whose name is indissolubly linked the founding of the Soviet school of the physics of electron and atom collisions, today generally acknowledged as one of the prominent trends in physics research.

The conference surveyed progress achieved in this vigorously developing branch of plasma physics over the period elasped since the fourth conference (Riga, 1970).

Until comparatively recently, the efforts of research scientists have been focused on the study of effects accompanying collisions of high-energy particles ($\approx$1 keV), which has been associated with the problem of radiation effects and problems involving materialization of the first stages in thermonuclear research programs. In recent years, with the progressive conquest and study of outer space, the availability and applications of high-power gas lasers, magnetohydrodynamics as a full-fledged low-power source, advances in chemical technology, and so forth, there has also been a concomitant and impressive expansion of research in the field of low-energy collisions.

A total of 281 papers were presented at the conference.* The conference deliberations took place in plenary sessions and at panel sessions.

Review papers delivered at the plenary sessions provided an overview of the general state of research in the physics of particle collisions. Reports by E. E. Nikitin surveyed opportunities associated with interpretations of measurements of differential cross sections for elastic scattering and inelastic scattering. Decoding the specific structure of the experimental dependence arrived at makes it possible to restore, quite precisely, the variation of the term-potentials of the interactions (by analogy with molecular spectroscopy, this led to the apparance of the term "collisional spectroscopy"). Some particularly intriguing possibilities have been opened up by analysis of data on inelastic scattering due to what has been termed intersection or crossing of terms. The theory of atomic collisions has long had at its disposal a mathematical tool-kit adequate for quantitative descriptions of such scattering, but this apparatus has not been put to practical use because of the lack of a reliable experiment. The development of experimental techniques has now rendered possible a comparison of theoretical predictions and measurements in this area, and has made it possible to determine quantitatively parameters which are crucial for the inelastic scattering process. This in turn makes it possible to establish the overall regularities and patterns in inelastic transitions.

The problem of how to exert control over a real chemical process (over its rate and direction) under conditions where the process is being intensified by a powerful activating agent (radiation or laser) is closely associated with our level of knowledge on the mechanism underlying the process, and on laws governing some distinct stages of the process. Until recently, all of our concepts of elementary reactions in gases has been based on comparisons of macroscopic reaction rates measured empirically and those calculated on the basis of a specific model. The inevitable statistical averaging of the effects of distinct collisions in counts of the observable macroscopic yield of reaction products generally tends to blur out the distinctions between models. This state of affairs is unsatisfactory, even from the standpoint of the prospective utilization of chemical processes in the generation of laser emission. In that sense, we see some unique

*Abstracts of the papers presented have been published under separate cover.

Translated from Atomnaya Énergiya, Vol. 34, No. 2, pp. 140-141, February, 1973.

possibilities and opportunities being opened up by research on chemical reactions with the aid of the method of colliding beams. Highly detailed information on the probability, dynamics, and energetics of the elementary collision process involving chemical transformation of partners has been obtained successfully in that research. The applied value of such research is quite evident, and the investigations are of inestimable value in terms of the development of a reliable theory to account for the elementary processes.

The results of beam investigations of elementary atomic – molecular processes typical of collisions in a low-temperature plasma was the subject of a report submitted by V. I. Gol'danskii, V. B. Leonas, and L. Yu. Rusin. In a manner similar to the chemical processes, molecular transport processes, excitation of internal degrees of freedom of molecules in gases, and such had been studied previously only on a macroscopic level. Successful elaboration of a reliable theory accounting for elementary atomic – molecular processes, and possibilities of subsequent quantitative applications of the theory, must be related to the direct information that can be secured in beam experiments on the potentials of pair interaction, and on the probabilities of translational – vibrational (and rotational) transitions.

The new approach to the study of elementary atomic – molecular processes (elastic scattering, energy exchange, chemical transformations) does not entail simply replacement of some methods by other methods; the purpose is to secure such experimental information as to make it possible to greatly improve the "predictability" of the theory called for by the demands of sophisticated industry of the current epoch. A paper presented by G. F. Drukarev was devoted to these "second-generation" experimental problems. Even the most perfectly conceived and worked-out experiments cannot yield complete information on collisional processes, because of the averaging effect due to the spectrum of spin states and due to the orientations of the interacting particles; this effect cannot yet be completely eliminated. The second-generation experiments are being devised to surmount this hurdle, and the report discussed prospective ways of achieving "polarized" collisions.

A paper by V. V. Titov demonstrated two aspects of research investigations on atomic collisions. On the one hand, the paper showed the possibility and fruitfulness of utilizing the concept of pair collisions in the problem dealing with the motion of a high-energy particles in a periodic structure of the atomic lattice type, and on the other hand, it was clearly demonstrated how the procedure of a purely physical experiment can become the basis of a new technological process for fabricating solid-state electronic devices with prespecified parameters.

The research done at Uzhgorod on optical excitation cross sections in collisions involving electrons, ions, and atoms came through in some of the papers presented at the conference. A detailed study of excitation of inner and outer envelopes of atoms was covered by papers submitted by staff scientists of the A. F. Ioffe Physicotechnical Institute. A novel procedure for investigating the energy levels of highly excited negative ions was also devised and is now in use. There was considerable interest manifested in a report on a large-scale facility for investigating chemical reactions in intersecting beams that has been built at the institute of Chemical Physics of the Academy of Sciences of the USSR.

Consequently, the conference was a demonstration of the qualitative and quantitative expansion of research in this area; the growth and high scientific level of the theoretical research were again put in evidence. Some shortcomings also came to light. Given the generally high stress put on theoretical research, there is unjustifiably scant attention being given to analysis of collisions of atoms and molecules at low energies. The data adduced on processes occurring at thermal energies are generally acquired on the basis of measurements of macroscopic properties, and are converted into cross sections of microscopic processes only with the observance of certain assumptions (some of which are quite open to question). The insufficient attention given to the development of beam experiments in the range of low energies was reflected in the discussion on techniques and equipment.

The next All-Union conference on this topic is scheduled for 1975.

SOVIET — SWEDISH SYMPOSIUM ON THE PHYSICS OF THERMAL AND FAST REACTORS

I. D. Rakhitin

The first Soviet–Swedish joint symposium on the physics of thermal reactors and fast reactors was held September 11-5, 1972, at Dubna. The renowned Swedish specialists I. Jung, B. Pershagen, E. Hellstrand, R. Persson, E. Tenerts, and others took part in the work of the symposium, and subsequently visited leading Soviet scientific research institutes.

Over thirty papers were heard and discussed, including about twelve delivered by Soviet experts. The report by V. T. Rudenko describes the IBR fast pulsed reactor, and problems solved through the use and operation of that reactor at JINR. The study of the physical features of fast reactors with BFS physical assemblies was the subject of reports by Yu. A. Kazanskii and V. A. Dulin. Theoretical and experimental aspects of the physics of thermal reactors were reflected in reports by I. N. Aborina, V. I. Naumov, and colleagues.

Various topics in the calculations and design of fast reactors, working out requirements for nuclear physics data, compiling libraries of nuclear data and reactor programs, were addressed in remarks by R. I. Nikol'skii, S. M. Zaritskii, I. P. Markelov, and M. N. Zizin.

Soviet reports on the most urgent topics in the mathematical theory of nuclear reactors, development of new methods for solving reactor equations, and the development of concepts in reactor theory, met with great interest (such reports were presented by V. V. Khromov, I. D. Rakitin, V. N. Artamkin, A. V. Voronkov, B. P. Kochurov, E. S. Tsapelkin, and N. I. Laletin).

Swedish specialists delivered some informative reports.

The head of the Reactor design division, E. Tenerts, presented an account of reactor physics research problems and developments in design and determination of the characteristics of thermal reactor cores. He reported that old-standing problems in reactor physics, such as the calculation of critical mass, for example, or calculations of neutron flux, of reactivity coefficients, of the reactivity balance and burnup, are now being solved with greater accuracy than actually required for reactor operation.

Today's problems are a combination of heat transfer, hydraulics, neutron physics, reactor control, and economics. Reactor physics comprises a component part of reactor technology, and all the problems relating to it have to be studied simultaneously.

General problems pertaining to the development of Sweden's nuclear power industry and requirements applicable to reactor physics are covered in a report by B. Pershagen.

Until the mid-Sixties, attention had been centered on pressure vessel type heavy-water reactors. The first such reactor built at Agesta was started up in 1963. Its thermal power output level stood at about 80 MW. Construction of a straight-flow boiling heavy water reactor at Marviken, with a rating of 140 MW(e), was cut short in 1970 because of the competition by ordinary-water boiling-water reactors (BWR).

Construction work was begun, in 1965, on the first full-scale water-cooled water-moderated boiling-water reactor, BWR type, rated 440 MW(e), at Oskarshamn. This reactor was started up in August 1971, and went on the line producing electric power in February 1972.

The nuclear power developmental outlook in Sweden is reflected in the following figures:

Translated from Atomnaya Énergiya, Vol. 34, No. 2, pp. 141-143, February, 1973.

Year	Power station output, MW(e)	Nuclear power station fractional contribution to total national electric power production, %
1975	2600	15
1980	8600	30
1985	16,500	50
1990	25,500	60

The construction of industrial fast breeders is scheduled for no earlier than the decade 1980–1990 in Sweden.

The core of the Agesta heavy-water reactor was designed on the basis of a simple two-group procedure, with experimental verification using the ZEBRA exponential assembly. The calculations were found to agree closely with experiment.

More rigorous design techniques were developed for the Marviken reactor. For example, a computational program for FLEF cells was compiled on the basis of a solution of the kinetic many-group equation in integral form.

Several many-group two-dimensional and three-dimensional programs based on a heterogeneous method of the source – sink type, and written in FORTRAN language, were devised to the aid the study of macrodistributions of neutron fields in heavy-water reactors.

Extensive research on the physics of BWR and PWR type ordinary-water reactors is underway in Sweden.

Computational techniques were verified both during the startup of the Oskarshamn-1 reactor and in the performance of the KRITZ high-temperature assembly (R. Persson). One of the outstanding results of these search efforts was the pinpointing of systematic discrepancies between the theoretically predicted and experimental values of the temperature coefficient of reactivity.

At the present time, a program for aiding studies of lattices with fuel in the form of plutonium dioxide is being worked out. The plutonium fuel elements were obtained from USAEC.

In the design techniques developed in Sweden, attention is centered on predictions of the characteristics of reactors while in operation, and optimization of fuel reloading, as well as on the study of the plutonium cycle in thermal reactors. The BUXY two-dimensional many-group program (M. Edenius), used in the preparation of macroscopic constants for diffusional calculations of power distribution fields in large power reactors by the POLCA program, based on a three-dimensional grid network one-group solution of the diffusion equation, is used on the widest scale for calculations of lattice parameters. This BUXY program incorporates thermohydraulic calculations of two-phase flow, and carries out iterations in terms of coolant density as a function of reactor output power, with xenon poisoning taken into consideration.

Startup operations and beginnings of reactor operation yielded rich information, in the case of the Oskarshamn-1 reactor, useful in verifying the BUXY – POLCA computational system, including data on reactivity, field distributions, and the effects of control rods. As E. Tenerts pointed out, the agreement between calculations and experiment was much better than expected.

The study of fast reactor physics was begun in Sweden in 1964, with the startup of the FRO critical assembly at Studsvik (loading of 600 kg 20%-enriched uranium metal). A cycle of major experiments was staged with this fuel assembly (E. Hellstrand). In this way the effective cross sections of ten different isotopes in fission products in three different spectra of a fast reactor were determined, as well as the mean number of fast fission neutrons $\bar{\nu}$ for U^{235} and Pu^{239}. The calculated and empirical $\bar{\nu}$ values agreed within the limits of error of the experiment. Finally, experiments were staged to aid investigation of reaction rates in different configurations of breeding blankets.

Investigations of the Doppler effect and comparison of those data and the theoretical data are dealt with in a report by H. Heggblum. The results of this comparison are fully satisfactory, if we bear in mind heterogeneous effects in experimental specimens, as well as the fine structure of the spectrum and the overlapping resonances.

Extensive work on estimates and compilation of nuclear data, a very timely topic at this time, is being done in Sweden.

In the SPENG program, the neutron spectrum is computed in 2000 energy groups, for a finite homogeneous mixture, and effective cross sections and group constants are worked out for any group decomposition whatever. For those groups where resonance self-shielding and overlapping resonances are essential, the averaged cross sections are computed according to the DORIX program as a function of the temperature and a function of the effective potential cross section. The report by H. Heggblum presents a method for determining estimated neutron data with simultaneous consideration of a large number (51) of macroscopic characteristics obtained in work on fast reactors (31 critical assemblies). It is interesting to note that the fission cross section of U^{235} and the capture cross section of U^{238} are much lower than the data available in the famous ENDF/B-11 library, in the range of energies of greatest importance for fast reactors.

Starting 1966, design projects have been underway in Sweden on three distinct types of fast breeders rated at 1000 MW(e), with sodium, gas, and steam as coolants, and with attention focused on sodium-cooled fast reactors. It is proposed that the initial construction work on an industrial fast breeder get underway not earlier than the 1980's.

Work on the development of computational techniques and programs for fast reactors was reported by K. Jirlov. The basic purpose of the system of programs is to determine the appropriate geometry and composition of the core, as well as the effective fuel cycle for conditions where the percentage burnup and the specific output power in the core and in the breeding blanket will not surpass reasonable limits.

In conclusion, we may note that the meeting between the Soviet and Swedish scientists was most fruitful.

The understanding in effect calls for a return Swedish–Soviet symposium to be held in Sweden during 1973, to discuss engineering topics relating to nuclear reactor safety.

The second CERN school on digital computer processing of experimental data was held September 10-24 in Austria.

Attending the school session were young physicists and computing scientists from 19 European countries, including two from the USSR. The lectures delivered by scientists from CERN member nations encompassed a wide range of topics: translation procedure; the use of desktop computers in physics; system programming; use of large computing systems.

Experimental physicists were most interested in the second round of lectures. These included a particularly interesting lecture course given by W. Zacharow (Britain) developing the general principles of the design and software of desktop computer systems for on-line processing of experimental data.

An example of a well-conceived and organized system with on-line computing equipment is the CERN Omega-project, a general-purpose magnetic spectrometer capable of recording and analyzing the most widely varied processes in high-energy physics (R. Russell).

An arrangement for investigations of nuclear reactions at intermediate energies (BOL) has been devised at the Amsterdam Nuclear Research Institute for research at the synchrocyclotron (J. Obersky). The recording system operates with two PDP-8 computers, which are in turn hooked up to an EL-X8 machine.

One of the lectures was devoted to on-borad computers of satellites (M. A. Perrie, Netherlands).

R. Kaiser (CERN) and J. Schraml (West Germany) demonstrated the possibilities of utilizing computers in the control of accelerators and radio telescopes.

One round of lectures (F. James, G. Wind, CERN) was devoted to general topics in the mathematical processing of large blocks of information. In particular, G. Wind presented an intriguing method of geometrical restoration of tracks in the presence of large statistics, such that machine memory capacity could be greatly conserved by utilizing precomputed coefficients.

On the whole, the materials presented at the CERN school on computer processing of experimental physics data were of great interest.

In line with the terms of an agreement of collaboration in the field of peaceful uses of atomic energy, contracted between the GKAE SSSR and the Canadian state agency Atomic Energy of Canada, a delegation of Canadian specialists on nuclear reactor coolants, headed by P. J. Dean, visited the Soviet Union September 18-28, 1972.

The delegation members vistited the I. V. Kurchatov Institute of Atomic Energy, the G. M. Krzhizhanovskii Power Institute, the Power Physics Institute at Obninsk, the Thermal Physics Institute of the Siberian Division of the Academy of Sciences of the USSR, the Moscow Power Institute, and also the V. I. Lenin Atomic Reactor Scientific Research Institute [NIIAR] in Dimitrovgrad.

The interest of the delegation was focused on the following topics: heat removal when using boiling water as reactor coolant; chemistry of the water coolant, i.e., how the required composition and the necessary quantity of salts can be sustained in the coolant, as well as the required amounts of oxygen and hydrogen; corrosion of the surfaces of loops and entrainment of corrosion productions in the loop stream; activation of corrosion products and deposition of corrosion products on the loop surfaces; the radiation environment and repair and maintenance of process equipment. Soviet scientists and specialists delivered reports on these topics. For their part, the Canadian specialists gave accounts of work in progress in Canada on the investigation of burnout and postburnout phenomena and conditions, and also on the use of organic coolants in reactors.

Translated from Atomnaya Energiya, Vol.34, No. 2, pp. 143-144, February, 1973.

The encounters took place in a cordial atmosphere and setting. The members of the Canadian delegation expressed their satisfaction with the reports and discussions.

The tenth session of the French — Soviet commission on scientific questions was held September 26-28, 1972 at the Institute of High-Energy Physics in Serpukhovo. Basic reviews of joint work on a set of experimental facilities at the Institute of High-Energy Physics including the French Mirabel liquid-hydrogen bubble chamber, and systems producing a separated beam targeted on that bubble chamber, were discussed at the sessions of the commission.

During the period elapsed since the last session, the Mirabel bubble chamber has been functioning satisfactorily on the whole. In the May 1972 campaign, about 22,000 photographs were taken in a beam of K^--mesons of 34 GeV/c momentum.

Analysis of the data accumulated in the processing and inspection of 950 plates made it possible to determine the approximate composition of the beam: 93% K^--mesons, 2% μ-mesons, 5% miscellaneous. The background amounted to 20% of the beam. Work was impossible with the beam of K^+-mesons, because the background due to μ-mesons was five to six times greater than the background observed in the beam of K^--mesons. Future plans call for strengthening the shielding in the leading portion of the channel and in front of the bubble chamber, so as to improve background conditions appreciably.

The commission reviewed and discussed the results of processing events in pp-interactions with momenta of 70 and 50 GeV/c, at both IFVE and Saclay. The combined data, with total statistics of 10,000 events at 70 GeV/c momentum and 2,000 event at 50 GeV/c momentum, were reported out at the Sixteenth International Conference on High-Energy Physics in Batavia (USA). The energy dependence of the mean multiplicity of the charged particles is described satisfactorily by both logarithmic and power function of $\sqrt{S}$. Topological cross sections were measured to high accuracy.

Data were obtained on the mean multiplicity of charged particles and on topological cross sections determined as a result of analyzing 800 plates in π^-p-interactions at 50 GeV/c momentum and 6,000 plates in K^-p-interactions at 34 GeV/c momentum. The mean multiplicity of charged particles in the π^-p-interactions is 5.8 ± 0.1. These results were also reported out at the Batavia high-energy physics conference.

At one of the sessions of the commission, information was divulged on the status of inspecting and measuring equipment and computer programming software in French and Soviet laboratories, and also in the laboratories of other CERN member nations. The commission discussed the work program drawn up for the Mirabel bubble chamber for the October-December 1972 period, and the approximate schedule of beam work with the bubble chamber drawn up tentatively for 1973, with not less than 300,000 high-quality photographs to be processed.

The commission elected R. M. Sulyaev (USSR) chairman and A. Bertheleau (France) vice-chairman.

A conference of IAEA experts on the radiative capture of charged particles was held in Vienna, October 9-13, 1972. Participating were representatives of Great Britain, the USSR, the USA, France, West Germany, and other countries. A broad range of topics pertaining to nuclear spectoscopy investigations of $p\gamma$ and $\alpha\gamma$ reactions based on the use of low-energy accelerators was discussed, as well as research on the giant dipole resonance and high isospin analog states in radiative capture of charged particles.

The conference worked out recommendations for small laboratories engaged in such research, and took note of the need to stiffen the requirements on analysis of data, theoretical interpretation of data, and so on.

The reports and the discussion of them constituted a complete review of current research into the radiative capture of charged particles and also contained recommendations for future development in this direction.

The proceedings of the conference will be published by IAEA.

A consultation meeting of Soviet and French specialists on prospective topics in the construction of nuclear reactor power stations was held at GKAE SSSR (USSR State commission on peaceful uses of atomic energy) in late Ocober 1972.

The delegation of French specialists was headed by the leading official of the Division of Reactor Physics and Applied Mathematics, J. Busacq. The introductory remarks by J. Busacq pointed out that French specialists hoped to make use of the experience available in the USSR in the construction of power stations of high unit power output based on channel type graphite-moderated uranium-fueled reactors. Academician N. A. Dollezhal' delivered a brief report on work done by Soviet officials in the design of reactor power-generating stations in the USSR. Next the following reports were read: "Design features of the uranium-graphite channel type reactor at the Leningrad nuclear power station; nuclear steam superheat in channel type reactors"; "Heat burnout in the flow of boiling water along bundles of fuel rods"; Prospects for the development of nuclear power stations with reactors of the type built at the I. V. Kurchatov nuclear power station at Belyi Yar; uranium-graphite channel type natural-coolant-circulation reactor (based on developments and experience at the Bilibin combined nuclear-fueled and fossil-fueled electric power generating station)."

The reports and papers evoked a lively discussion from representatives of both parties present; a useful exchange of opinions took place.

The members of the French delegation visited the Power Physics Institute, the world's First Nuclear Power Station at Obninsk, the I. V. Kurchatov Institute of Atomic Energy, and the Belyi Yar nuclear power station, where they were familiarized with the scientific research laboratories, and with the basic equipment and instrumentation of the Belyi Yar nuclear power plant.

During the concluding talks, J. Busacq thanked the Soviet delegation for the excellent organization of the reception, and the opportunity of visiting institutes in this country, and noted that many interesting points came up in the scientific discussions, with some exhaustive answers forthcoming in all of the areas of mutual interest.

breaking the language barrier

WITH COVER-TO-COVER ENGLISH TRANSLATIONS OF SOVIET JOURNALS

in physics

Title	# of Issues	Subscription Price
Astrophysics *Astrofizika*	4	$100.00
Fluid Dynamics *Izvestiya Akademii Nauk SSSR mekhanika zhidkosti i gaza*	6	$160.00
High-Energy Chemistry *Khimiya vysokikh énergii*	6	$155.00
High Temperature *Teplofizika vysokikh temperatur*	6	$125.00
Journal of Applied Mechanics and Technical Physics *Zhurnal prikladnoi mekhaniki i tekhnicheskoi fiziki*	6	$150.00
Journal of Engineering Physics *Inzhenerno-fizicheskii zhurnal*	12 (2 vols./yr. 6 issues ea.)	$150.00
Magnetohydrodynamics *Magnitnaya gidrodinamika*	4	$100.00
Mathematical Notes *Matematicheskie zametki*	12 (2 vols./yr. 6 issues ea.)	$185.00
Polymer Mechanics *Mekhanika polimerov*	6	$120.00
Radiophysics and Quantum Electronics (Formerly Soviet Radiophysics) *Izvestiya VUZ. radiofizika*	12	$160.00
Solar System Research *Astronomicheskii vestnik*	4	$ 95.00
Soviet Applied Mechanics *Prikladnaya mekhanika*	12	$160.00
Soviet Atomic Energy *Atomnaya énergiya*	12 (2 vols./yr. 6 issues ea.)	$160.00
Soviet Physics Journal *Izvestiya VUZ. fizika*	12	$160.00
Soviet Radiochemistry *Radiokhimiya*	6	$155.00
Theoretical and Mathematical Physics *Teoreticheskaya i matematicheskaya fizika*	12 (4 vols./yr. 3 issues ea.)	$145.00

Back volumes are available. For further information, please contact the Publishers.

SEND FOR YOUR FREE EXAMINATION COPIES

PLENUM PUBLISHING CORPORATION
227 WEST 17th STREET
NEW YORK, N. Y. 10011
Plenum Press • Consultants Bureau
• IFI/Plenum Data Corporation

In United Kingdom
Plenum Publishing Co. Ltd., Davis House (4th Floor)
8 Scrubs Lane, Harlesden, NW10 6SE, England